FELINE CORONAVIRUS INFECTION: IMPLICATIONS FOR THE TREATMENT OF FELINE INFECTIOUS PERITONITIS

A Dissertation

Presented to the Faculty of the Graduate School

of Cornell University

In Partial Fulfillment of the Requirements for the Degree of

Doctor of Philosophy

by

Andrew Douglas Regan

February 2010

FELINE CORONAVIRUS INFECTION: IMPLICATIONS FOR THE TREATMENT OF FELINE INFECTIOUS PERITONITIS

Andrew Douglas Regan, Ph.D.

Cornell University 2010

Feline infectious peritonitis (FIP) is an untreatable and terminal disease of cats caused by systemic infection with a feline coronavirus termed feline infectious peritonitis virus (FIPV). This thesis investigates the cellular entry of FIPV in order to discover targets which may be of therapeutic value in treating this disease. This thesis demonstrates that FIPV utilizes the lectin DC-SIGN to enhance cellular uptake. This is significant because macrophages and dendritic cells, which express DC-SIGN at high levels, are infected by FIPV to initiate the disease process. This thesis also shows that FIPV activates the p38 MAPK signaling pathway in infected cells, and that this induces the overproduction of pro-inflammatory cytokines observed in cats with FIP. Finally this thesis demonstrates that feline coronaviruses require cathepsin cysteine proteases during entry to cleave and activate the viral spike protein. In addition, specific proteases are preferred over others depending on the pathogenicity of the virus. It is also shown that certain molecular inhibitors of cysteine proteases can block viral infection in primary feline cells, presumably by preventing cleavage of the spike protein during viral entry. These data highlight new therapeutic strategies for the treatment of FIP which will be discussed in the conclusion.

BIOGRAPHICAL SKETCH

Andrew Regan was born in Newport, Rhode Island, USA in December of 1978. He grew up in Portsmouth, Rhode Island and graduated from Portsmouth High School in 1996. Over the next few years he lived in Connecticut, Colorado and Oregon. In 2000 he began attending Oregon State University in Corvallis, Oregon, where he conducted viral research in the laboratory of Dr. Theo Dreher and graduated with a Bachelor of Science in Microbiology cum laude. In 2004 he began his doctoral studies in the Department of Microbiology and Immunology at the Cornell University College of Veterinary Medicine, Ithaca, New York. He has since been conducting research in the laboratory of Dr. Gary Whittaker on viral pathogens such as influenza, SARS, VSV and FIPV. At Cornell he met his wife, Rebecca Cohen Regan, DVM, whom he married in May of 2009 on the shore of Cayuga Lake in Aurora, New York.

I dedicate this work to my parents Richard and Jane.

ACKNOWLEDGMENTS

I would like to thank Gary Whittaker for his guidance and wisdom. I would also like to thank the members of my advisory committee Rick Cerione and Colin Parish, and my A-examination committee Jim Casey and Joel Baines. I would like to thank Ed Dubovi, Fred Scott, Ruth Collins, Pete Rahl, Sandrine Boulezard and Marc Antoniak who have given me significant help and advice during my doctoral studies, and all the members of the Whittaker Lab, Collins Lab and Cerione Lab. I would also like to thank my family, specifically my wife Rebecca who has given me strength throughout the pursuit of my doctoral research.

TABLE OF CONTENTS

LIST OF FIGURES

LIST OF FIGURES (continued)

LIST OF FIGURES (continued)

LIST OF TABLES

CHAPTER ONE

INTRODUCTION

1.1 Feline Infectious Peritonitis

Feline infectious peritonitis (FIP) is a disease of cats with a spectrum of pathological outcomes, all of which are lethal. FIP was first described as a disease in the 1960's (26), however later analysis of necropsy records showed that it first appeared in cats during the previous decade (51). The causative agent of FIP is a coronavirus designated as feline coronavirus (FCoV) (75, 81). There are two dominant manifestations of FIP in cats. The more common wet (effusive) form is characterized by the accumulation of fluid in the peritoneal or thoracic cavity due to pyrogranulomatous endothelial lesions (75). The dry (non-effusive) form is often characterized by granulomatous lesions in the central nervous system (CNS) or eyes leading to neurological and ocular symptoms (42). However lesions in cats with the dry form of FIP have also been observed in a variety of other tissues (54). Lymphopenia, enteritis, fever, weight loss and lethargy are common symptoms in cats with both forms of FIP (1).

1.2 Virus Classification

Coronaviruses are enveloped and contain a single-stranded positive-sense RNA (+ssRNA) genome (33). They are divided into five groups (1a,1b,2a,2b,3) (Table 1.1) (20). Feline coronaviruses are members of group 1a, and most closely related to canine coronavirus (CCoV) and porcine transmissible gastroenteritis virus (TGEV) suggesting a common origin (27). Feline coronaviruses are further differentiated into serotype 1 (FCoV-1) and serotype 2 (FCoV-2) based on spike protein homology (43). Serotype 1 feline coronaviruses make up approximately 80% of field isolates, and are more closely related to serotype 1 canine coronavirus (CCoV-1) (37). Serotype 2 feline coronaviruses are less common, but may be more likely to cause FIP (36). They are more closely related to serotype 2 canine coronavirus

Table 1.1 Classification of coronaviruses. Significant coronaviruses representing the five groups (1a, 1b, 2a, 2b, 3) are listed. Also shown are major determinants of viral tropism (when known): the host-cell receptor and proteolytic enzymes that have been shown to cleave and activate the spike (S) protein. Aminopeptidase N (APN), angiotensin converting enzyme 2 (ACE2), carcinoembryonic antigen-related cell adhesion molecules (CEACAM), elastase (E), trypsin (T), furin (F), cathepsin B (B), cathepsin L (L).

Coronavirus	Host	Receptor	S Cleavage
Group 1a			
Feline coronavirus (type 1)	Cat	?	F, B (60)
Feline coronavirus (type 2)	Cat	APN (71)	B, L (61)
Canine coronavirus (type 1)	Dog	?	?
Canine coronavirus (type 2)	Dog	APN (71)	B, L (60)
Transmissible gastroenteritis virus	Pig	APN (71)	B, L (60)
Ferret coronavirus	Ferret	?	?
Group 1b			
Human coronavirus NL63	Human	ACE2 (23)	?
Human coronavirus 229E	Human	APN (80)	T, L (30)
Bat coronavirus (Trinidad)	Bat	?	?
Porcine epidemic diarrhea virus	Pig	APN (34)	?

Table 1.1 (continued)

Coronavirus	Host	Receptor	S Cleavage
Group 2a			
Human coronavirus OC43	Human	Sialic acid (74)	?
Human coronavirus HKU1	Human	?	?
Porcine hemagglutinating encephalomyelitis virus	Pig	Sialic acid (64)	?
Bovine coronavirus	Cow	Sialic acid (64)	?
Murine hepatitis virus	Mouse	CEACAM (25)	T (16), F (16), B (58)
Group 2b			
Severe acute respiratory syndrome (SARS) coronavirus	Human	ACE2 (35), DC/L-SIGN (40)	E (41), T (41), B (28), L (28)
Bat-SARS coronavirus	Bat	?	?
Group 3			
Infectious bronchitis virus	Chicken	Sialic acid (77)	F (79), T (79)
Turkey coronavirus	Turkey	?	?

(CCoV-2) and TGEV (37).

In addition to group and serotype, feline coronaviruses are divided into two biotypes based on their pathological outcome (53). Members of the nonpathogenic biotype are classified as feline enteric coronavirus (FECV), and are common throughout the world's population of domesticated and wild cats (55). FECV replicates mostly in the intestinal epithelial cells of the gut, and causes mild to unapparent enteritis (52). In contrast, feline coronaviruses that cause FIP can efficiently replicate in the immune cells of their host (67). These highly pathogenic viruses cause a lethal systemic infection, and are classified as the feline infectious peritonitis virus (FIPV) biotype (53).

1.3 Replication and Assembly

The feline coronavirus genome consists of an unsegmented 29kb +ssRNA which is translated by ribosomes after cellular entry (47). It codes for the viral replicase (1a/1b), four structural proteins (spike, envelope, membrane and nucleocapsid), and five accessory proteins (3a, 3b, 3c, 7a and 7b) (62). The viral replicase is activated by intramolecular proteolytic processing, and then proceeds to polymerize negative-sense copies of the viral genome (31). These serve as templates for the production of full length (genomic) and partial length (subgenomic) viral +ssRNA (14). Subgenomic and genomic +ssRNA are translated to produce the viral structural and accessory proteins (62). Genomic copies are also packaged into newly assembled viral particles (Figure 1.1) (8, 45).

The viral structural proteins spike, envelope and membrane are produced and incorporated into the membrane of the host cell endoplasmic reticulum (54). The nucleocapsid protein binds newly synthesized viral genomes and the membrane protein (44). Fully formed complexes bud into the ER to become internal viral

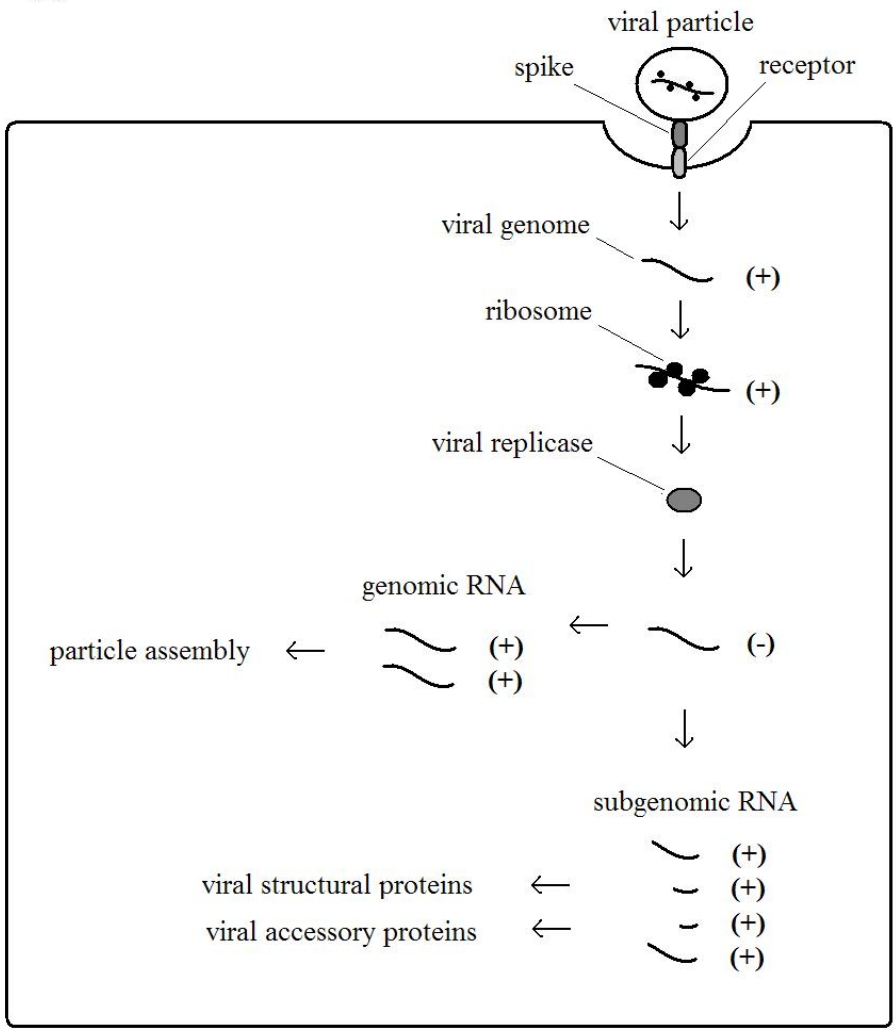

Figure 1.1 Diagram of coronavirus entry and replication. Spike protein on the surface of the viral particle binds a specific host receptor, and then mediates entry of the viral genome into the cell. Ribosomes translate the viral replicase from the +ssRNA viral genome. The replicase polymerizes -ssRNA templates which are used to make genomic +ssRNA which are packaged into new viral particles, and partial length subgenomic +ssRNA which is used as a template for the production of viral structural proteins and accessory proteins.

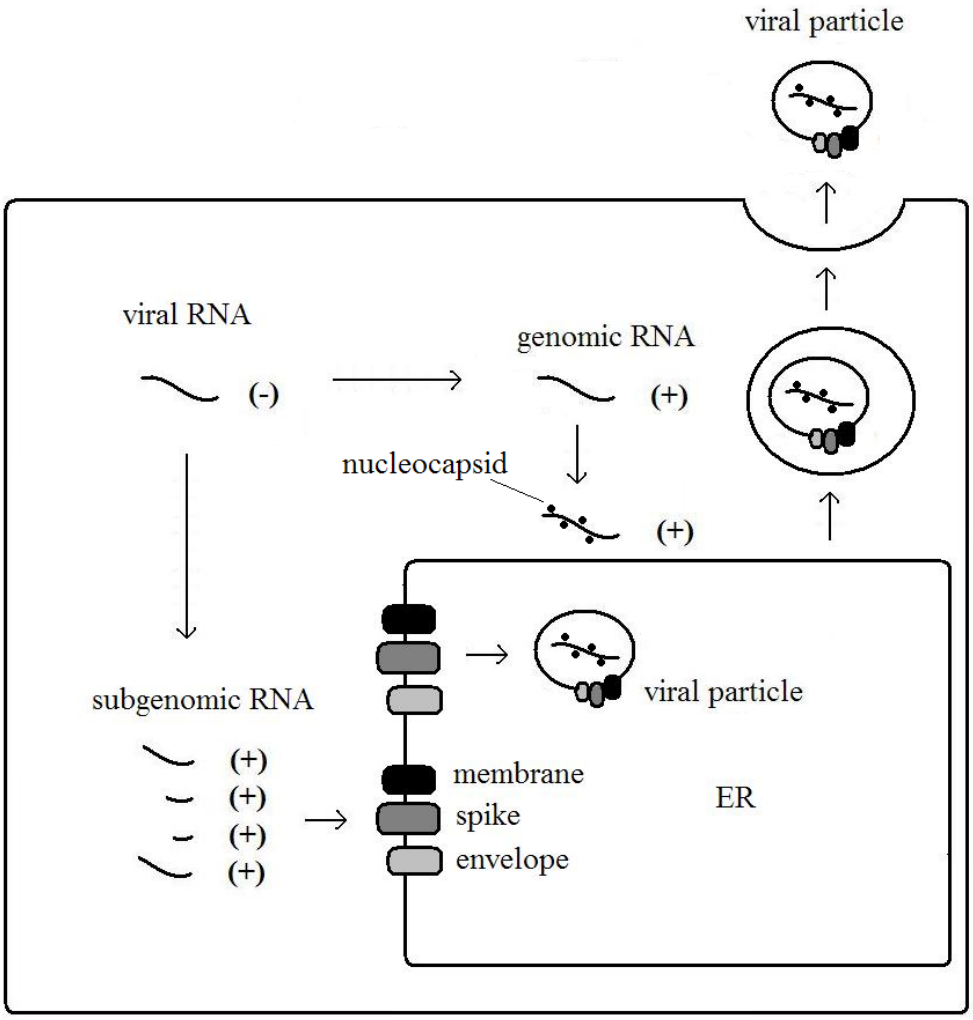

Figure 1.2 Diagram of coronavirus assembly. Viral structural proteins (membrane, spike, envelope, and nucleocapsid) are produced from subgenomic +ssRNA. Membrane, spike and envelope are membrane-bound proteins that are incorporated in the ER membrane. Nucleocapsid is a soluble protein which binds full length genomic +ssRNA. Nucleocapsid interacts with the membrane-bound structural proteins, and the entire complex buds into the ER lumen. These newly formed viral particles are then secreted through the Golgi and exocytosed from the cell.

particles (49). These particles are trafficked through the Golgi and released from the cell by exocytosis (Figure 1.2) (66).

1.4 Spike Protein

The coronavirus spike protein is a membrane-bound glycoprotein expressed on the surface of viral particles responsible for host cell receptor binding and virus-cell membrane fusion (17). The spike protein is categorized as a class I viral fusion protein and has characteristics in common with other class I viral fusion proteins such as influenza virus hemagglutinin (HA), retrovirus envelope (Env) and paramyxovirus fusion (F) (7, 12). The spike protein is divided into two domains designated as S1 and S2. S1 is responsible for host cell receptor binding, while S2 facilitates virus-host membrane fusion to facilitate cellular entry (3). Class I viral fusion proteins are "primed" for fusion by proteolytic cleavage, and then "activated" by receptor binding, low pH, or a combination of the two (32).

The spike proteins of group 2a coronaviruses (e.g. MHV-1) and group 3 coronaviruses (e.g. infectious bronchitis virus (IBV)) are cleaved by furin or furin-like enzymes in the secretory pathway during viral particle assembly and trafficking (4, 16). This occurs at specific sites containing the amino acids lysine or arginine, present at either the S1/S2 boundary, or at a conserved site within the S2 domain (4, 79). In contrast, the spike proteins of group 1a/1b and 2a coronaviruses remain uncleaved during assembly, except in a few cases (9, 57). It has recently been shown that some group 1a coronaviruses (e.g. human coronavirus 229E (HCoV-229E)) and group 2b coronaviruses (e.g. severe acute respiratory syndrome associated coronavirus (SARS-CoV)) are cleaved after assembly, either by trypsin- or elastase-like proteases in the extracellular space (76), or by cysteine proteases in the host cell endocytic pathway (28, 30).

1.5 Cellular Entry

Cellular entry commences when the spike protein on the surface of a viral particle binds to the extracellular domain of specific membrane-bound receptors on the host cell surface (65). Aminopeptidase N has been identified as the receptor for many group 1a and 1b coronaviruses, including FCoV-2, CCoV-2, TGEV, HCoV-229E and porcine epidemic diarrhea virus (PEDV) (34, 70, 71). FCoV-1 has been suggested to use a different unidentified receptor (11). The other exception is group 1b human coronavirus NL63 (HCoV-NL63) which utilizes angiotensin converting enzyme 2 (ACE2) instead of APN (23). The receptor for group 2a coronavirus MHV is CEACAM (25). Group 2b bovine coronavirus (BCoV) and porcine hemagglutinating encephalomyelitis virus (PHEV) utilize sialic acid (64). The group 2b SARS-CoV utilizes ACE2 as its receptor (35). The dendritic cell specific ICAM-3-grabbing nonintegrin (DC-SIGN) and liver/lymph node specific (L-SIGN) have also been shown to enhance entry of SARS-CoV (40). Both sialic acid and heparin have been reported to play a role in the entry of the group 3 coronavirus IBV (39, 77).

After receptor binding, a virus-host membrane fusion event occurs either at the cell surface, or after endocytosis of the viral particle (65). For many coronaviruses, it is still unclear which mechanism of entry is utilized. Recent evidence suggests that coronaviruses may have the ability to utilize either pathway dependent on the host environment. For example, SARS-CoV enters a host cell via endocytosis and cathepsin L-mediated spike protein cleavage (28); however if this pathway is blocked, the virus can enter by a trypsin- or elastase-mediated event the cell surface instead (41).

In addition to receptor binding, many coronaviruses are dependent on low-pH for cellular entry such as IBV (6), MHV (46) and SARS-CoV (28). IBV requires low pH for spike protein fusion activation, as is the case for other class I viral fusion

proteins like influenza HA (6). However, in the case of SARS-CoV, the cathepsin L mediated spike protein cleavage is the low-pH dependent step, not fusion itself (28).

1.6 Cathepsin B and L

Cathepsins are a group of cysteine proteases within the papain family of proteases, which also includes papain and related plant proteases (2). Cathepsins are localized mainly to the endocytic pathway of cells, but are also secreted and found at the cell surface (29). Most cathepsins possess endopeptidase activity, although some such as cathepsin B (catB) can also act as an exopeptidase (38). Some cathepsins have specific amino acid motifs which are required for cleavage to occur, whereas others are more promiscuous. Cat B prefers to cleave where the P1 position is an arginine or lysine (5). Cathepsin L (catL) prefers to cleave at an arginine or lysine as well, but also requires the P2 position be a bulky hydrophobic amino acid (5). CatB and catL are essential for entry of viruses such as reovirus (13), hendra virus (50), nipah virus (10) and coronaviruses such as SARS-CoV (28) and MHV-2 (58). A number of small molecule inhibitors have been created which target either one (e.g. CA-074Me inhibits catB) or all cathepsins (e.g. E-64-d) *in vitro* and *in vivo* with no reported toxicity in mice (72).

1.7 Transmission

FECV is shed at high titers in the feces of infected cats and is transmitted efficiently via the oral-fecal route (52). However cases of FIP are usually isolated incidents among a population suggesting that FIPV is not efficiently transmitted (54). An important observation was made when FECV and FIPV isolates from the same geographic area and serotype were shown to be more closely related to each other (98-99% homology) than to analogous isolates from different geographic regions (80-90%

homology), suggesting that separate strains of FECV and FIPV do not exist independently of each other (73). The currently accepted model claims that FECV infects a young naïve host via fecal-oral transmission, and is usually cleared by an appropriate immune response (52). However, an ineffective immune response may lead to the establishment of a persistent infection of FECV in the gut (54). The low fidelity viral replicase causes the production of mutant viruses during a persistent infection, some of which have the ability to infect immune cells and are now referred to as FIPV (67). Specific mutations in the spike protein and accessory protein 3c have been suggested to play a role in the conversion of FECV to FIPV, however the mechanism has yet to be described (54, 63).

1.8 T-cell Activation

In addition to mutations in the virus, the ability of FECV to convert to FIPV appears to depend on the immune system of the host. The accepted model suggests that the specific type of T-cell activation in the host defines the outcome of the disease (54). If the host mounts a "cell-mediated" type 1 T-helper cell (T_h1) immune response, then the initial FECV infection is eliminated. A persistent infection of FECV may become established in gut epithelial cells if the immune system mounts an "antibody-mediated" type 2 T-helper cell (T_h2) response; a mix of T_h1 and T_h2 responses; or a compromised T_h1 response (54). During a persistent FECV infection, FIPV mutants may arise and start to replicate in immune cells. If the host then mounts a potent T_h1 response, the virus can be eliminated from infected cells and disease is averted. If the host instead mounts a T_h2 antibody-mediated response, it actually enhances the disease by a process termed antibody-dependent (back off ADE) enhancement (ADE) (48). Antibodies usually bind viral particles and target them for destruction by immune cells such as macrophages, however FIPV is able to avoid

destruction and hijack the very cell attempting to destroy it (24). A T_h2 response also causes the accumulation of virus-antibody complexes on endothelial tissue, leading to the extreme vasculitis seen in cats with the wet form of FIP (56). If the host responds to FIPV with a mix of T_h1 and T_h2 responses, or a compromised T_h1 response, FIPV is only partially cleared from immune cells, and establishes a persistent infection in immune cells and certain tissues. This results in the non-effusive dry form of FIP, which may progress more slowly (54). The type of T-cell activation also dictates which cytokines are produced in response to infection (59). Cats suffering from FIP have been shown to produce high levels of T_h2-associated pro-inflammatory cytokines such as tumor necrosis factor alpha (TNFα), interleukin-1 beta (IL-1β) and interleukin-6 (IL-6), all of which are indicators of a poor outcome (18, 19, 68).

1.9 Current Treatments

There is no current recommended treatment for FIP, and a cat with a confirmed diagnosis is usually euthanized depending on the severity and progression of the disease (21). The use of immunosuppressant's such as glucocorticoids and cyclophosphamide have been reported to slow disease progression, but do not prevent a fatal outcome (22). Vaccines against FCoV have proven ineffective at preventing FIP, in some cases actually enhancing disease progression (69). A vaccine is currently marketed that confers protective immunity against FCoV-2, but cannot be administered until after 16 weeks when most kittens are already seropositive (78). In addition it does not cross-protect against the more common FCoV-1 and is therefore not recommended by the American Association of Feline Practitioners Feline Vaccine Advisory Panel (15).

REFERENCES

1. Addie, D., S. Belak, C. Boucraut-Baralon, H. Egberink, T. Frymus, T. Gruffydd-Jones, K. Hartmann, M. J. Hosie, A. Lloret, H. Lutz, F. Marsilio, M. G. Pennisi, A. D. Radford, E. Thiry, U. Truyen, and M. C. Horzinek. 2009. Feline infectious peritonitis ABCD guidelines on prevention and management. J Feline Med Surg 11:594-604.
2. Barrett, A., Rawlings, N., Woessner, J. 2004. Handbook of Proteolytic Enzymes Elsevier Academic Press.
3. Bosch, B., Rottier, P. 2008. Nidovirus entry into cells. Nidoviruses ASM Press:157–78.
4. Cavanagh, D., Davis, P., Pappin, D., Binns, M., Boursnell, M., Brown, T. 1986. Coronavirus IBV: partial amino terminal sequencing of spike polypeptide S2 identifies the sequence Arg-Arg-Phe-Arg-Arg at the cleavage site of the spike precursor propolypeptide of IBV strains Beaudette and M41. Virus Res 4:133–43.
5. Choe, Y., Leonetti, F., Greenbaum, D., Lecaille, F., Bogyo, M., Brömme, D., Ellman, J., Craik, C. 2006 Substrate profiling of cysteine proteases using a combinatorial peptide library identifies functionally unique specificities. J Biol Chem 281:128424-32.
6. Chu, V., McElroy, L., Chu, V., Bauman, B., Whittaker, G. 2006 The avian coronavirus infectious bronchitis virus undergoes direct low-pH-dependent fusion activation during entry into host cells. J Virol 80:3180-8.
7. Colman, P., Lawrence, M. 2003. The structural biology of type I viral membrane fusion. Nat Rev Mol Cell Biol 4:309-19.

8. Dalton, K., Casais, R., Shaw, K., Stirrups, K., Evans, S., Britton, P., Brown, T., Cavanagh, D. 2001 cis-acting sequences required for coronavirus infectious bronchitis virus defective-RNA replication and packaging. J Virol 75:125-33.

9. de Haan, C., Haijema, B., Schellen, P., Schreur, P., te Lintelo, .E, Vennema, H., Rottier, P. 2008 Cleavage of group 1 coronavirus spike proteins: how furin cleavage is traded off against heparan sulfate binding upon cell culture adaptation. J Virol 82:6078-83.

10. Diederich, S., Thiel, L., Maisner, A. 2008 Role of endocytosis and cathepsin-mediated activation in Nipah virus entry. Virology 375:391-400.

11. Dye, C., Temperton, N., Siddell, S. 2007 Type I feline coronavirus spike glycoprotein fails to recognize aminopeptidase N as a functional receptor on feline cell lines. J Gen Virol 88:1753-60.

12. Earp, L., Delos, S., Park, H., White, J. 2005. The many mechanisms of viral membrane fusion proteins. Curr Top Microbiol Immunol 285:25-66.

13. Ebert, D., Deussing, J., Peters, C., Dermody, T. 2002 Cathepsin L and cathepsin B mediate reovirus disassembly in murine fibroblast cells. J Biol Chem 277:24609-17.

14. Enjuanes, L., Almazán, F., Sola, I., Zuñiga, S. 2006. Biochemical aspects of coronavirus replication and virus-host interaction. Annu Rev Microbiol 60.

15. Fehr, D., Holznagel, E., Bolla, S. 1997. Placebo-controlled evaluation of a modified life virus vaccine against feline infectious peritonitis: safety and efficacy under field conditions. Vaccine 15.

16. Frana, M., Behnke, J., Sturman, L., Holmes, K. 1985. Proteolytic cleavage of the E2 glycoprotein of murine coronavirus: host-dependent differences in proteolytic cleavage and cell fusion. J. Virol 56:912–20.

17. Gallagher, T., Buchmeier, M. 2001. Coronavirus spike proteins in viral entry and pathogenesis. Virology 279:371-4.

18. Goitsuka, R., Ohashi, T., Ono, K., Yasukawa, K., Koishibara, Y., Fukui, H., Ohsugi, Y., Hasegawa, A. 1990 IL-6 activity in feline infectious peritonitis. J Immunol 144:2599-603.

19. Goitsuka, R., Onda, C., Hirota, Y., Hasegawa, A., Tomoda, I. 1988 Feline interleukin 1 production induced by feline infectious peritonitis virus. Nippon Juigaku Zasshi 50:209-14.

20. Gorbalenya, A. 2008. Genomics and evolution of the Nidovirales. Nidoviruses ASM Press:15-28.

21. Hartmann, K. 2005 Feline infectious peritonitis. Vet Clin North Am Small Anim Pract 35:39-79.

22. Hartmann, K., Ritz, S. 2008 Treatment of cats with feline infectious peritonitis. Vet Immunol Immunopathol 123:172-5.

23. Hofmann, H., Pyrc, K., van der Hoek, L., Geier, M., Berkhout, B., Pöhlmann, S. 2005 Human coronavirus NL63 employs the severe acute respiratory syndrome coronavirus receptor for cellular entry. Proc Natl Acad Sci U S A 102:7988-93.

24. Hohdatsu, T., Nakamura, M., Ishizuka, Y., Yamada, H., Koyama, H. 1991. A study on the mechanism of antibody-dependent enhancement of feline infectious peritonitis virus infection in feline macrophages by monoclonal antibodies. Arch Virol 120:207-217.

25. Holmes, K., Boyle, J., Weismiller, D., Compton, S., Williams, R., Stephensen, C., Frana, M. 1987. Identification of a receptor for mouse hepatitis virus. Adv Exp Med Biol 218:197-202.

26. Holzworth, J. 1963. Some important disorders of cats. Cornell Vet 53:157-60.

27. Horzinek, M., Lutz, H., Pedersen, N. 1982 Antigenic relationships among homologous structural polypeptides of porcine, feline, and canine coronaviruses. Infect Immun 37:1148-55.

28. Huang, I., Bosch, B., Li, F., Li, W., Lee, K., Ghiran, S., Vasilieva, N., Dermody, T., Harrison, S., Dormitzer, P., Farzan, M., Rottier, P., Choe, H. 2006 SARS coronavirus, but not human coronavirus NL63, utilizes cathepsin L to infect ACE2-expressing cells. J Biol Chem 281:198-203.

29. Jane, D., Morvay, L., Dasilva, L., Cavallo-Medved, D., Sloane, B., Dufresne, M. 2006 Cathepsin B localizes to plasma membrane caveolae of differentiating myoblasts and is secreted in an active form at physiological pH. Biol Chem 387:223-34.

30. Kawase, M., Shirato, K., Matsuyama, S., Taguchi, F. 2009. Protease-mediated entry via the endosome of human coronavirus 229E. J Virol 83:712-21.

31. Kim, J., Spence, R., Currier, P., Lu, X., Denison, M. 1995 Coronavirus protein processing and RNA synthesis is inhibited by the cysteine proteinase inhibitor E64d. Virology 208:1-8.

32. Klenk, H., Garten, W. 1994. Activation cleavage of viral spike proteins by host proteases. Cellular Receptors for Animal Viruses Cold Spring Harbor Press:241–80.

33. Lai, M., Holmes, K. 2001. Coronaviridae: the viruses and their replication. In: Knipe, D.M., Howely, P.M. (Eds.), Fields Virology Lippincott Wilkins and Williams.

34. Li, B., Ge, J., Li, Y. 2007 Porcine aminopeptidase N is a functional receptor for the PEDV coronavirus. Virology 365:166-72.

35. Li, W., Moore, M., Vasilieva, N., Sui, J., Wong, S., Berne, M., Somasundaran, M., Sullivan, J., Luzuriaga, K., Greenough, T., Choe, H., Farzan, M. 2003

Angiotensin-converting enzyme 2 is a functional receptor for the SARS coronavirus. Nature 426:450-4.

36. Lin, C., Su, B., Wang, C., Hsieh, M., Chueh, T., Chueh, L. 2009 Genetic diversity and correlation with feline infectious peritonitis of feline coronavirus type I and II: a 5-year study in Taiwan. Vet Microbiol 136:233-9.

37. Lorusso, A., Decaro, N., Schellen, P., Rottier, P., Buonavoglia, C., Haijema, B., de Groot, R. 2008. Gain, preservation, and loss of a group 1a coronavirus accessory glycoprotein. J Virol 82:10312-7.

38. Lutgens, S., Cleutjens, K., Daemen, M., Heeneman, S. 2007. Cathepsin cysteine proteases in cardiovascular disease. FASEB J 12:3029-41.

39. Madu, I., Chu, V., Lee, H., Regan, A., Bauman, B., Whittaker, G. 2007 Heparan sulfate is a selective attachment factor for the avian coronavirus infectious bronchitis virus Beaudette. Avian Dis 51:45-51.

40. Marzi, A., Gramberg, T., Simmons, G., Möller, P., Rennekamp, A., Krumbiegel, M., Geier, M., Eisemann, J., Turza, N., Saunier, B., Steinkasserer, A., Becker, S., Bates, P., Hofmann, H., Pöhlmann, S. 2004 DC-SIGN and DC-SIGNR interact with the glycoprotein of Marburg virus and the S protein of severe acute respiratory syndrome coronavirus. J Virol 78:12090-5.

41. Matsuyama, S., Ujike, M., Morikawa, S., Tashiro, M., Taguchi, F. 2005 Protease-mediated enhancement of severe acute respiratory syndrome coronavirus infection. Proc Natl Acad Sci U S A 102:12543-7.

42. Montali, R., Strandberg, J. 1972. Extraperitoneal lesions in feline infectious peritonitis. Vet Pathol 9.

43. Motokawa, K., Hohdatsu, T., Hashimoto, H., Koyama, H. 1996. Comparison of the amino acid sequence and phylogenetic analysis of the peplomer, integral

membrane and nucleocapsid proteins of feline, canine and porcine coronaviruses. Microbiol Immunol 40:425-33.

44. Narayanan, K., Kim, K., Makino, S. 2003 Characterization of N protein self-association in coronavirus ribonucleoprotein complexes. Virus Res 98:131-40.

45. Narayanan, K., Makino, S. 2001 Cooperation of an RNA packaging signal and a viral envelope protein in coronavirus RNA packaging. J Virol 75:9059-67.

46. Nash, T., Buchmeier, M. 1997 Entry of mouse hepatitis virus into cells by endosomal and nonendosomal pathways. Virology 233:1-8.

47. Olsen, C. 1993. A review of feline infectious peritonitis virus: molecular biology, immunopathogenesis, clinical aspects, and vaccination. Vet Microbiol 36:1-37.

48. Olsen, C., Corapi, W., Ngichabe, C., Baines, J., Scott, F. 1992 Monoclonal antibodies to the spike protein of feline infectious peritonitis virus mediate antibody-dependent enhancement of infection of feline macrophages. J Virol 66:956-65.

49. Opstelten, D., Raamsman, M., Wolfs, K., Horzinek, M., Rottier, P. 1995 Envelope glycoprotein interactions in coronavirus assembly. J Cell Biol 131:339-49.

50. Pager, C., Dutch, R. 2005 Cathepsin L is involved in proteolytic processing of the Hendra virus fusion protein. J Virol 79:12714-20.

51. Pedersen, N. 1976. Feline infectious peritonitis: Something old, something new. Feline Pract 6:42-51.

52. Pedersen, N., Allen, C., Lyons, L. 2008 Pathogenesis of feline enteric coronavirus infection. J Feline Med Surg 10:529-41.

53. Pedersen, N., Black, J., Boyle, J., Evermann, J., McKeirnan, A., Ott, R. 1984. Pathogenic differences between various feline coronavirus isolates. Adv Exp Med Biol 173:365-80.

54. Pedersen, N. C. 2009. A review of feline infectious peritonitis virus infection: 1963-2008. J Feline Med Surg 11:225-58.

55. Perlman, S. 1998. Pathogenesis of coronavirus-induced infections. Adv Exp Med Biol 440:503-13.

56. Perlman, S., Dandekar, A. 2005 Immunopathogenesis of coronavirus infections: implications for SARS. Nat Rev Immunol 12:917-27.

57. Pratelli, A., Martella, V., Decaro, N., Tinelli, A., Camero, M., Cirone, F., Elia, G., Cavalli, A., Corrente, M., Greco, G., Buonavoglia, D., Gentile, M., Tempesta, M., Buonavoglia, C. 2003 Genetic diversity of a canine coronavirus detected in pups with diarrhoea in Italy. J Virol Methods 110:9-17.

58. Qiu, Z., Hingley, S., Simmons, G., Yu, C., Das Sarma, J., Bates, P., Weiss, S. 2006. Endosomal proteolysis by cathepsins is necessary for murine coronavirus mouse hepatitis virus type 2 spike-mediated entry. J Virol 80:5768-76.

59. Rautajoki, K., Kylaniemi, M., Raghav, S., Rao, K., Lahesmaa, R. 2008. An insight into molecular mechanisms of human T helper cell differentiation. Ann Med 40:322-35.

60. Regan, A. 2009. Unpublished results.

61. Regan, A., Shraybman, R., Cohen, R., Whittaker, G. 2008 Differential role for low pH and cathepsin-mediated cleavage of the viral spike protein during entry of serotype II feline coronaviruses. Vet Microbiol 132:235-48.

62. Rottier, P. 1999 The molecular dynamics of feline coronaviruses. Vet Microbiol 69:117-25.

63. Rottier, P., Nakamura, K., Schellen, P., Volders, H., Haijema, B. 2005 Acquisition of macrophage tropism during the pathogenesis of feline infectious peritonitis is determined by mutations in the feline coronavirus spike protein. J Virol 79:14122-30.

64. Schultze, B., Herrler, G. 1993. Recognition of N-acetyl-9-O-acetylneuraminic acid by bovine coronavirus and hemagglutinating encephalomyelitis virus. Adv Exp Med Biol 342:299-304.

65. Sieczkarski, S., Whittaker, G. 2005. Viral entry. Curr Top Microbiol Immunol 285.

66. Siu, Y., Teoh, K., Lo, J., Chan, C., Kien, F., Escriou, N., Tsao, S., Nicholls, J., Altmeyer, R., Peiris, J., Bruzzone, R., Nal, B. 2008. The M, E, and N structural proteins of the severe acute respiratory syndrome coronavirus are required for efficient assembly, trafficking, and release of virus-like particles. J Virol 82:11318-30.

67. Stoddart, C., Scott, F. 1989 Intrinsic resistance of feline peritoneal macrophages to coronavirus infection correlates with in vivo virulence. J Virol 63:436-40.

68. Takano, T., Hohdatsu, T., Toda, A., Tanabe, M., Koyama, H. 2007 TNF-alpha, produced by feline infectious peritonitis virus (FIPV)-infected macrophages, upregulates expression of type II FIPV receptor feline aminopeptidase N in feline macrophages. Virology 364:64-72.

69. Takano, T., Kawakami, C., Yamada, S., Satoh, R., Hohdatsu, T. 2008 Antibody-dependent enhancement occurs upon re-infection with the identical serotype virus in feline infectious peritonitis virus infection. J Vet Med Sci 70:1315-21.

70. Tresnan, D., Holme,s K. 1998. Feline aminopeptidase N is a receptor for all group I coronaviruses. Adv Exp Med Biol 440:69-75.

71. Tresnan, D., Levis, R., Holmes, K. 1996 Feline aminopeptidase N serves as a receptor for feline, canine, porcine, and human coronaviruses in serogroup I. J Virol 70:8669-74.

72. Vasiljeva, O., Reinheckel, T., Peters, C., Turk, D., Turk, V., Turk, B. 2007. Emerging roles of cysteine cathepsins in disease and their potential as drug targets. Curr Pharm Des 13:387-403.

73. Vennema, H., Poland, A., Foley, J., Pedersen, N. 1998 Feline infectious peritonitis viruses arise by mutation from endemic feline enteric coronaviruses. Virology 243:150-7.

74. Vlasak, R., Luytjes, W., Spaan, W., Palese, P. 1988 Human and bovine coronaviruses recognize sialic acid-containing receptors similar to those of influenza C viruses. Proc Natl Acad Sci U S A 85:4526-9.

75. Ward, J. 1970. Morphogenesis of a virus in cats with experimental feline infectious peritonitis. Virology 41.

76. Watanabe, R., Matsuyama, S., Shirato, K., Maejima, M., Fukushi, S., Morikawa, S., Taguchi, F. 2008. Entry from the cell surface of severe acute respiratory syndrome coronavirus with cleaved S protein as revealed by pseudotype virus bearing cleaved S protein. J Virol 82:11985-91.

77. Winter, C., Schwegmann-Wessels, C., Cavanagh, D., Neumann, U., Herrler, G. 2006 Sialic acid is a receptor determinant for infection of cells by avian Infectious bronchitis virus. J Gen Virol 87:1209-16.

78. Wolf, A. 1997. Feline infectious peritonitis, part 2. Feline Pract 25:24-8.

79. Yamada, Y., Liu, D. 2009 Proteolytic activation of the spike protein at a novel RRRR/S motif is implicated in furin-dependent entry, syncytia formation and

infectivity of coronavirus infectious bronchitis virus in cultured cells. J Virol Epub ahead of print.

80. Yeager, C., Ashmun, R., Williams, R., Cardellichio, C., Shapiro, L., Look, A., Holmes, K. 1992 Human aminopeptidase N is a receptor for human coronavirus 229E. Nature 357:420-2.

81. Zook, B., King, N., Robinson, R., McCombs, H. 1968. Ultrastructural evidence for the viral etiology of feline infectious peritonitis. Pathol Vet 5:91-5.

CHAPTER TWO

UTILIZATION OF DC-SIGN FOR ENTRY OF FELINE CORONAVIRUSES INTO HOST CELLS*

*** A.D. Regan and G.R. Whittaker**. 2008. Utilization of DC-SIGN for Entry of Feline Coronaviruses into Host Cells. Journal of Virology. 82(23): 11992–11996.

2.1 Summary

The entry and dissemination of viruses in several families can be mediated by C-type lectins such as DC-SIGN. We showed that entry of the serotype II feline coronavirus strains feline infectious peritonitis virus (FIPV) WSU 79-1146 and DF2 into nonpermissive mouse 3T3 cells can be rescued by the expression of human DC-SIGN (hDC-SIGN) and that infection of a permissive feline cell line (Crandall-Reese feline kidney) was markedly enhanced by the overexpression of hDC-SIGN. Treatment with mannan considerably reduced infection of feline monocyte-derived cells expressing DC-SIGN, indicating a role for FIPV infection in vivo.

2.2 Introduction

The entry of coronaviruses (CoVs) is mediated by a primary receptor, which in many cases has been well characterized (29). Aminopeptidase N (APN, or CD13) acts as a primary receptor for the entry of serotype II feline coronaviruses (FCoVs) in both feline infectious peritonitis virus (FIPV) and feline enteric coronavirus (FECV) biotypes (10, 29), as well as in transmissible gastroenteritis virus and human CoV strain 229E (HCoV-229E) (27). In addition to having a primary receptor, it is becoming increasingly clear that coronaviruses also make use of a variety of nonspecific receptors during entry, including sialic acid and C-type lectins (29). Notably, severe acute respiratory syndrome CoV was shown to utilize liver/lymph nonspecific ICAM-3-grabbing nonintegrin (L-SIGN/CD209L) as a receptor in *cis* (11, 17), possibly in combination with a specific receptor, ACE2. Severe acute respiratory syndrome CoV also interacts with dendritic cell (DC)-specific ICAM-3- grabbing nonintegrin (DC-SIGN/CD209) in *cis* (11), as well as with DC-SIGN and/or L-SIGN in *trans* (19, 30). L-SIGN and DC-SIGN have also been shown to promote the entry of HCoV-229E and HCoV-NL63, respectively (12, 16).

The utilization of C-type lectins as entry factors was first demonstrated for human immunodeficiency virus type 1 (1, 9), and it is now known that viruses in various families use DC-SIGN and/or L-SIGN for entry and dissemination, acting either in *cis* or in *trans* (3, 18). C-type lectins act as entry factors by preferentially recognizing viral glycoproteins containing high-mannose carbohydrate residues (3, 7). Compared to that in the human system, the use of C-type lectins as entry factors in nonhuman animal viruses has received little attention. A notable exception is the demonstration that feline immunodeficiency virus can specifically interact with human DC-SIGN and allow virus transmission to target cells in *cis* and in *trans* (6). Based on this finding and the established role of L-SIGN/DC-SIGN for certain coronaviruses, we reasoned that FCoVs might be able to utilize C-type lectins as entry cofactors, with human DC-SIGN (hDC-SIGN) able to serve in this role.

2.3 Results and Discussion

To examine the possible role of hDC-SIGN in FIPV infection, we first analyzed the infection of mouse 3T3 cell lines stably expressing hDC-SIGN (NIAID AIDS Research and Reference Reagent Program) and compared it to that of nonpermissive wild-type 3T3 cells and permissive Crandall-Reese feline kidney (CRFK) cells (ATCC). Cells were infected with either serotype II FIPV strain WSU 79-1146 (FIPV-1146) or FIPV-DF2 at a final concentration of 1 X 10^6 PFU/ml (multiplicity of infection (MOI) = 10 infectious units/cell), as determined by standard plaque assay of CRFK cells. The supernatants were collected, and the production of virus was determined at 24 h postinfection by 50% tissue culture infective dose assay of CRFK cells (Figure 2.1 A). As expected, 3T3 cells were not able to support FIPV infection; however, 3T3-hDCSIGN cells propagated the virus to a relatively high titer. The production of virus was approximately 2 log units lower than in permissive CRFK

cells. To confirm that productive infection was mediated specifically by the expression of hDC-SIGN, we transfected wild-type 3T3 cells with plasmid pcDNA3-DCSIGN (NIAID AIDS Research and Reference Reagent Program) to transiently express hDC-SIGN. At twenty-four hours posttransfection, cells were infected with FIPV-1146 or FIPV-DF2 at a final concentration of 1 X 10^6 PFU/ml, and at 9 h postinfection, the cells were fixed. Cells were analyzed by immunofluorescence microscopy, using the anti-DC-SIGN monoclonal antibody (MAb) 120526 (an immunoglobulin G2a [IgG2a] isotype; NIAID AIDS Research and Reference Reagent Program) and the anti-FCoV nucleocapsid MAb 17B7.1 (an IgG2b isotype) (21) followed by isotype-specific secondary antibodies conjugated to Alexa Fluor 488 or Alexa Fluor 569 (Invitrogen). Infection of 3T3 cells by either FIPV-1146 or FIPV-DF2 strictly correlated with hDC-SIGN expression (Figure 2.1 B).

To examine how DC-SIGN might function in the context of FIPV infection of permissive cells, we created CRFK cells lines stably expressing hDC-SIGN. CRFK or CRFK-hDCSIGN cells were infected with FIPV-1146 and FIPV-DF2 at a low MOI of 0.01 infectious units/cell (1 X 10^3 PFU/ml). Cells were fixed at 6 h postinfection and analyzed by immunofluorescence microscopy after being stained with the IgG2a anti-hDC-SIGN MAb 120526 and the IgG2b anti-FCoV nucleocapsid MAb 17B7.1. Infection of CRFK cells was markedly increased in CRFK-hDCSIGN cells (Figure 2.2 A). To quantify the increase in infection following hDC-SIGN expression, the experiments were repeated with inocula of various amounts of FIPV (0.0005 to 1.0 infectious units/cell), and images from at least three independent experiments (~1,000 cells) were scored for infection. As shown in figure 2.2 B, the expression of hDC-SIGN significantly enhanced infection of FIPV over a range of MOI values but with more-limited effects at the lowest and highest infectious doses.

To confirm that the enhancement of FIPV infection following DC-SIGN expression was specific, we infected CRFK or CRFK-DCSIGN cells with FIPV-1146 and FIPV-DF2 at an MOI of 0.01 infectious unit/cell (1 X 10^3 PFU/ml) in the presence of mannan (50 mg/ml) as a competitor of DC-SIGN binding or in the presence of the anti-DC-SIGN MAbs 9E9A8 and 120526 (20 mg/ml; NIAID AIDS Research and Reference Reagent Program) (Figure 2.3). Both mannan and the two MAbs tested reduced FIPV infection to the control levels found in the absence of hDC-SIGN expression.

Dissemination of FIPV in the cat relies on the ability of the virus to infect monocytes and macrophages (10). To examine the role of DC-SIGN in such in vivo situations, we isolated primary feline monocytes (23) and cultured them for 4 days in the presence of 20% fetal bovine serum. These cells were specifically recognized by the hDC-SIGN MAb DC6 (NIAID AIDS Research and Reference Reagent Program) indicating that they had undergone differentiation and were expressing DC-SIGN. We then treated these cells with either the MAb R-G-4 (200 mg/ml) to inhibit infection via the feline aminopeptidase N (fAPN) receptor (14) or with mannan (50 mg/ml). Monocytes were then infected with FIPV strains 1146 and DF2 at 1 X 10^6 PFU/ml (MOI = 10 infectious units/cell). Cells were fixed at 6 h postinfection and analyzed by immunofluorescence microscopy as described above. Compared to the untreated controls, both cells treated with R-G-4 and those treated with mannan showed a significant inhibition of FIPV infection, in both cases to around 15% of the level for the untreated cells (Figure 2.4). The addition of R-G-4 and mannan combined resulted in an almost complete blockage of FIPV infection (Figure 2.4). These data confirm previous reports that the blockage of fAPN with R-G-4 alone could not completely inhibit the infection of feline macrophages with serotype II FIPV (24) and suggest that both APN and DC-SIGN are important for infection in vivo.

Our studies show that the C-type lectin hDC-SIGN can rescue FIPV infection of nonpermissive cells and enhance infection of permissive cells, acting in *cis*. To date, we have not examined the use of hDC-SIGN in *trans* for FIPV infection in vivo. As the feline homolog of hDC-SIGN has not yet been cloned (6), the role of FCoV-DC-SIGN interactions in cats remains to be demonstrated, and we have not examined serotype I FCoVs due to the difficulty in propagating these viruses in the laboratory. In our studies, we also examined human L-SIGN, which was able to rescue infection with FIPV-1146. However, as L-SIGN is as yet unreported except in humans, this was not examined further.

It is interesting to note that both APN and DC-SIGN are localized to cell surface microdomains, or lipid rafts (2, 20), and that this localization is important for the function of DCSIGN during virus entry (2). This suggests that the colocalization of the two cell surface molecules may be a factor in successful FCoV entry into host cells. At present, however, little is known regarding the internalization pathway of FCoVs, although HCoV-299E (which uses a combination of APN and L-SIGN for entry) is believed to enter cells via cell surface microdomains that contain caveolin (20). Other likely factors in the successful use of DC-SIGN as an entry factor for coronaviruses are that viral spike proteins are heavily glycosylated and that the virus buds from the endoplasmic reticulum-Golgi intermediate compartment (13); the coronavirus spike protein is therefore likely to contain high-mannose sugars that would be a recognition site for C-type lectins (3, 4, 7).

The majority of natural infections with FCoVs are classified as being in the FECV biotype and cause, at most, mild enteritis in the intestinal epithelial tract. It is believed that mutations within FECV viruses allow the dissemination and systemic spread of the newly generated FIPV biotype viruses, and monocytes and macrophages are well established as cell types that act as a conduit for such systemic

spread (10). DC-SIGN is considered to be widely expressed in monocyte-derived macrophages which are thought to be the targets of FIPV infection in vivo (10), so in the course of our studies, we examined whether there were any differences in the utilization of DCSIGN by FIPV-1146 and the FECV biotype WSU 79-1638. However, we found no significant difference in the effects of hDC-SIGN expression between these two viruses, which suggests that any change in cell tropism between these viruses appears to occur at a post-receptor step of infection. At present, there is only limited information on the possible role of DCs in the dissemination of FIPV. With increased characterization of feline DCs (8, 25), it will be very interesting to explore these cells in the context of FIPV infection in cats.

Although murine APN is not considered to support FIPV infection by itself (28), it remains possible that the entry of serotype II FCoV is mediated through a combination of DCSIGN and mouse APN. In this scenario, DC-SIGN would act as an entry cofactor, allowing for the use of mouse APN as a viral receptor. Alternatively, DC-SIGN may act an alternate receptor for FCoV rather than acting as an accessory factor. Such APN-independent entry of FIPV has been known for some time, based on Fc-mediated uptake of the virus into mouse macrophages in the presence of anti-S antibodies (5, 15, 22, 26). To address these possible models, hDC-SIGN was overexpressed in primary fibroblast cells from an APN knockout mouse and from a parental wild-type mouse (kindly provided by Renata Pasqualini and Wadih Arap, Anderson Cancer Center, Houston, TX). While overexpression of hDC-SIGN in wild-type murine fibroblasts rescued infection by FIPV, it did not allow infection in APN knockout cells (data not shown), suggesting that DC-SIGN does not act as an alternate receptor for FIPV but rather acts as an entry cofactor. However, it cannot be ruled out that DC-SIGN may act as an independent FCoV receptor under certain conditions.

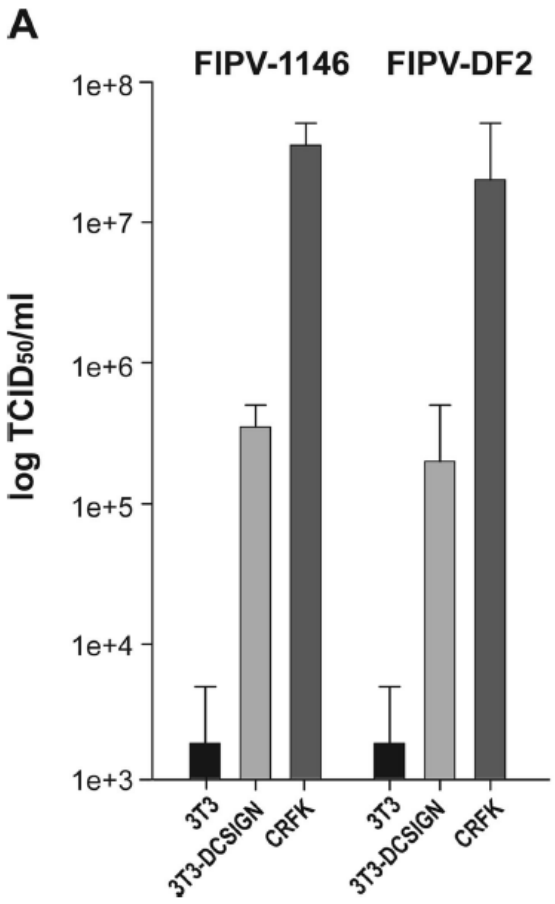

Figure 2.1 Expression of hDC-SIGN rescues FCoV infection of nonpermissive cells. (A) 3T3, 3T3-DCSIGN, or CRFK cells were infected with FIPV-1146 or FIPV-DF2 at a MOI of 10. Cells were rinsed and placed in fresh media after 2 h. At 24 h, cells and the supernatants were collected. The production of virus was determined from at least three independent replicates of the experiment by 50% tissue culture infective dose ($TCID_{50}$) assay. Error bars represent the standard deviations of the means. (B) 3T3 cells were transfected with pCDNA3-hDCSIGN. Twenty-four hours posttransfection, cells were infected with virus at a MOI of 10. Cells were fixed 9 h postinfection and stained for immunofluorescence microscopy with the IgG2a anti-hDC-SIGN MAb 120526 and the IgG2b anti-FCoV nucleocapsid (anti-FIPV N) MAb 17B7.1.

Figure 2.1 (continued)

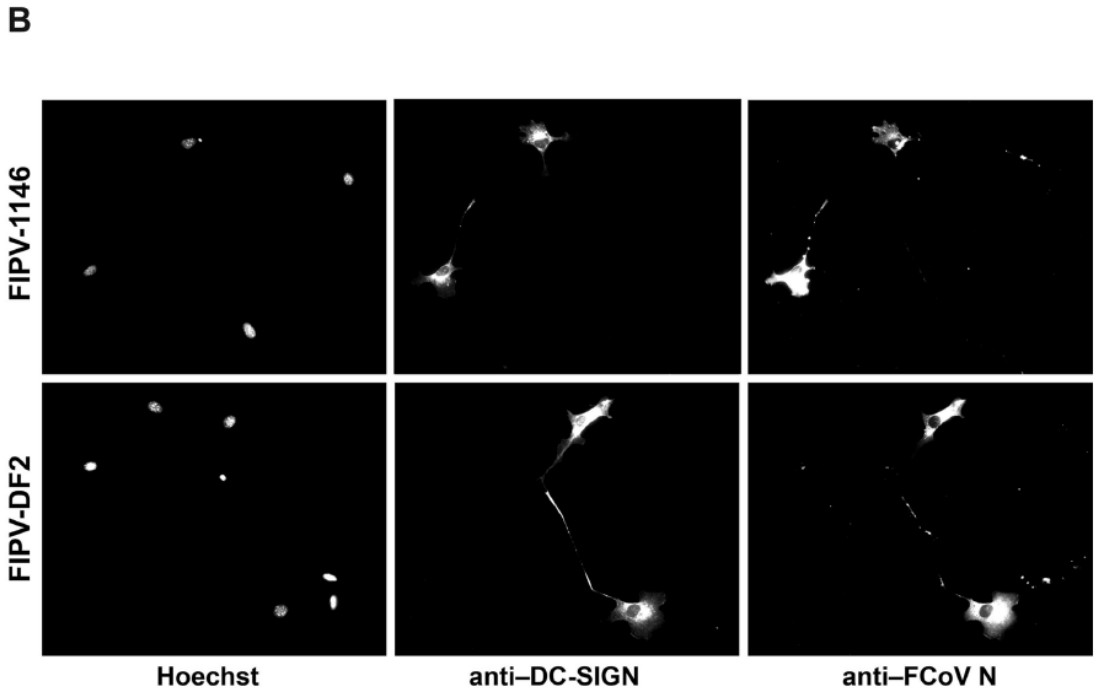

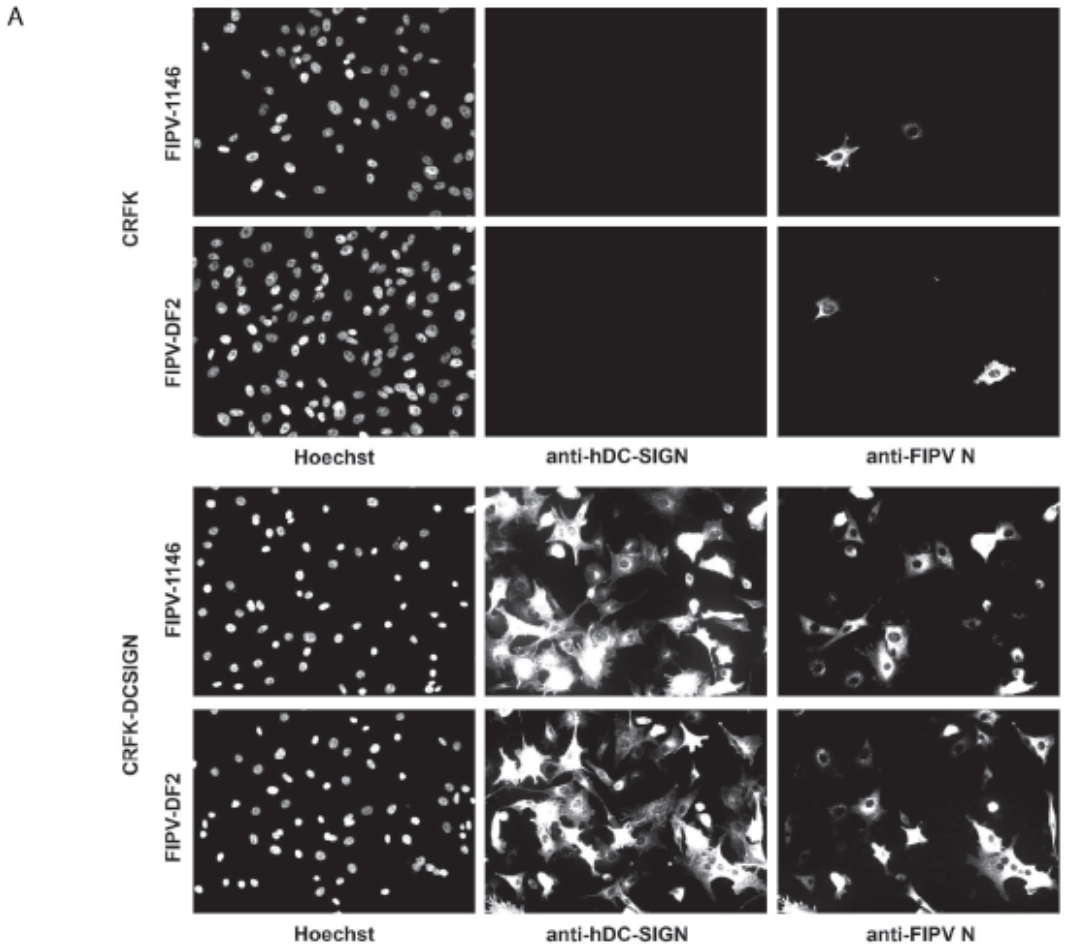

Figure 2.2 Expression of hDC-SIGN enhances FCoV infection of permissive cells. (A) CRFK or CRFK-hDCSIGN cells were infected with FIPV-1146 or FIPV-DF2 at a MOI of 0.01. Six hours postinfection, cells were fixed and stained for immunofluorescence microscopy with the IgG2a anti-hDC-SIGN MAb 120526 and the IgG2b anti-FCoV nucleocapsid (anti-FIPV N) MAb 17B7.1. (B) CRFK or CRFK-hDCSIGN cells were infected with FIPV-1146 or FIPV-DF2 at the indicated concentrations. Six hours postinfection, cells were fixed and stained for immunofluorescence microscopy with the anti-FCoV nucleocapsid MAb 17B7.1. Images from at least three independent experiments were captured and quantified. For quantification, ~1,000 cells from three independent replicates of each experimental condition were scored. Error bars represent the standard deviations of the means.

Figure 2.2 (continued)

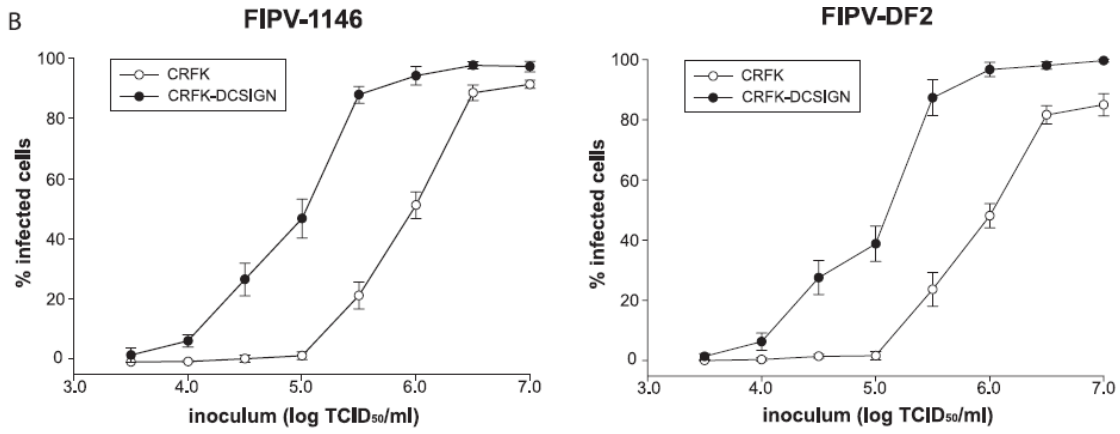

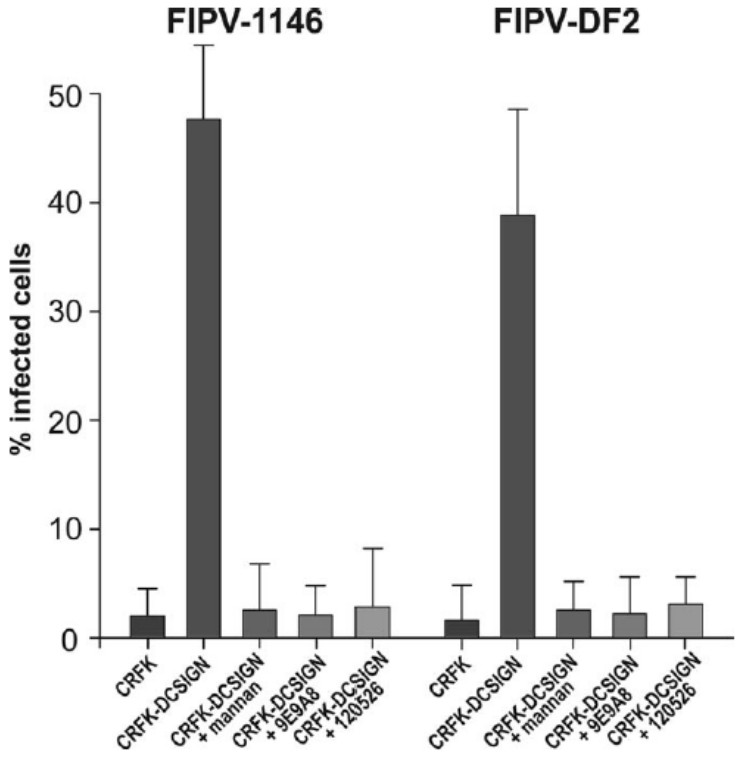

Figure 2.3 Mannan and anti-hDC-SIGN MAbs block the enhancement of infection by FCoVs. CRFK, CRFK-hDCSIGN, or CRFK-hDCSIGN cells pretreated with either mannan (50 μg/ml), anti-hDC-SIGN MAb 9E9A8 (20 μg/ml), or anti-hDC-SIGN MAb 120526 (20 μg/ml) were infected with FIPV-1146 or FIPV-DF2 at a MOI of 0.01. Cells were fixed at 6 h postinfection and stained for immunofluorescence microscopy with the anti-FCoV nucleocapsid MAb 17B7.1. Images from at least three independent experiments were captured and quantified. For quantification, ~1,000 cells from three independent replicates of each experimental condition were scored. Error bars represent the standard deviations of the means.

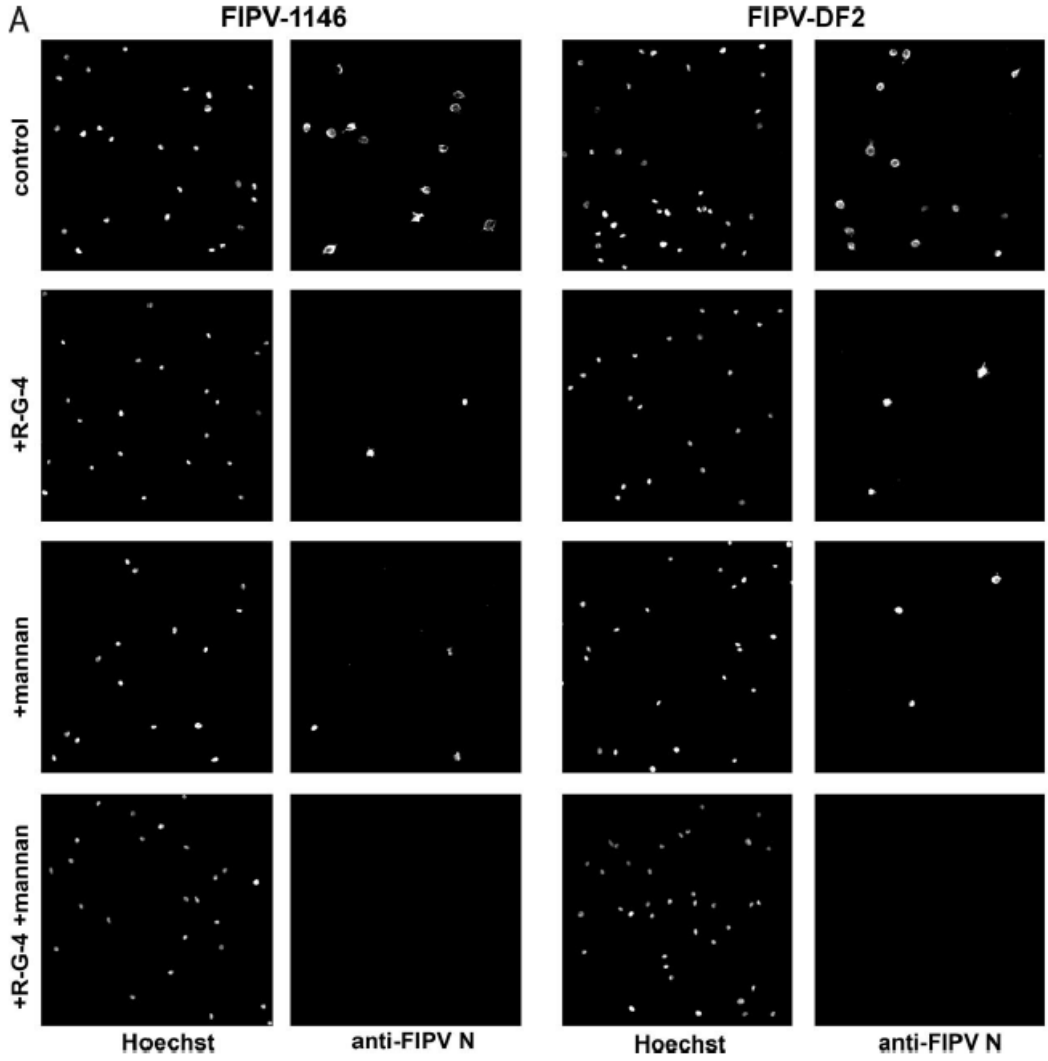

Figure 2.4 Mannan inhibits FCoV infection of primary feline monocyte-derived cells expressing DC-SIGN. (A) Primary feline cells expressing DC-SIGN were pretreated with mannan (50 μg/ml), anti-fAPN MAb R-G-4 (200 μg/ml), or both in combination for 60 min before being infected with FIPV-1146 or FIPV-DF2 at a MOI of 10. Cells were fixed 12 h postinfection and stained for immunofluorescence microscopy with the anti-FCoV nucleocapsid (anti-FCoV N) MAb 17B7.1. (B) Images from at least three independent experiments were captured and quantified. For quantification, ~250 cells from three independent replicates of each experimental condition were scored. Error bars represent the standard deviations of the means.

Figure 2.4. (continued)

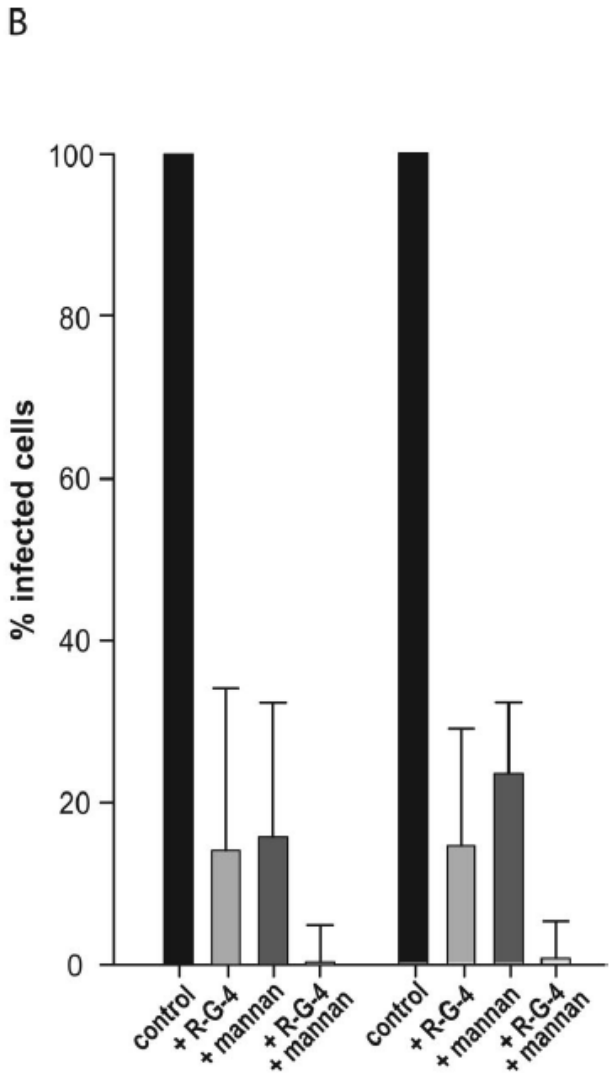

2.4. Acknowledgements

We thank Fred Scott, Joel Baines, and Sandrine Belouzard for helpful advice and discussions during the course of this work and Ed Dubovi for kind provision of reagents. We also thank A. Damon Ferguson for technical assistance and Renata Pasqualini and Wadih Arap for provision of cells from APN-null mice. This work was supported in part by a research grant (to G.R.W.) from the Winn Feline Foundation. A.D.R. was supported by grant T32AI007618 (Training in Molecular Virology and Pathogenesis) from the National Institutes of Health.

REFERENCES

1. Baribaud, F., S. Pohlmann, and R. W. Doms. 2001. The role of DC-SIGN and DC-SIGNR in HIV and SIV attachment, infection, and transmission. Virology 286:1 6.
2. Cambi, A., F. de Lange, N. M. van Maarseveen, M. Nijhuis, B. Joosten, E. M. van Dijk, B. I. de Bakker, J. A. Fransen, P. H. Bovee-Geurts, F. N. van Leeuwen, N. F. Van Hulst, and C. G. Figdor. 2004. Microdomains of the C-type lectin DC-SIGN are portals for virus entry into dendritic cells. J. Cell Biol. 164:145–155.
3. Cambi, A., M. Koopman, and C. G. Figdor. 2005. How C-type lectins detect pathogens. Cell Microbiol. 7:481–488.
4. Cavanagh, D. 1983. Coronavirus IBV glycopolypeptides: size of their polypeptide moieties and nature of their oligosaccharides. J. Gen. Virol. 64:1187–1191.
5. Corapi, W. V., R. J. Darteil, J. C. Audonnet, and G. E. Chappuis. 1995. Localization of antigenic sites of the S glycoprotein of feline infectious peritonitis virus involved in neutralization and antibody-dependent enhancement. J. Virol. 69:2858–2862.
6. de Parseval, A., S. V. Su, J. H. Elder, and B. Lee. 2004. Specific interaction of feline immunodeficiency virus surface glycoprotein with human DCSIGN. J. Virol. 78:2597–2600.
7. Feinberg, H., D. A. Mitchell, K. Drickamer, and W. I. Weis. 2001. Structural basis for selective recognition of oligosaccharides by DC-SIGN and DCSIGNR. Science 294:2163–2166.

8. Freer, G., D. Matteucci, P. Mazzetti, L. Bozzacco, and M. Bendinelli. 2005. Generation of feline dendritic cells derived from peripheral blood monocytes for in vivo use. Clin. Diagn. Lab. Immunol. 12:1202–1208.

9. Geijtenbeek, T. B., D. S. Kwon, R. Torensma, S. J. van Vliet, G. C. van Duijnhoven, J. Middel, I. L. Cornelissen, H. S. Nottet, V. N. KewalRamani, D. R. Littman, C. G. Figdor, and Y. van Kooyk. 2000. DC-SIGN, a dendritic cell-specific HIV-1-binding protein that enhances *trans*-infection of T cells. Cell 100:587–597.

10. Haijema, B. J., P. J. Rottier, and R. J. de Groot. 2007. Feline coronaviruses: a tale of two-faced types, p. 183–203. *In* V. Thiel (ed.), Coronaviruses. Molecular and cellular biology. Caister Academic Press, Norfolk, United Kingdom.

11. Han, D. P., M. Lohani, and M. W. Cho. 2007. Specific asparagine-linked glycosylation sites are critical for DC-SIGN- and L-SIGN-mediated severe acute respiratory syndrome coronavirus entry. J. Virol. 81:12029–12039.

12. Hofmann, H., G. Simmons, A. J. Rennekamp, C. Chaipan, T. Gramberg, E. Heck, M. Geier, A. Wegele, A. Marzi, P. Bates, and S. Pohlmann. 2006. Highly conserved regions within the spike proteins of human coronaviruses 229E and NL63 determine recognition of their respective cellular receptors. J. Virol. 80:8639–8652.

13. Hogue, B. G., and C. E. Machamer. 2008. Coronavirus structural proteins and virus assembly, p. 179–200. *In* S. Perlman, T. Gallagher, and E. J. Snijder (ed.), Nidoviruses. ASM Press, Washington, DC.

14. Hohdatsu, T., Y. Izumiya, Y. Yokoyama, K. Kida, and H. Koyama. 1998. Differences in virus receptor for type I and type II feline infectious peritonitis virus. Arch. Virol. 143:839–850.

15. Hohdatsu, T., J. Tokunaga, and H. Koyama. 1994. The role of IgG subclass of mouse monoclonal antibodies in antibody-dependent enhancement of feline infectious peritonitis virus infection of feline macrophages. Arch. Virol. 139:273–285.

16. Jeffers, S. A., E. M. Hemmila, and K. V. Holmes. 2006. Human coronavirus 229E can use CD209L (L-SIGN) to enter cells. Adv. Exp. Med. Biol. 581: 265–269.

17. Jeffers, S. A., S. M. Tusell, L. Gillim-Ross, E. M. Hemmila, J. E. Achenbach, G. J. Babcock, W. D. Thomas, Jr., L. B. Thackray, M. D. Young, R. J. Mason, D. M. Ambrosino, D. E. Wentworth, J. C. Demartini, and K. V. Holmes. 2004. CD209L (L-SIGN) is a receptor for severe acute respiratory syndrome coronavirus. Proc. Natl. Acad. Sci. USA 101:15748–15753.

18. Lozach, P. Y., L. Burleigh, I. Staropoli, and A. Amara. 2007. The C type lectins DC-SIGN and L-SIGN: receptors for viral glycoproteins. Methods Mol. Biol. 379:51–68.

19. Marzi, A., T. Gramberg, G. Simmons, P. Moller, A. J. Rennekamp, M. Krumbiegel, M. Geier, J. Eisemann, N. Turza, B. Saunier, A. Steinkasserer, S. Becker, P. Bates, H. Hofmann, and S. Pohlmann. 2004. DC-SIGN and DC-SIGNR interact with the glycoprotein of Marburg virus and the S protein of severe acute respiratory syndrome coronavirus. J. Virol. 78:12090–12095.

20. Nomura, R., A. Kiyota, E. Suzaki, K. Kataoka, Y. Ohe, K. Miyamoto, T. Senda, and T. Fujimoto. 2004. Human coronavirus 229E binds to CD13 in rafts and enters the cell through caveolae. J. Virol. 78:8701–8708.

21. Olsen, C. W., W. V. Corapi, C. K. Ngichabe, J. D. Baines, and F. W. Scott. 1992. Monoclonal antibodies to the spike protein of feline infectious peritonitis

virus mediate antibody-dependent enhancement of infection of feline macrophages. J. Virol. 66:956–965.

22. Perlman, S., and A. A. Dandekar. 2005. Immunopathogenesis of coronavirus infections: implications for SARS. Nat. Rev. Immunol. 5:917–927.

23. Regan, A. D., R. Shraybman, R. D. Cohen, and G. R. Whittaker. 29 May 2008, posting date. Differential role for low pH and cathepsin-mediated cleavage of the viral spike protein during entry of serotype II feline coronaviruses. Vet. Microbiol.

24. Rottier, P. J., K. Nakamura, P. Schellen, H. Volders, and B. J. Haijema. 2005. Acquisition of macrophage tropism during the pathogenesis of feline infectious peritonitis is determined by mutations in the feline coronavirus spike protein. J. Virol. 79:14122–14130.

25. Sprague, W. S., M. Pope, and E. A. Hoover. 2005. Culture and comparison of feline myeloid dendritic cells vs macrophages. J. Comp. Pathol. 133:136–145.

26. Takano, T., Y. Katada, S. Moritoh, M. Ogasawara, K. Satoh, R. Satoh, M. Tanabe, and T. Hohdatsu. 2008. Analysis of the mechanism of antibody dependent enhancement of feline infectious peritonitis virus infection: aminopeptidase N is not important and a process of acidification of the endosome is necessary. J. Gen. Virol. 89:1025–1029.

27. Tresnan, D. B., R. Levis, and K. V. Holmes. 1996. Feline aminopeptidase N serves as a receptor for feline, canine, porcine, and human coronaviruses in serogroup I. J. Virol. 70:8669–8674.

28. Tusell, S. M., S. A. Schittone, and K. V. Holmes. 2007. Mutational analysis of aminopeptidase N, a receptor for several group 1 coronaviruses, identifies key determinants of viral host range. J. Virol. 81:1261–1273.

29. Wentworth, D. E., and K. V. Holmes. 2007. Coronavirus binding and entry, p. 3–31. *In* V. Thiel (ed.), Coronaviruses. Molecular and cellular biology. Caister Academic Press, Norfolk, United Kingdom.

30. Yang, Z. Y., Y. Huang, L. Ganesh, K. Leung, W. P. Kong, O. Schwartz, K. Subbarao, and G. J. Nabel. 2004. pH-dependent entry of severe acute respiratory syndrome coronavirus is mediated by the spike glycoprotein and enhanced by dendritic cell transfer through DC-SIGN. J. Virol. 78:5642–5650.

CHAPTER THREE

DIFFERENTIAL ROLE FOR LOW PH AND CATHEPSIN-MEDIATED CLEAVAGE OF THE VIRAL SPIKE PROTEIN DURING ENTRY OF SEROTYPE II FELINE CORONAVIRUSES*

*** A.D. Regan, R. Schraybman, R.D. Cohen, G.R. Whittaker**. 2008. Differential role for low pH and cathepsin-mediated cleavage of the viral spike protein during entry of serotype II feline coronaviruses. Veterinary Microbiology. 132(3-4): 235-48.

3.1 Summary

Feline infectious peritonitis (FIP) is a terminal disease of cats caused by systemic infection with a feline coronavirus (FCoV). FCoV biotypes that cause FIP are designated feline infectious peritonitis virus (FIPV), and are distinguished by their ability to infect macrophages and monocytes. Antigenically similar to their virulent counterparts are FCoV biotypes designated feline enteric coronavirus (FECV), which usually cause only mild enteritis and are unable to efficiently infect macrophages and monocytes. The FCoV spike protein mediates viral entry into the host cell and has previously been shown to determine the distinct tropism exhibited by certain isolates of FIPV and FECV, however, the molecular mechanism underlying viral pathogenesis has yet to be determined. Here we show that the FECV strain WSU 79-1683 (FECV 1683) is highly dependent on host cell cathepsin B and cathepsin L activity for entry into the host cell, as well as on the low pH of endocytic compartments. In addition, both cathepsin B and cathepsin L are able to induce a specific cleavage event in the FECV-1683 spike protein. In contrast, host cell entry by the FIPV strains WSU 79 1146 (FIPV-1146) and FIPV-DF2 proceeds independently of cathepsin L activity and low pH, but is still highly dependent on cathepsin B activity. In the case of FIPV-1146 and FIPV-DF2, infection of primary feline monocytes was also dependent on host cell cathepsin B activity, indicating that host cell cathepsins may play a role in the distinct tropisms displayed by different feline coronavirus biotypes.

3.2 Introduction

Coronaviruses are enveloped positive-stranded RNA viruses that replicate in the cytoplasm (31, 43). They have a distinctive set of club-shaped spikes on their envelope, comprised of the viral spike protein (S). The coronavirus S protein is a primary determinant of cell tropism and pathogenesis, being responsible (and

apparently sufficient) for receptor binding and fusion (19). Overall, the coronavirus S protein is categorized as a class I fusion protein (15) based on the presence of characteristic heptad repeats (4, 6, 29); as such it shows characteristic features of fusion proteins of influenza virus (HA), retroviruses (Env) and paramyxoviruses (F) for which there is extensive characterization at a structural and biophysical level (9). Many viral fusion proteins are known to be activated following cleavage by host cell proteases (27). This has been most extensively documented for orthomyxo- and paramyxoviruses. In the case of high pathogenicity avian influenza strains, mutations in the region of the cleavage site that modify it from a trypsin-like (monobasic) to a furin-like (polybasic) cleavage site allow systemic spread within the host and hence show drastically increased virulence (28). Although coronaviruses do show structural similarities to canonical class I fusion proteins, they appear to have significant differences in regard to the role of proteolytic cleavage for fusion activation (3). Coronavirus S proteins consist of two principal domains (S1 and S2), with S1 responsible for receptor binding, and S2 mediating membrane fusion. In group 3 coronaviruses (e.g., infectious bronchitis virus; IBV) there is ubiquitous cleavage of the S precursor protein to form the S1 and S2 subunits (5), with cleavage apparently carried out by furin. In group 2 viruses (e.g., for mouse hepatitis virus; MHV), S1/S2 cleavage is variable (18).The ability to be cleaved at the S1/S2 boundary has been studied quite extensively for MHV-1 and 4 (58). While there is some correlation between S1/S2 cleavage and increased cell–cell fusion, in general there appears to be no direct link between syncytia formation (and by analogy S1/S2 protein cleavage) and pathogenicity (25). For the group 2MHV-2, the S protein remains uncleaved in the virus particle (45). For group 1 viruses (e.g., human coronavirus NL63 and feline coronavirus; FCoV), S1/S2 cleavage is not considered to occur (56), however, recent identification of a group 1 coronavirus with a furin-like motif at S1/S2 (44) suggests

this may not be the case with all group 1 members. Infection of cells by several coronaviruses has been shown to be sensitive to the presence of lysosomotropic agents, such as NH_4Cl, which raise the pH of the endosome (2, 20, 24, 32, 35). These data suggest a pH-dependent route of coronavirus entry through endosomes. In some cases (e.g., IBV and MHV-4), the coronavirus fusion reaction has been clearly shown to be triggered by low pH (8, 17), whereas in other cases, e.g., SARS-CoV, it is suggested that the low pH of the endosome is important for activation of cathepsin proteases that prime the fusion event (49), with fusion activation itself considered to be pH-independent. The classical cathepsins are cysteine proteases typically present within the endosome/lysosome system of host cells (1). While a role for cathepsins during entry of the non-enveloped reoviruses has been known for some time (16, 21), it has recently become apparent that the fusion proteins from several families of enveloped viruses can be cleaved by these proteases. Such examples are the recently identified paramyxoviruses Hendra and Nipah (13, 39, 40), as well as Ebola virus (7, 47, 48) and Moloneymurine leukemia virus (30). In the case of coronaviruses, SARS-CoV and MHV-2 are thought to require cathepsin activation (26, 45, 49, 50), with cathepsin L predominantly involved in SARS-CoV entry, and cathepsin B mediating MHV-2 cleavage during virus entry. For SARS-CoV, neither the site of cathepsin L mediated proteolysis nor the cleaved products produced are known, although for MHV-2 cathepsin B may cleave at the S1/S2 junction (45). Other coronaviruses such as MHV-4, HCoV-NL63 and IBV are not considered to be dependent on cathepsins (8, 26, 45).

Feline infectious peritonitis (FIP) is a highly lethal systemic infection of cats caused by a group I feline coronavirus (FCoV) of the FIPV biotype (23, 36). However, under normal circumstances FCoVs cause only mild and often inapparent enteritis; in this case the virus is classified as the feline enteric coronavirus (FECV)

biotype (11, 23). FCoVs can exist as either serotype I, or less commonly as serotype II, in which case the spike protein share extensive similarity with canine coronavirus (CCoV) and transmissible gastroenteritis virus (TGEV). Due to the relative ease of growth in cell culture, the serotype II FCoVs have been subject to some degree of molecular characterization. In particular, two strains of serotype II FCoV, WSU 79-1683 and WSU 79-1146, have served as model viruses that cause either mild enteritis or FIP, respectively (41, 42). The viruses are thus referred to as FECV-1683 and FIPV-1146. In the ‘‘internal mutation’’ model of FIP it is believed that a process of mutation within an individual cat confers the ability of a FECV to infect macrophages and monocytes, and so allow systemic spread and become a virus that causes FIP (57). Despite extensive study, the genomic differences that determine whether an FCoV will behave as an FECV or an FIPV are still largely unknown (23). However, in the case of the serotype II FCoVs, mapping studies between the FECV-1683 and FIPV-1146 spike proteins have determined critical domains involved in the switch to FIPV. Surprisingly, the S1 domain (receptor binding) domain is not important, and the critical region was mapped to the C-terminal part of the S2 (fusion) domain (46).

In light of the recently determined involvement of cathepsins in activation of other coronavirus S proteins, we reasoned that the FCoV spike protein might be a target of cathepsins during virus entry, which might explain some of the unusual pathogenic properties of FIPV. Here we examined the entry pathway of feline coronaviruses and show a differential role for low pH and spike protein cleavage by cathepsin B and cathepsin L.

3.3 Materials and methods

Cell lines and primary feline monocytes Crandell–Rees feline kidney (CRFK) cells and feline fetal lung cells (AK-D) were obtained from the American Type

Culture Collection (ATCC). A-72 cells were provided by Dr. Colin Parrish (Cornell University, Baker Institute for Animal Health). Fc2Lu cells were provided by Dr. Ed Dubovi (Animal Health Diagnostic Center, New York State College of Veterinary Medicine, Cornell University). Primary feline monocytes were individually purified from the blood of three SPF cats (Liberty Research, Inc., Waverly, NY) using a standard Ficoll-paque gradient (GE Healthcare) as specified by the manufacturer. Monocytes were seeded in 24-well plates and allowed to attach to culture-treated glass coverslips overnight. After washing, the purity of monocyte preparations was checked by immunofluorescence microscopy using the monocyte marker DH59B. CRFK, Fc2Lu, AK-D and A-72 cells were grown in the presence of 5% CO2 at 37 8C in RPMI-1640 media pH 7.4 supplemented with 10% fetal bovine serum (FBS), 2 mM glutamine, 100 U/ml penicillin and 10 mg/ml streptomycin. Monocytes were cultured under the same conditions except the media was supplemented with 20% FBS.

FIPV WSU 79-1146 (FIPV-1146) was obtained from the ATCC. FECV WSU 79-1683 (FECV-1683) and FIPV-DF2 were provided by Dr. Ed Dubovi (Animal Health Diagnostic Center, New York State College of Veterinary Medicine, Cornell University). FIPV-1146 and FECV-1683 were grown in A-72 cells and FIPV-DF2 was grown in CRFK cells, and supernatant collected after CPE was observed in 80% of cells. Supernatant was clarified by a low speed centrifugation step (1250 X g for 10 min) and viral particles were then pelleted by centrifugation at 28,000 rpm in a SW28 rotor (Sorvall) for 60 min. Pellets were resuspended in either phosphate-buffered saline pH 7.4 for infection assays, or acetate buffer pH 5.0 for cathepsin cleavage assays. Virus titers were determined with $TCID_{50}$ assays on CRFK cells, using standard techniques (22). Anti-FCoV nucleocapsid (17B7.1) (37) and spike (22G6.4) monoclonal antibodies were provided by Dr. Ed Dubovi (Animal Health Diagnostic Center, New York State College of Veterinary Medicine, Cornell University). The

monocyte marker antibody (anti-CD127a mAb DH59B) was obtained from Veterinary Medical Research & Development, Inc. (Pullman, WA).

The cysteine protease inhibitor (2S,3S)-trans-epoxysuccinyl-L-leucylamido-3-methylbutane ethyl ester loxistatin (E-64d), the cathepsin B inhibitor [L-3-trans-(propylcarbamoyl)oxirane-2-carbonyl]-L-isoleucyl-L-proline methyl ester (CA074-Me), the cathepsin K inhibitor 1-(N-benzyloxycarbonyl-leucyl)-5-(NBoc-phenylalanyl-leucyl)carbohydrazide (Boc-l) and bafilomycin A1 were purchased Calbiochem (San Diego, CA). The cathepsin L inhibitor Z-Phe-Tyr(t-Bu)-diazomethylketone (Z-FY-(t-Bu)-DMK) was purchased from Axxora (San Diego, CA).

For growth assays, A-72 cells were seeded to 75% confluency on 24-well tissue culture-treated plates. Cells were pre-incubated with specified treatments in serum-free media for 60 min before addition of virus to a final concentration of 10^6 $TCID_{50}$/ml. After 3 h, cells were washed and media replaced with fresh serum-free media. After 9 h, supernatant was collected and frozen at -80ºC until later determination of viral titer by $TCID_{50}$ assay. For infection assays, cells were seeded to 75% confluency on 24-well plates with tissue culture-treated glass coverslips. Cells were treated with inhibitors as specified, either 60 min before, or 60 min after the addition of virus. Virus was added to a final concentration of 10^6 $TCID_{50}$/ml, which infected 20–50% of control cells under the conditions tested. 6 h post-infection, cells were fixed in 3% paraformaldehyde and stained with the anti-FCoV nucleocapsid mAb 17B7.1, essentially as described previously (Chu et al., 2006). Influenza virus and Sendai virus infection assays were performed as previously described (8). All assays were repeated at least three times and 8–15 widefield images were captured and quantified per experimental replicate. Cells were viewed on a Nikon Eclipse E600 fluorescence microscope, and images were captured with a Sensicam EM camera and

IPLab software before transfer into ImageJ software (http:// rsb.info.nih.gov/ij/) for determination of infection frequency.

Concentrated viral particles (10^{12} $TCID_{50}$/ml) were suspended in acetate buffer pH 5.0. 50 ml of virus preparation was incubated with either purified cathepsin L (Calbiochem, San Diego, CA) or purified cathepsin B (Calbiochem, San Diego, CA) at a final concentration of 1 mM for 1 h at 37 8C, followed by the addition of 500 U PNGase F (New England Biolabs, Ipswich, MA) to allow differentiation of any multiply glycosylated species. SDS sample buffer was added and the reaction was heated at 95ºC before separation using a 4–20% SDS-PAGE gel at 200 V for 2 h. Gels were electroblotted to PVDF membrane, blocked with 5% bovine serum albumin and probed with the anti-FCoV spike protein mAb 22G6.4. Membranes were developed using anti-mouse antibody linked to horseradish peroxidase (SouthernBiotech, Birmingham, AL) and ECL substrate (Pierce, Rockford, IL) and images captured using a Fujifilm LAS-3000 CCD camera. Western blot densitometry analysis of spike protein cleavage was performed using ImageJ software. Percent cleavage was determined by dividing pixel intensity of the cleaved spike protein band by total pixel intensity of the cleaved and uncleaved spike protein bands combined.

3.4. Results and Discussion

To determine the role of cysteine proteases in the life cycle of FIPV-1146 and FECV-1683, we first pretreated A-72 cells with the cell-permeable irreversible cysteine protease inhibitor E-64d, which non-selectively inhibits a range of cysteine proteases. Cells were then infected with either FIPV-1146 or FECV-1683. As a control, cells were infected with influenza virus, which is not believed to require proteolytic activation by cysteine proteases during entry. We collected cell supernatants at 9 h post-infection and assayed virus production by $TCID_{50}$ assay. Pre-

treatment with E-64d significantly reduced the production of both FIPV-1146 and FECV-1683 viral particles, as compared to control cells pre-treated with DMSO alone (Figure 3.1). As expected, E-64d had no effect on influenza virus infection. To further investigate the potential roles of cathepsins in the growth of FIPV-1146 and FECV-1683, cells were then pre-treated with specific inhibitors of cathepsin B (CA074-Me), cathepsin L (Z-FY-(t-Bu)-DMK) and cathepsin K (Boc1). As shown figure 3.1, the cathepsin B inhibitor considerably limited the production of both FIPV-1146 and FECV-1683. In contrast, the cathepsin L inhibitor had only a negligible effect on FIPV-1146; however, it greatly diminished the propagation of FECV-1683. Cathepsin K inhibitor had no significant effect on either virus (Figure 3.1). The specific cathepsin inhibitors also had no effect on influenza virus infection. These data indicate that both FIPV-1146 and FECV-1683 require cathepsin B activity for propagation, whereas FECV-1683 selectively requires cathepsin L activity.

To establish if the effects of the cathepsin B and L inhibitors occurred during virus entry, A-72 cells were treated with five log dilutions of inhibitor either 60 min pre-infection, or 60 min post-infection, and infected with FIPV-1146 or FECV-1683. Cells were fixed 6 h post-infection, and infected cells were detected by immunofluorescence microscopy using the anti-FCoV nucleocapsid monoclonal antibody 17B7.1, and quantified (Figure 3.2). Pre-incubation with the specific cathepsin B inhibitor almost completely blocked infection by FIPV-1146, however, treatment after entry had no effect (Figure 3.2). Consistent with data from viral growth assays, the cathepsin L inhibitor had no effect on FIPV-1146 entry, except for some limited effect at the highest concentration tested (Figure 3.2 B). Pre-incubation with either cathepsin B or cathepsin L inhibitor both potently blocked infection by FECV-1683, and again treatment after entry with either inhibitor had no effect. As a control, cells were treated with inhibitors and infected with influenza virus. Infected cells

were fixed 6 h post-infection and detected by immunofluorescence microscopy with the anti-influenza nucleoprotein monoclonal antibody H19 (Figure 3.2). Neither the cathepsin B nor the cathepsin L inhibitor had an effect on influenza virus entry. Pretreatment with the cathepsin K inhibitor had no effect on the cellular entry of either FIPV-1146, FECV-1683 or influenza virus. These data show that the inhibitory effects of the cathepsin inhibitors are manifested during virus entry.

Lysosomotropic agents such as NH_4Cl and bafilomycin A are well established to disrupt the acidic environment of endocytic compartments. To assess the role of low pH during entry of FIPV-1146 and FECV-1683, A-72 cells were pre-treated with either NH_4Cl or bafilomycin A1. We first assessed the effect of NH4Cl, a weak base that acts to neutralize the low pH of the endosome. Pre-treatment with 10 mM NH4Cl only partially inhibited entry of FIPV-1146 (approximately 20% inhibition), however, the same concentration almost completely blocked entry by FECV-1683 (Figure 3.3). Even following pre-treatment with 30 mM NH4Cl, FIPV-1146 entry was only partially blocked as compared to FECV-1683. As controls for these experiments, we used influenza virus and Sendai virus. Influenza virus is well established to require low pH to trigger its fusion mechanism and was completely inhibited by pre-treatment with 10 mM NH_4Cl, analogous to the results obtained with FECV-1683 (Figure 3.3). Sendai virus is known to fuse at a neutral pH and accordingly showed no reduction in entry with cell pre-treated with NH_4Cl (Figure 3.3). We next assessed the effect of bafilomycin A1, an inhibitor of the vacuolar-type H+-ATPase. Pre-treatment of cells with 50 nM bafilomycin A1 completely blocked entry of both FECV-1683 and influenza virus, but only partially blocked entry by FIPV-1146 (approximately 40% inhibition). Sendai virus entry was unaffected by bafilomycin A1 at the concentrations tested. Treatment after entry with both NH_4Cl and bafilomycin A1 had a minimal effect on FIPV-1146 and FECV-1683 at the concentrations shown in Fig. 3, however,

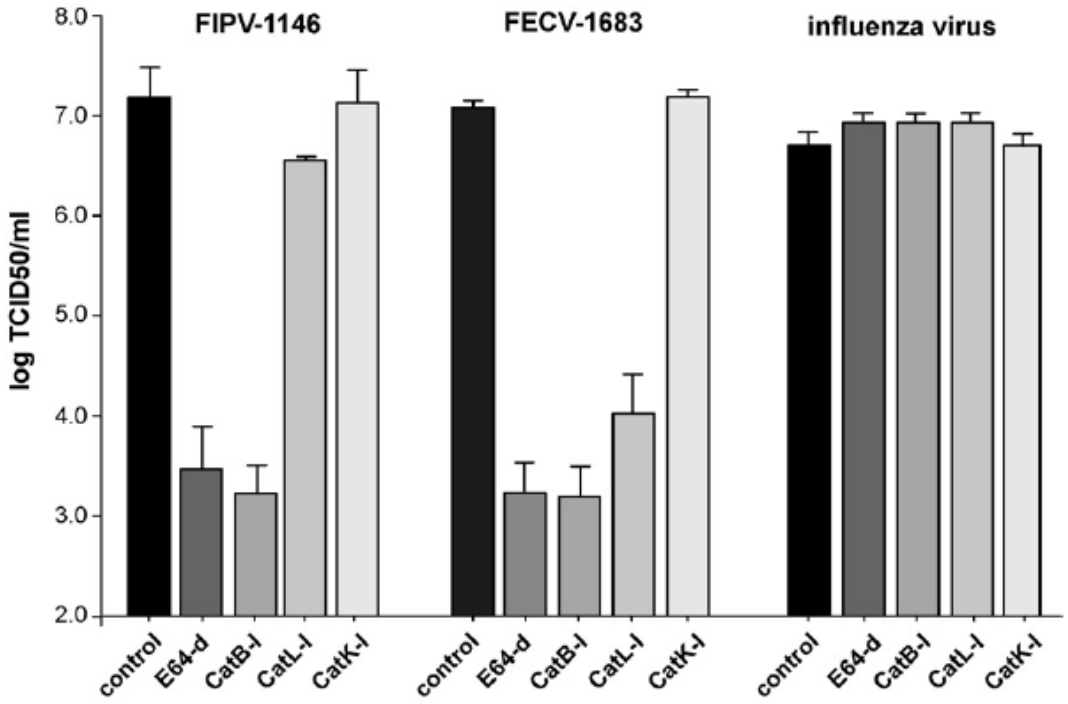

Figure 3.1 The effect of cysteine protease inhibitors on the growth of FIPV-1146 and FECV-1683. A-72 cells were pre-treated with specified inhibitors at a concentration of 10 mM and then infected with virus. 3 h post-infection, fresh media without inhibitor was added to cells and 9 h post-infection media was collected. Production of extracellular virus from at least three independent experiments was determined by $TCID_{50}$ assay. Error bars represent the standard deviation of the mean.

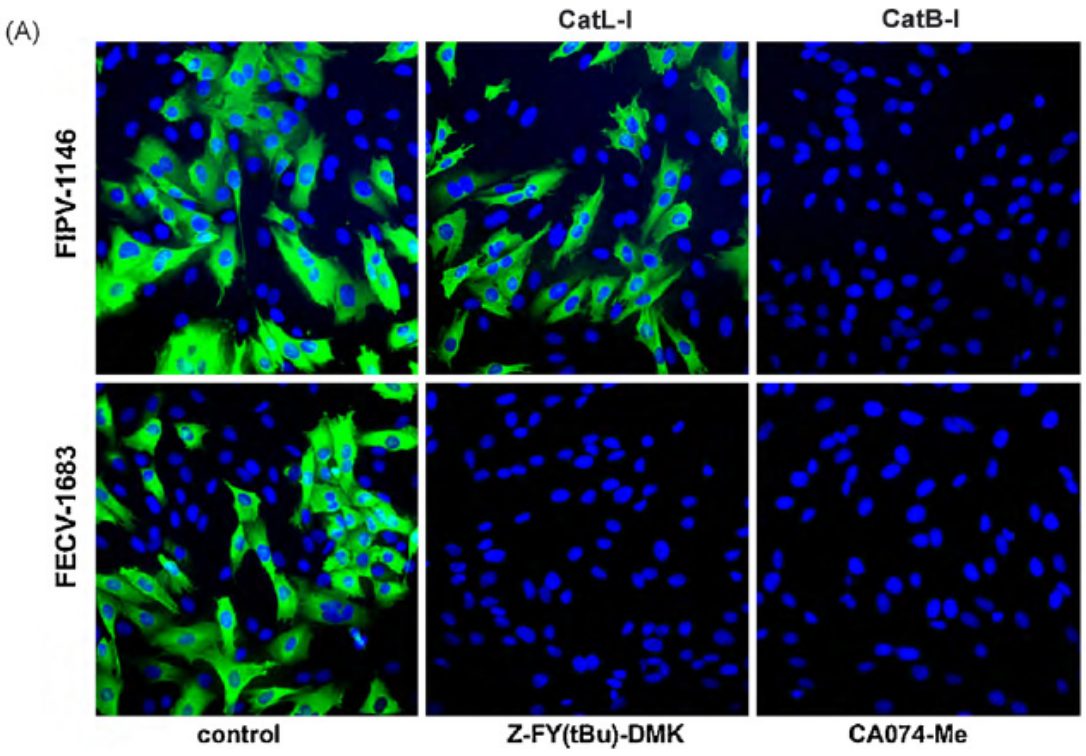

Figure 3.2 The effect of cathepsin L and cathepsin B inhibitors on the entry of FIPV-1146 and FECV-1683. A-72 cells were pre-treated with the cathepsin L inhibitor Z-FY-(t-Bu)-DMK (CatL-I) or the cathepsin B inhibitor CA074-Me (CatB-I) at the concentration specified, and then infected with virus. 6 h post-infection cells were fixed and stained for immunofluorescence microscopy with the anti-FCoV nucleocapsid mAb 17B7.1 (A). Images from at least three independent experiments were processed and quantified (B). To control for non-specific effects on replication, cells were also treated with inhibitors 1 h post-infection. For quantification, >1000 cells were scored from three independent replicates of each experimental condition. Error bars represent the standard deviation of the mean.

Figure 3.2 (continued)

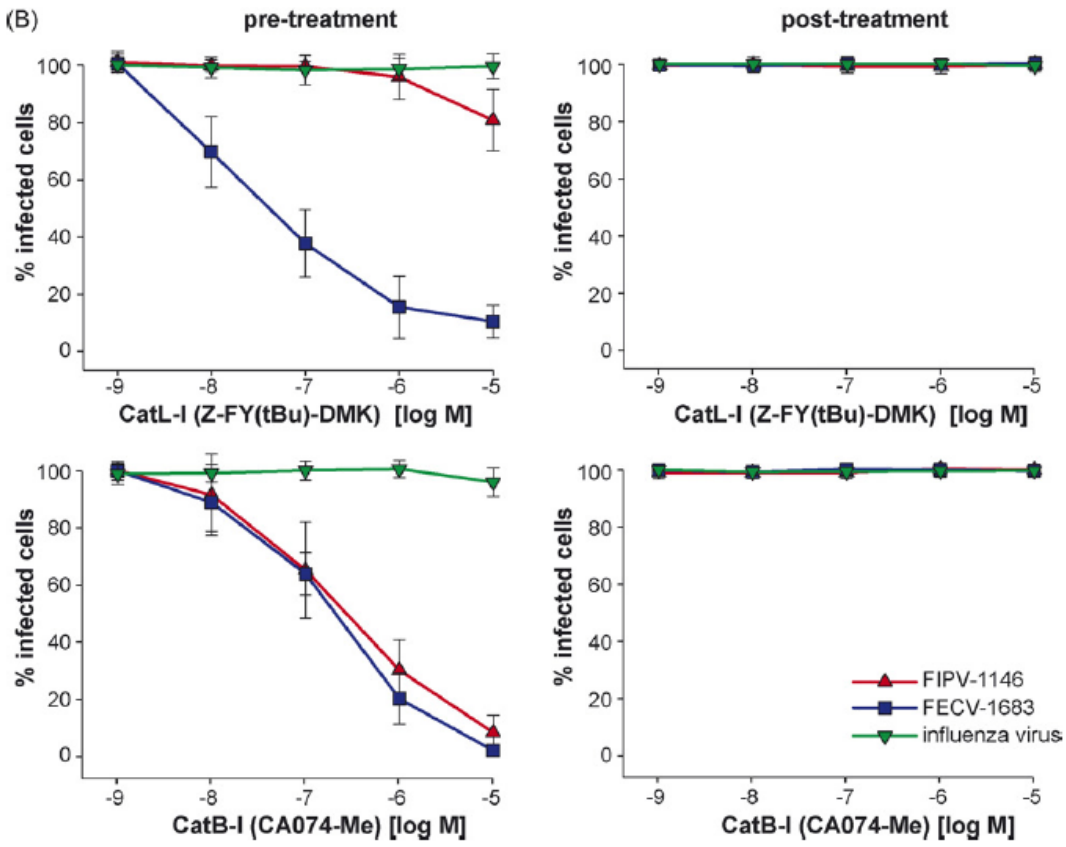

higher concentrations (>100 nM bafilomycin A1 and >30 mM NH_4Cl) were able to significantly reduce infectivity of both viruses. Post-treatment with bafilomycin had no effect on influenza or Sendai virus infection at the concentrations shown in figure 3.3. Overall these data show that FECV-1683 entry is highly dependent on low endosomal pH, whereas FIPV-1146 is much less dependent on low pH during entry.

To determine whether the effects of low pH and cathepsin inhibitors were more generally applicable to serotype II coronavirus infections, we repeated key experiments using an additional feline coronavirus strain (FIPV-DF2), and also tested a variety of established feline cell lines (CRFK, AK-D and Fc2Lu). As shown in figure 3.4, the results were consistent with our previous data (see figures 3.1 and 3.2). The cathepsin B inhibitor CA074-Me almost completely prevented infection of all the feline coronaviruses tested, whereas the cathepsin L inhibitor Z-FY-(t-Bu)-DMK, selectively inhibited FECV-1683, but showed little or no effect on infection by FIPV-1146 or FIPV-DF2. Likewise, the weak base NH_4Cl selectively inhibited FECV-1683 in all the cell lines tested, but showed only a marginal effect on the FIPV biotypes.

To investigate whether the effect of cathepsins B and L occurred at the level of spike protein cleavage, concentrated FIPV-1146 and FECV-1683 viral particles were incubated with purified, activated cathepsin B and cathepsin L for 1 h at 37ºC, and then analyzed by Western blot with the anti-FCoV monoclonal antibody 22G6.4, specific for the S protein. As shown in figure 3.5, cathepsin L was unable to cleave the spike protein of FIPV-1146 under the conditions tested, but was clearly able to cleave the FECV-1683 spike protein, with an obvious cleavage product of approximately 150–160 kDa. In contrast, cathepsin B was able to cleave both FIPV-1146 and FECV-1683 spike proteins, also producing a cleavage product of approximately 150–160 kDa (Figure 3.5). The samples shown in figure 3.5 were treated with the endoglycosidase PNGase F, which resulted in a clearer representation of the cleaved product by

Western blot, compared to samples without PNGaseF pre-treatment, most likely due to heterogenous glycosylation of the spike protein in samples without the glycosidase. Overall, these data indicate that cathepsin L selectively cleaves the S protein of FECV-1683, whereas cathepsin B can cleave the S protein of both FECV-1683 and FIPV-1146.

The in vivo targets of the highly virulent coronaviruses FIPV-1146 and FIPV-DF2 include feline monocytes and macrophages. In order to assess whether cathepsins B and L might play a role in the entry of FIPV-1146 and FIPV-DF2 into its in vivo target, we isolated CD172a-positive, primary feline blood monocytes, pre-treated the cells with the cathepsin B inhibitor CA074-Me, or the cathepsin L inhibitor Z-FY-(t-Bu)-DMK, and then infected them with FIPV-1146 or FIPV-DF2. As shown in figure 3.6, the cathepsin B inhibitor significantly reduced infection by FIPV-1146 and FIPV-DF2 (approximately 85–95% inhibition), however, the block was not as complete as observed in cell lines (see figures 3.2 and 3.4). In line with our data using cell lines, the cathepsin L inhibitor showed no significant effect on FIPV infection of primary feline monocytes. As expected (12), primary feline blood monocytes were only negligibly susceptible to infection with FECV-1683, hence a role for cathepsin B or L cannot be determined in this case (Figure 3.6). These data indicate that cathepsin B-mediated cleavage of FIPV-1146 and FIPV-DF2 may play an important role in cells infected in vivo during the course of FIP.

We show here the effects of low pH and cathepsin cleavage of the serotype II feline coronavirus spike protein, with a differential effect of low pH, and cathepsin B versus cathepsin L cleavage for the FECV and FIPV biotypes. The two biotypes are genotypically very similar and the strains FECV-1683 and FIPV-1146, in particular, are known to share a high degree of amino acid identity in their spike protein (>95%) yet cause radically different clinical outcomes—lethal vasculitis for FIPV-1146,

compared to mild enteritis for FECV-1683 (23). Previous studies have shown that the S2 domain of the viral spike protein is a critical discriminating factor in FECV-1683 and FIPV-1146 pathogenesis (46). The studies presented here raise the possibility that differential proteolysis of the spike (S2) protein might be an important factor in explaining the different pathogenic properties of these viruses.

At present, we cannot definitely determine the exact point in the FCoV infectious cycle that cathepsin cleavage would occur. However, the in vivo localization of cathepsins to the endosome/lysosome system, together with absence of any obvious cleaved product in purified extracellular FCoV particles unless exogenous activated cathepsin is added, would strongly suggest that cleavage occurs in the endosome during virus entry. In support of this, we find that addition of cathepsin inhibitors after virus entry has occurred has no detectable effect on viral replication. While the use of feline aminopeptidase N (fAPN) as a receptor for serotype II feline coronaviruses is well established (51, 53, 54), many other aspects of the entry pathway have not been explored in great detail for these viruses. Based on the effects of lysosomotropic agents shown here, we suggest that all serotype II feline coronaviruses enter the endocytic pathway for virus entry, where they are primed for fusion activation by cathepsin cleavage, but that FECV-1683 is much more dependent on endosomal function, suggesting that FIPV-1146 and FIPV-DF2 may escape into the cytosol earlier in the endocytic pathway. Possibilities that might account for this are the differential cleavage of the FIPV spike protein by cathepsin L, or alternatively a lower threshold for any necessary low pH-dependent conformational changes for FIPV spike. It remains to be determined whether a similar situation with cathepsin cleavage exists for the serotype I FCoVs, which are not considered to share the same receptor as FECV-1683 and FIPV-1146 (14). In general, the cleavage site of cathepsins is difficult to predict based on sequence specificity, and so we cannot at

present determine specifically where in the spike protein cathepsin B or L might cleave. However, based on the single 150–160 kDa cleaved product seen in Fig. 5 for both cathepsin B and L, it does appear that the spike protein is subject to single, distinct cleavage event for both proteases, most likely occurring at the same approximate position in S. We used the monoclonal antibody 22G6.4 to show this specific cleavage event, and while the epitope recognized by 22G6.4 is not known, by analogy to the many other S specific FCoV monoclonal antibodies that have epitopes in S1 (10, 38), we tentatively suggest that the 22G6.4-reactive epitope is also most likely to be within the S1 domain. Based on the cleavage pattern shown in figure 3.5 it does not appear that cleavage occurs at the S1/S2 boundary, but rather, the 150–160 kDa cleavage products observed may represent cleavage within the C-terminal part of S2. As the C-terminal part of FCoV S2 has been previously considered to specify the pathogenic properties of FIPV (46), it will be interesting to determine if any of the specific mutations in the FIPV-1146 spike can account for the differential cathepsin-sensitivity observed here. Interestingly, treatment with cathepsins L or B resulted in only a fraction of the spike protein being cleaved (approximately 17–34% cleaved depending on the cathepsin/virus combination; see figure 3.5 B). This may indicate that the cleavage site is relatively inaccessible, and that only a small number of spike proteins are cleaved during virus entry. In this regard, it is noteworthy that in many cases cleavage activation of a viral fusion protein does not necessarily occur on all copies of the protein (34). Our data also indicate that for FECV-1683 (which is cleaved by both cathepsin B and L), cleavage occurs to a greater degree than with cathepsin B (Figure 3.5). These data are consistent with inhibitor treatments where cathepsin B inhibitor had a greater effect on virus infection than cathepsin L inhibitor. Thus we consider that cathepsin B may be the more important protease mediating FCoV entry, with cathepsin L possibly having a more secondary role. Cysteine

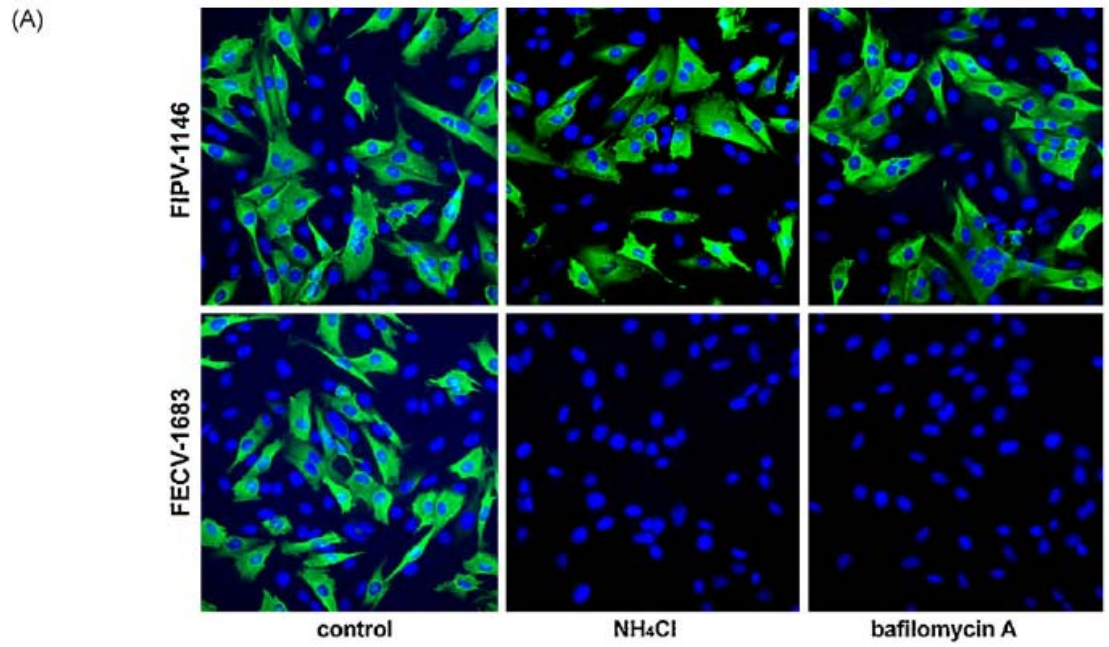

Figure 3.3 The effect of lysosomotropic agents on the entry of FIPV-1146 and FECV 1683. A-72 cells were pre-treated with NH_4Cl or bafilomycin A at the specified concentration and then infected with virus. 6 h post-infection cells were fixed and stained for immunofluorescence microscopy with the anti-FCoV nucleocapsid mAb 17B7.1 (A). Images from at least three independent experiments were processed and quantified (B). To control for non-specific effects on replication, cells were also treated with lysomotrophic agents 1 h post-infection. For quantification, >1000 cells were scored from three independent replicates of each experimental condition. Error bars represent the standard deviation of the mean.

Figure 3.3 (continued)

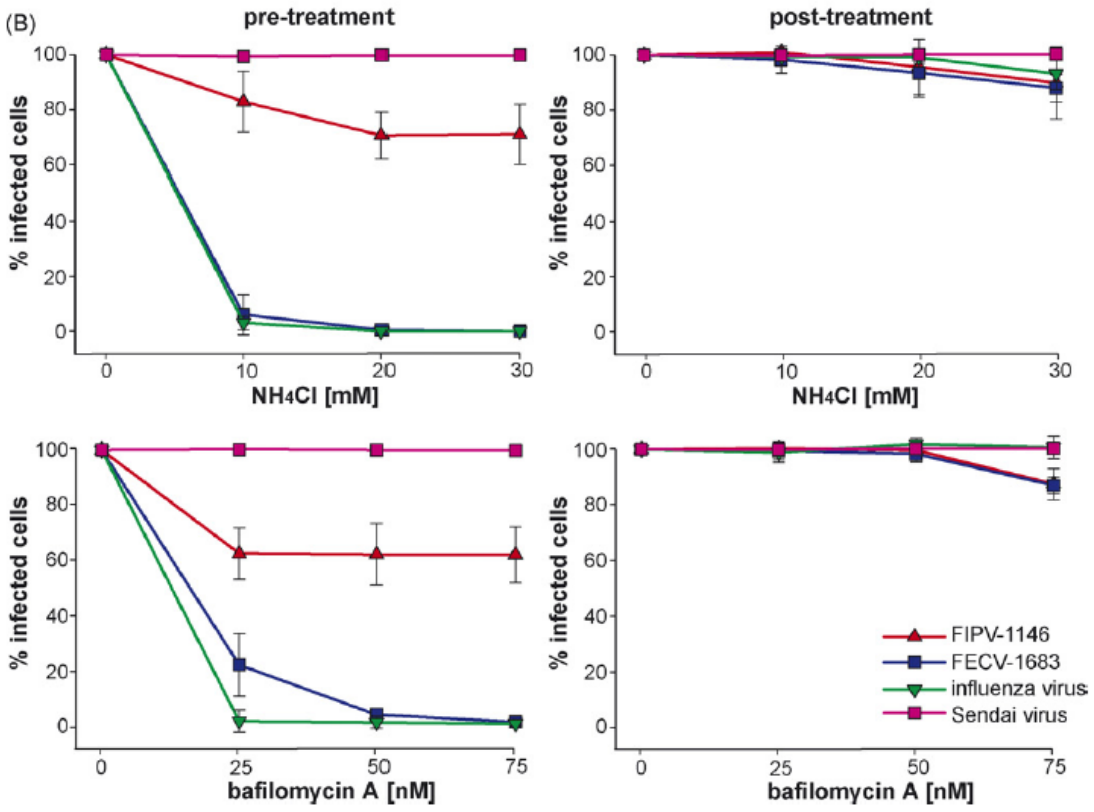

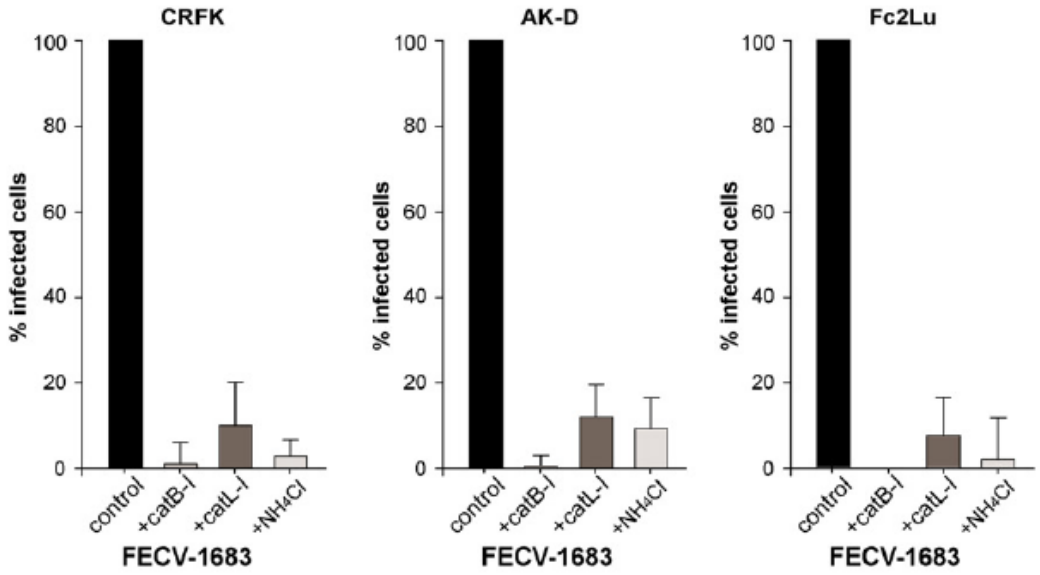

Figure 3.4 The effects of cathepsin L and cathepsin B inhibitors, and low pH, on the infection of feline cells by serotype II FCoVs. CRFK, AK-D or Fc2Lu cells were pre-treated with either 10 mM cathepsin B inhibitor CA074-Me (CatB-I), 10 mM cathepsin L inhibitor Z-FY-(t-Bu)-DMK (CatL-I), or 10 mM NH_4Cl, and then infected with virus. 6 h post-infection cells were fixed and stained for immunofluorescence microscopy with the anti-FCoV nucleocapsid mAb 17B7.1. Images from at least three independent experiments were processed and quantified. For quantification >500 cells were scored from three independent replicates. Error bars represent the standard deviation of the mean.

Figure 3.4 (continued)

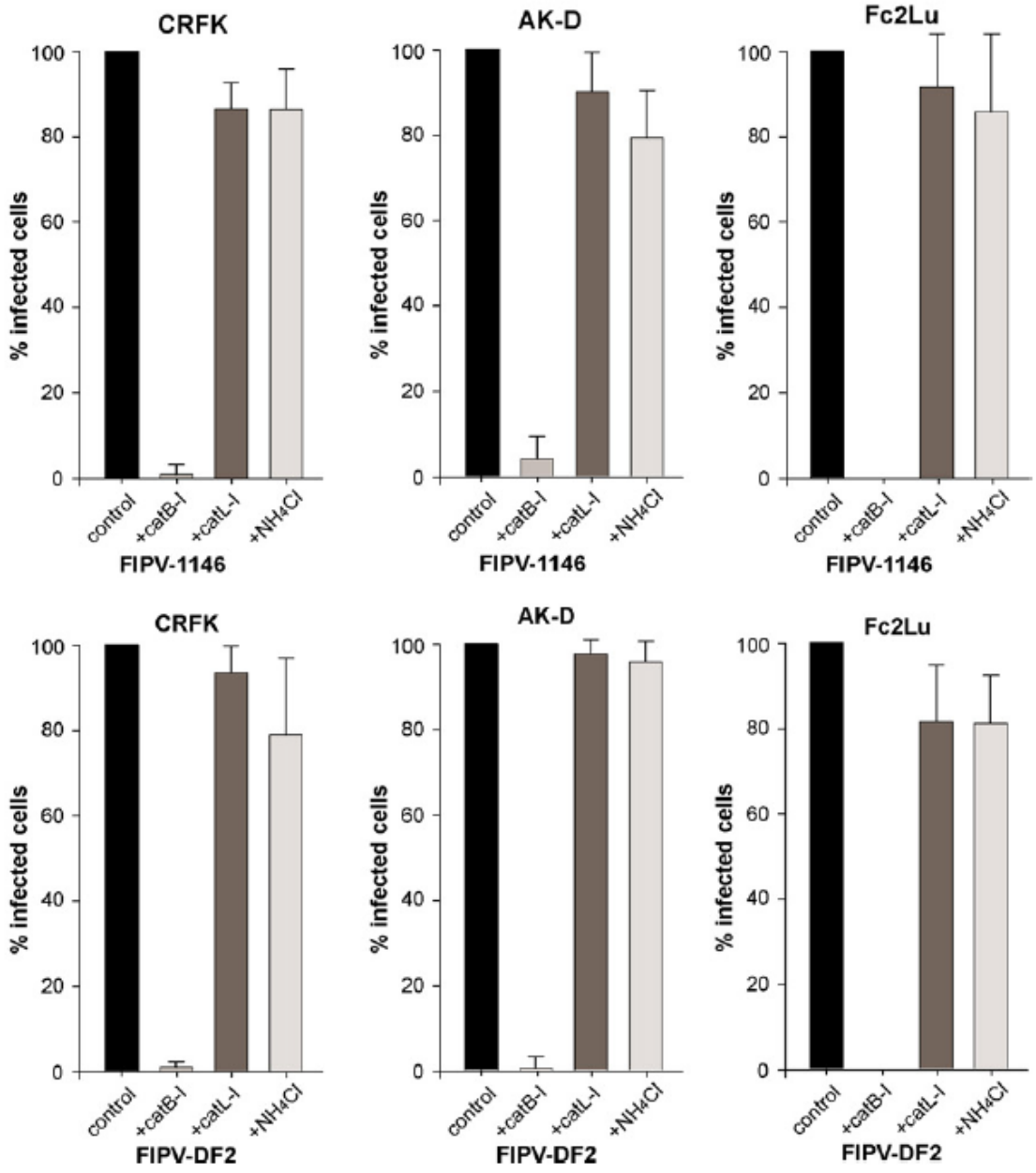

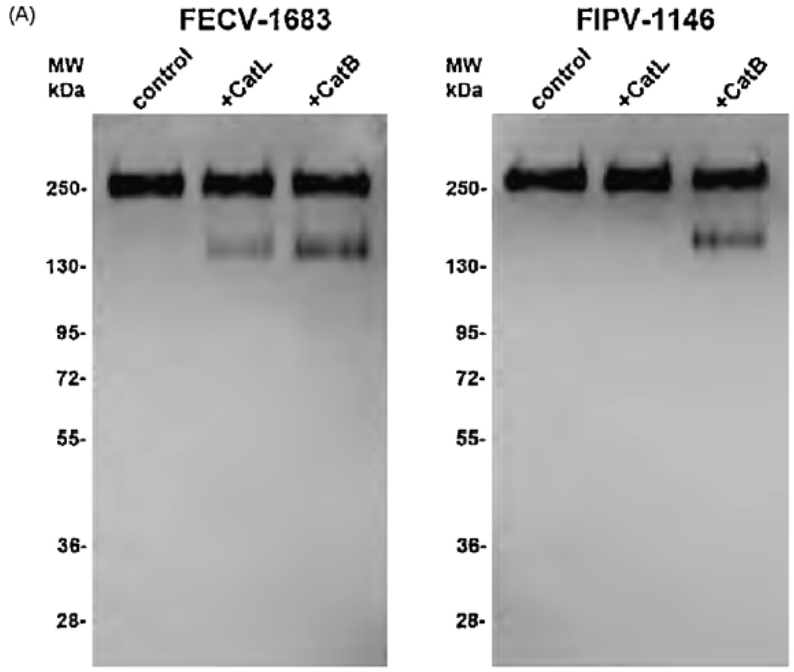

(B)

FECV-1683 (% cleaved product)	FIPV-1146 (% cleaved product)
control (0%)	control (0%)
+ cathepsin L (17%)	+ cathepsin L (0%)
+ cathepsin B (34%)	+ cathepsin B 26%)

Figure 3.5 Cleavage of FIPV-1146 and FECV-1683 by purified cathepsins. Concentrated virus preparations were incubated with purified cathepsin B, cathepsin L, or buffer alone for 1 h at 37ºC, followed by treatment with PNGase F. (A) Samples were then analyzed by western blot with the anti-FCoV spike mAb 22G6.4. (B) Quantification of western blot to show degree of cleavage. (CatL-I), or 10 mM NH_4Cl, and then infected with virus. 6 h post-infection cells were fixed and stained for immunofluorescence microscopy with the anti-FCoV nucleocapsid mAb 17B7.1. Images from at least three independent experiments were processed and quantified. For quantification >500 cells were scored from three independent replicates. Error bars represent the standard deviation of the mean.

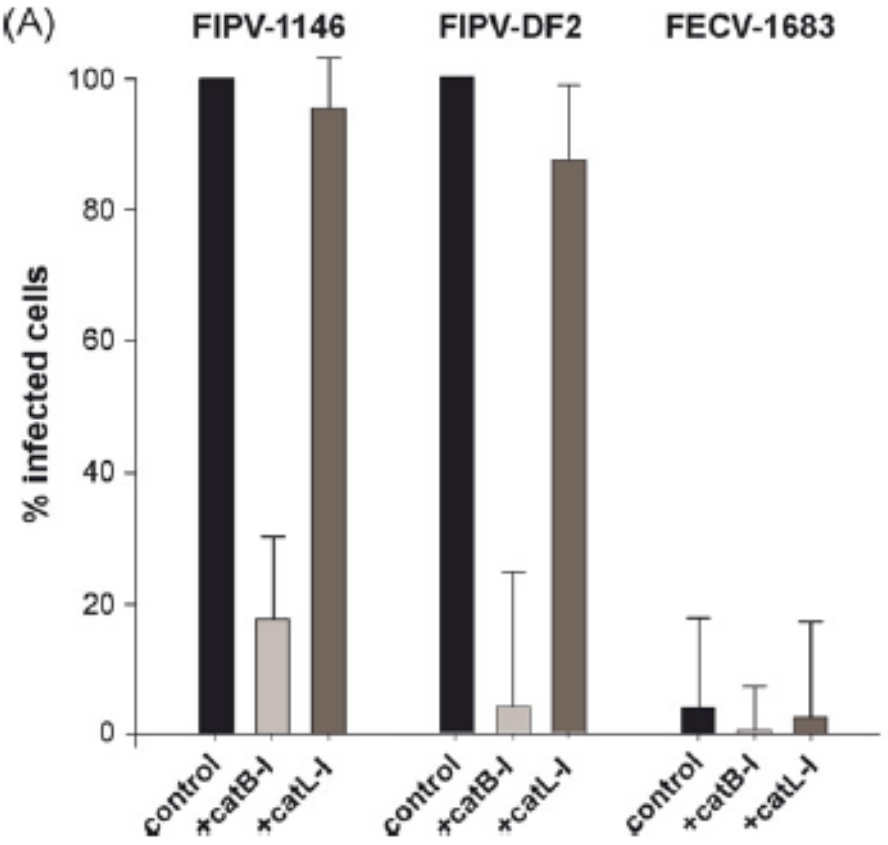

Figure 3.6 The effect of cathepsin inhibitors on the infection of primary feline blood monocytes. Monocytes were purified from the blood of SPF cats, pre-treated with the cathepsin B inhibitor CA074-Me (CatB-I) or the cathepsin L inhibitor Z-FY-(t-Bu)-DMK (CatL-I) at a concentration 10 mM, and infected with virus. 12 h post-infection, cells were fixed and stained for immunofluorescence microscopy with the anti-FCoV nucleocapsid mAb 17B7.1 (A). Images from at least three independent experiments were processed and quantified (B). For quantification, >200 cells were scored from three independent replicates of each experimental condition. Error bars represent the standard deviation of the mean.

Figure 3.6 (continued)

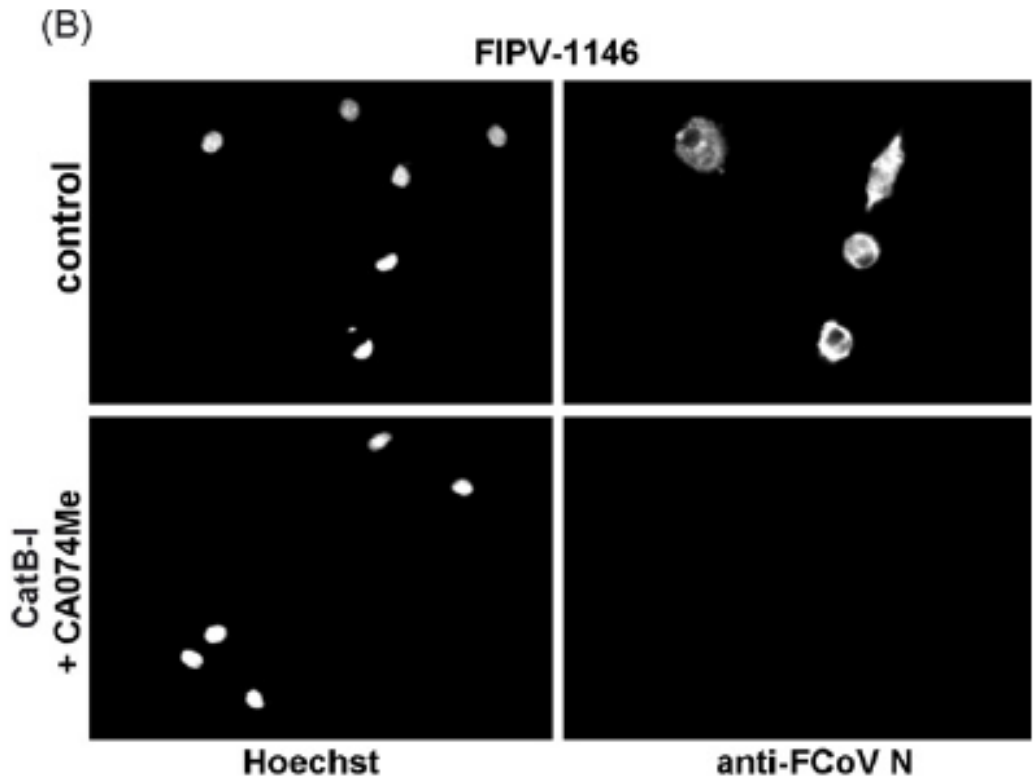

proteases such as cathepsins B, L, K and S, are emerging as therapeutic targets for a range of diseases, including cancer, osteoarthritis and autoimmune disorders, with some candidate drugs currently in clinical trials (52, 55). Cathepsin inhibitors also show promise as drugs targeting virus entry (55). Our results show a clear role for cathepsin B during entry of serotype II feline coronaviruses, raising the possibility that cathepsin B inhibitors may be effective therapeutics to treat this incurable and lethal affliction of cats.

3.4. Acknowledgements

We thank Fred Scott, Joel Baines and Sandrine Belouzard for helpful advice and discussions during the course of this work, and Ed Dubovi for kind provision of reagents. We also thank A. Damon Ferguson for technical assistance. A.D.R. was supported by grant T32AI007618 (Training in Molecular Virology and Pathogenesis) from the National Institutes of Health. This work was supported by a research grant from the Winn Feline Foundation.

REFERENCES

1. Barrett, A.J., Rawlings, N.D., Woessner, J.F., 2004. Handbook of Proteolytic Enzymes. Elsevier Academic Press, London.
2. Blau, D.M., Holmes, K.V., 2001. Human coronavirus HCoV-229E enters susceptible cells via the endocytic pathway. Adv. Exp. Med. Biol. 494, 193–198.
3. Bosch, B.J., Rottier, P.J., 2008. Nidovirus entry into cells. In: Perlman, S., Gallagher, T., Snijder, E.J. (Eds.), Nidoviruses. ASM Press, Washington, DC, pp. 157–178.
4. Bosch, B.J., van der Zee, R., de Haan, C.A., Rottier, P.J., 2003. The coronavirus spike protein is a class I virus fusion protein: structural and functional characterization of the fusion core complex. J. Virol. 77, 8801–8811.
5. Cavanagh, D., Davis, P.J., Pappin, D.J., Binns, M.M., Boursnell, M.E., Brown, T.D., 1986. Coronavirus IBV: partial amino terminal sequencing of spike polypeptide S2 identifies the sequence Arg-Arg-Phe-Arg-Arg at the cleavage site of the spike precursor propolypeptide of IBV strains Beaudette and M41. Virus Res. 4, 133–143.
6. Chambers, P., Pringle, C.R., Easton, A.J., 1990. Heptad repeat sequences are located adjacent to hydrophobic regions in several types of virus fusion glycoproteins. J. Gen. Virol. 71 (Pt 12), 3075–3080.
7. Chandran, K., Sullivan, N.J., Felbor, U., Whelan, S.P., Cunningham, J.M., 2005. Endosomal proteolysis of the Ebola virus glycoprotein is necessary for infection. Science 308, 1643–1645.

8. Chu, V.C., McElroy, L.J., Chu, V., Bauman, B.E., Whittaker, G.R., 2006. The avian coronavirus infectious bronchitis virus undergoes direct low-pH-dependent fusion activation during entry into host cells. J. Virol. 80, 3180–3188.

9. Colman, P.M., Lawrence, M.C., 2003. The structural biology of type I viral membrane fusion. Nat. Rev.Mol. Cell Biol. 4, 309–319.

10. Corapi, W.V., Darteil, R.J., Audonnet, J.C., Chappuis, G.E., 1995. Localization of antigenic sites of the S glycoprotein of feline infectious peritonitis virus involved in neutralization and antibody-dependent enhancement. J. Virol. 69, 2858–2862.

11. de Groot-Mijnes, J.D., van Dun, J.M., van der Most, R.G., de Groot, R.J., 2005. Natural history of a recurrent feline coronavirus infection and the role of cellular immunity in survival and disease. J. Virol. 79, 1036–1044.

12. Dewerchin, H.L., Cornelissen, E., Nauwynck, H.J., 2005. Replication of feline coronaviruses in peripheral blood monocytes. Arch. Virol. 150, 2483–2500.

13. Diederich, S., Moll, M., Klenk, H.D., Maisner, A., 2005. The nipah virus fusion protein is cleaved within the endosomal compartment. J. Biol. Chem. 280, 29899–29903.

14. Dye, C., Temperton, N., Siddell, S.G., 2007. Type I feline coronavirus spike glycoprotein fails to recognize aminopeptidase N as a functional receptor on feline cell lines. J. Gen. Virol. 88, 1753–1760.

15. Earp, L.J., Delos, S.E., Park, H.E., White, J.M., 2005. The many mechanisms of viral membrane fusion proteins. Curr. Top. Microbiol. Immunol. 285, 25–66.

16. Ebert, D.H., Deussing, J., Peters, C., Dermody, T.S., 2002. Cathepsin L and cathepsin B mediate reovirus disassembly in murine fibroblast cells. J. Biol. Chem. 277, 24609–24617.

17. Eifart, P., Ludwig, K., Bottcher, C., de Haan, C.A., Rottier, P.J., Korte, T., Herrmann, A., 2007. Role of endocytosis and low pH in murine hepatitis virus strain A59 cell entry. J. Virol. 81, 10758–10768.

18. Frana, M.F., Behnke, J.N., Sturman, L.S., Holmes, K.V., 1985. Proteolytic cleavage of the E2 glycoprotein of murine coronavirus: host-dependent differences in proteolytic cleavage and cell fusion. J. Virol. 56, 912–920.

19. Gallagher, T.M., Buchmeier, M.J., 2001. Coronavirus spike proteins in viral entry and pathogenesis. Virology 279, 371–374.

20. Gallagher, T.M., Escarmis, C., Buchmeier, M.J., 1991. Alteration of the pH dependence of coronavirus-induced cell fusion: effect of mutations in the spike glycoprotein. J. Virol. 65, 1916–1928.

21. Golden, J.W., Bahe, J.A., Lucas, W.T., Nibert, M.L., Schiff, L.A., 2004. Cathepsin S supports acid-independent infection by some reoviruses. J. Biol. Chem. 279, 8547–8557.

22. Gray, J., 1999. Assays for virus infection. In: Cann, A.J. (Ed.), Virus Culture. Oxford University Press, Oxford, pp. 81–109.

23. Haijema, B.J., Rottier, P.J., de Groot, R.J., 2007. Feline coronaviruses: a tale of two-faced types. In: Thiel, V. (Ed.), Coronaviruses. Molecular and Cellular Biology. Caister Academic Press, Norfolk, UK, pp. 183–203.

24. Hansen, G.H., Delmas, B., Besnardeau, L., Vogel, L.K., Laude, H., Sjostrom, H., Noren, O., 1998. The coronavirus transmissible gastroenteritis virus causes infection after receptor-mediated endocytosis and acid-dependent fusion with an intracellular compartment. J. Virol. 72, 527–534.

25. Hingley, S.T., Leparc-Goffart, I., Seo, S.H., Tsai, J.C., Weiss, S.R., 2002. The virulence of mouse hepatitis virus strain A59 is not dependent on efficient spike protein cleavage and cell-to-cell fusion. J. Neurovirol. 8, 400–410.

26. Huang, I.C., Bosch, B.J., Li, F., Li, W., Lee, K.H., Ghiran, S., Vasilieva, N., Dermody, T.S., Harrison, S.C., Dormitzer, P.R., Farzan, M., Rottier, P.J., Choe, H., 2005. SARS coronavirus, but not human coronavirus NL63, utilizes cathepsin L to infect ACE2-expressing cells. J. Biol. Chem. 10, 3198–3203.

27. Klenk, H.-D., Garten, W., 1994. Activation cleavage of viral spike proteins by host proteases. In: Wimmer, E. (Ed.), Cellular Receptors for Animal Viruses. Cold Spring Harbor Press, Cold Spring Harbor, NY, pp. 241–280.

28. Klenk, H.-D., Matrosovich, M., Stech, J., 2008. Avian influenza: molecular mechansims of pathogenesis. In: Mettenleiter, T.C., Sobrino, F. (Eds.), Animal Viruses: Molecular Biology. Caister Academic Press, Norfolk, UK, pp. 253–303.

29. Kliger, Y., Levanon, E.Y., 2003. Cloaked similarity between HIV-1 and SARS-CoV suggests an anti-SARS strategy. BMC Microbiol. 3, 20.

30. Kumar, P., Nachagari, D., Fields, C., Franks, J., Albritton, L.M., 2007. Host cell cathepsins potentiate Moloney murine leukemia virus infection. J. Virol. 81, 10506–10514.

31. Lai, M.M.C., Holmes, K.V., 2001. Coronaviridae: the viruses and their replication. In: Knipe, D.M., Howely, P.M. (Eds.), Fields Virology. Lippincott Wilkins and Williams, Philadelphia.

32. Li, D., Cavanagh, D., 1990. Role of pH in syncytium induction and genome uncoating of avian infectious bronchitis coronavirus (IBV). Adv. Exp. Med. Biol. 276, 33–36.

33. Li, D., Cavanagh, D., 1992. Coronavirus IBV-induced membrane fusion occurs at near-neutral pH. Arch. Virol. 122, 307–316.

34. Michalski,W.P., Crameri, G.,Wang, L., Shiell, B.J., Eaton, B., 2000. The cleavage activation and sites of glycosylation in the fusion protein of Hendra virus. Virus Res. 69, 83–93.

35. Mizzen, L., Hilton, A., Cheley, S., Anderson, R., 1985. Attenuation of murine coronavirus infection by ammonium chloride. Virology 142, 378–388.

36. Olsen, C.W., 1993. A review of feline infectious peritonitis virus: molecular biology, immunopathogenesis, clinical aspects, and vaccination. Vet. Microbiol. 36, 1–37.

37. Olsen, C.W., Corapi, W.V., Ngichabe, C.K., Baines, J.D., Scott, F.W., 1992. Monoclonal antibodies to the spike protein of feline infectious peritonitis virus mediate antibody-dependent enhancement of infection of feline macrophages. J. Virol. 66, 956–965.

38. Olsen, C.W., Corapi,W.V., Jacobson, R.H., Simkins, R.A., Saif, L.J., Scott, F.W., 1993. Identification of antigenic sites mediating antibody-dependent enhancement of feline infectious peritonitis virus infectivity. J. Gen. Virol. 74 (Pt 4), 745–749.

39. Pager, C.T., Dutch, R.E., 2005. Cathepsin L is involved in proteolytic processing of the Hendra virus fusion protein. J. Virol. 79, 12714–12720.

40. Pager, C.T., Craft Jr., W.W., Patch, J., Dutch, R.E., 2006. A mature and fusogenic form of the Nipah virus fusion protein requires proteolytic processing by cathepsin L. Virology 346, 251–257.

41. Pedersen, N.C., Black, J.W., Boyle, J.F., Evermann, J.F., McKeirnan, A.J., Ott, R.L., 1984a. Pathogenic differences between various feline coronavirus isolates. Adv. Exp. Med. Biol. 173, 365–380.

42. Pedersen, N.C., Evermann, J.F., McKeirnan, A.J., Ott, R.L., 1984b. Pathogenicity studies of feline coronavirus isolates 79-1146 and 79-1683. Am. J. Vet. Res. 45, 2580–2585.

43. Perlman, S., Gallagher, T., Snijder, E.J., 2008. Nidoviruses. ASM Press, Washington, DC.

44. Pratelli, A., Martella, V., Decaro, N., Tinelli, A., Camero, M., Cirone, F., Elia, G., Cavalli, A., Corrente, M., Greco, G., Buonavoglia, D., Gentile, M., Tempesta, M., Buonavoglia, C., 2003. Genetic diversity of a canine coronavirus detected in pups with diarrhoea in Italy. J. Virol. Methods 110, 9–17.

45. Qiu, Z., Hingley, S.T., Simmons, G., Yu, C., Das Sarma, J., Bates, P., Weiss, S.R., 2006. Endosomal proteolysis by cathepsins is necessary for murine coronavirus mouse hepatitis virus type 2 spike-mediated entry. J. Virol. 80, 5768–5776.

46. Rottier, P.J., Nakamura, K., Schellen, P., Volders, H., Haijema, B.J., 2005. Acquisition of macrophage tropism during the pathogenesis of feline infectious peritonitis is determined by mutations in the feline coronavirus spike protein. J. Virol. 79, 14122–14130.

47. Sanchez, A., 2007. Analysis of filovirus entry into vero e6 cells, using inhibitors of endocytosis, endosomal acidification, structural integrity, and cathepsin (B and L) activity. J. Infect. Dis. 196 (Suppl. 2), S251–258.

48. Schornberg, K., Matsuyama, S., Kabsch, K., Delos, S., Bouton, A., White, J., 2006. Role of endosomal cathepsins in entry mediated by the Ebola virus glycoprotein. J. Virol. 80, 4174–4178.

49. Simmons, G., Gosalia, D.N., Rennekamp, A.J., Reeves, J.D., Diamond, S.L., Bates, P., 2005. Inhibitors of cathepsin L prevent severe acute respiratory syndrome coronavirus entry. Proc. Natl. Acad. Sci. U.S.A. 102, 11876–11881.

50. Simmons, G., Reeves, J.D., Rennekamp, A.J., Amberg, S.M., Piefer, A.J., Bates, P., 2004. Characterization of severe acute respiratory syndrome-associated coronavirus (SARS-CoV) spike glycoprotein-mediated viral entry. Proc. Natl. Acad. Sci. U.S.A. 101, 4240–4245.

51. Tresnan, D.B., Levis, R., Holmes, K.V., 1996. Feline Aminopeptidase N serves as a receptor for feline, canine, porcine, and human coronaviruses in serogroup I. J. Virol. 70, 8669–8674.

52. Turk, D., Guncar, G., 2003. Lysosomal cysteine proteases (cathepsins): promising drug targets. Acta Crystallogr. D: Biol. Crystallogr. 59, 203–213.

53. Tusell, S.M., Schittone, S.A., Holmes, K.V., 2007. Mutational analysis of aminopeptidase N, a receptor for several group 1 coronaviruses, identifies key determinants of viral host range. J. Virol. 81, 1261–1273.

54. Van Hamme, E., Dewerchin, H.L., Cornelissen, E., Nauwynck, H.J., 2007. Attachment and internalization of feline infectious peritonitis virus in feline blood monocytes and Crandell feline kidney cells. J. Gen. Virol. 88, 2527–2532.

55. Vasiljeva, O., Reinheckel, T., Peters, C., Turk, D., Turk, V., Turk, B., 2007. Emerging roles of cysteine cathepsins in disease and their potential as drug targets. Curr. Pharm. Des. 13, 387–403.

56. Vennema, H., Heijnen, L., Zijderveld, A., Horzinek, M.C., Spaan, W.J., 1990. Intracellular transport of recombinant coronavirus spike proteins: implications for virus assembly. J. Virol. 64, 339–346.

57. Vennema, H., Poland, A., Foley, J., Pedersen, N.C., 1998. Feline infectious peritonitis viruses arise by mutation from endemic feline enteric coronaviruses. Virology 243, 150–157.

58. Wentworth, D.E., Holmes, K.V., 2007. Coronavirus binding and entry. In: Thiel, V. (Ed.), Coronaviruses. Molecular and Cellular Biology. Caister Academic Press, Norfolk, UK, pp. 3–31.

CHAPTER FOUR

ACTIVATION OF P38 MAPK BY FELINE INFECTIOUS PERITONITIS VIRUS REGULATES PRO-INFLAMMATORY CYTOKINE PRODUCTION IN PRIMARY BLOOD DERIVED MONONUCLEAR CELLS*

* A.D. Regan, R.D. Cohen, G.R. Whittaker. 2009. Activation of p38 MAPK by feline infectious peritonitis virus regulates pro-inflammatory cytokine production in primary blood derived feline mononuclear cells. Virology. 384(1): 135-43.

4.1. Summary

Feline infectious peritonitis (FIP) is an invariably fatal disease of cats caused by systemic infection with a feline coronavirus (FCoV) termed feline infectious peritonitis virus (FIPV). The lethal pathology associated with FIP (granulomatous inflammation and T-cell lymphopenia) is thought to be mediated by aberrant modulation of the immune system due to infection of cells such as monocytes and macrophages. Overproduction of pro-inflammatory cytokines occurs in cats with FIP, and has been suggested to play a significant role in the disease process. However, the mechanism underlying this process remains unknown. Here we show that infection of primary blood-derived feline mononuclear cells by FIPV WSU 79-1146 and FIPV-DF2 leads to rapid activation of the p38 MAPK pathway and that this activation regulates production of the pro-inflammatory cytokine tumor necrosis factor alpha (TNF-alpha) and interleukin-1 beta (IL-1 beta). FIPV-induced p38 MAPK activation and pro-inflammatory cytokine production was inhibited by the pyridinyl imidazole inhibitors SB 203580 and SC 409 in a dose-dependent manner. FIPV-induced p38 MAPK activation was observed in primary feline blood-derived mononuclear cells individually purified from multiple SPF cats, as was the inhibition of TNF-alpha production by pyridinyl imidazole inhibitors.

4.2. Introduction

Coronaviruses are a diverse family of enveloped positive-stranded RNA viruses that infect a wide range of species including humans. Coronaviruses are divided into three groups in which group 1 and 2 infect mammals and group 3 infects birds (37). Feline coronaviruses (FCoVs) belongs to group 1 and are classified as either serotype I or II depending on the sequence of their spike (S) protein (40). In addition, each serotype is divided into two biotypes designated as either feline enteric

coronavirus (FECV) or feline infectious peritonitis virus (FIPV) based on their pathological outcome in cats (47). FECV is ubiquitous amongst felines and causes mild to often unapparent enteritis, while FIPV leads to a lethal systemic infection marked by severe granulomatous inflammation (35, 36, 50). The mechanism underlying this drastic difference in disease between the two biotypes remains elusive, namely because FECV and FIPV isolates from the same serotype are virtually indistinguishable on the genetic and antigenic level. However it has been shown that the two biotypes possess markedly different abilities to infect cells of the immune system, with FIPV isolates possessing an extended tropism that allows for the infection of macrophages and monocytes (43). Recent studies have suggested that this alteration in tropism may be due to mutations in the S protein that affect protein cleavage and fusion activation during entry (39, 41).

Viral pathogens that infect immune cells (e.g. human immunodeficiency virus (HIV) and Dengue Virus) are known to induce aberrant cytokine production, a process which is proposed to play a role in the pathological outcome of their respective diseases (10, 20, 26). Studies of cats with FIP have shown that cytokine expressions are altered as compared to healthy animals (7, 21). Specifically it has been noted that expression of the pro-inflammatory cytokine tumor necrosis factor alpha (TNF-alpha), interleukin-1 beta (IL-1 beta) and interleukin-6 (IL-6) are significantly increased in cats with FIP, and are likely produced by infected macrophages and monocytes (21, 45, 46). It has been shown that TNF-alpha is able to induce feline T-cell apoptosis, making it the most likely causative agent of T-cell lymphopenia in FIPV-infected cats (7, 46). In addition TNF-alpha has been shown to increase expression of the FCoV receptor aminopeptidase N (APN) causing target cells to be more susceptible to viral infection and further exacerbate the disease (46). However despite their critical role in the pathological outcome of FIP, the mechanism regulating FIPV-induced

upregulation of pro-inflammatory cytokines remains undescribed. Mitogen-activated protein kinases (MAPKs) are a family of proteins that serve as components of signaling pathways within cells in order to process and respond to extracellular stimuli (38). Typically, receptors on the cell surface initiate signaling cascades, which lead to phosphorylation and translocation of MAPKs to the nucleus where they regulate transcriptional activators (51). In recent years, it has become clear that MAPKs also regulate processes outside of the nucleus such as mRNA translation and cytoskeletal remodeling (12, 19). Three major MAPK pathways have been identified which are conserved in all eukaryotic cells ranging from yeast to mammals. These pathways are designated as Extracellular Signal-Regulated Kinases 1 and 2 (ERK1/2), c-Jun N-terminal Kinases (JNK1) and p38 MAPK (34). In general the ERK pathway is activated by proliferative stimuli, while the JNK and p38 MAPK pathways are activated by extracellular stresses such as ultraviolet light, heat and osmotic shock (34). p38 MAPK was originally identified as the target of pyridinyl imidazole compounds that were shown to inhibit the production of IL-1 and TNF-alpha in lipopolysaccharide (LPS)-stimulated human monocytes (23). Subsequent studies have shown that the p38 MAPK pathway is responsible for the phosphorylation of a large group of transcriptional and translational response elements which directly regulate the expression of a wide variety of pro-inflammatory cytokines (22). Due to its involvement in cytokine regulation, we reasoned that the p38 MAPK pathway might play a role in the increased production of pro-inflammatory cytokines observed in cats with FIP. In this study we examined the activation of the p38 MAPK pathway in response to infection by FIPV in primary feline blood-derived mononuclear cells. We also investigated the role of p38 MAPK in TNF-alpha, IL-1 beta and IL-6 production, and the effect of p38 MAPK inhibitors on these processes.

4.3. Materials and methods

Primary feline blood-derived mononuclear (PFBM) cells were individually purified from four male SPF cats (animal ID# 07PJO7, 07PGP2, 07PGV4, 07PGV5) and three female SPF cats (animal ID# 07FGR2, 07FGV6, 07FJM5) (Liberty Research, Waverly, NY) using a standard Ficoll-paque gradient (GE Healthcare) as specified by the manufacturer. Cells were seeded in 24-well plates with tissue culture treated glass coverslips and allowed to attach overnight. After washing, cells were incubated in the presence of 5% CO2 at 37 °C in RPMI-1640 media pH7.4 supplemented with 10% Fetal Bovine Serum (FBS), 2 mM glutamine, 100 U/ml penicillin and 10 μg/ml streptomycin. The purity of PFBM preparations were routinely checked by immunofluorescence microscopy using the marker DH59B (Veterinary Medical Research & Development Inc., Pullman, WA). Crandell-Reese Feline Kidney cells were obtained from the American Type Culture Collection (ATCC) and cultured and maintained according to ATCC guidelines.

FIPV WSU 79-1146 (FIPV-1146) was obtained from the ATCC. FIPVDF2 was provided by Dr. Ed Dubovi (Animal Health Diagnostic Center, New York State College of Veterinary Medicine, Cornell University). Both viruses were grown by inoculating CRFK cells at a MOI of 0.01 and collecting supernatant after CPE was observed in 80% of cells which typically occurred between 48 and 72 h. Supernatant was clarified by a low speed centrifugation step (1250 X g for 10 min) and viral particles were then pelleted by centrifugation at 28,000 rpm in a SW28 rotor (Sorvall) for 60 min. Pellets were resuspended in phosphate-buffered saline (PBS). Virus titers were determined by plaque assays on CRFK cells using standard techniques. For UV inactivation, a thin layer of viral suspension was exposed to UV light (30 W) at a distance of 10 cm for 5 min. Inactivation was verified by performing infection assays in CRFK and PFBM cells as described.

The anti-phospho-p38 MAPK (Thr180/Tyr182) (3D7) rabbit monoclonal antibody (mAb) was obtained from Cell Signaling Technologies (Danvers, MA). The anti-p38 MAPK (N-20) goat polyclonal antibody (pAb) and anti-TNF-alpha (N-19) goat pAb were obtained from Santa Cruz Biotechnology (Santa Cruz, CA). The anti-FIPV nucleocapsid (N) protein mAb (17B7.1) was provided by Dr. Ed Dubovi (Animal Health Diagnostic Center, New York State College of Veterinary Medicine, Cornell University). Anti-CD127a mAb DH59B was obtained from Veterinary Medical Research and Development, Inc. (Pullman, WA). The feline TNF-alpha ELISA kit (TNF-alpha/TNFSF1A), feline IL-1 beta ELISA kit (IL-1 beta/IL-1F2), feline IL-6 ELISA kit, and associated antibodies and detection reagents were obtained from R&D Systems (Minneapolis, MN). The p38 MAPK inhibitors 4-(4-Fluorophenyl)-2-(4-methylsulfinylphenyl)-5-(4-pyridyl)1H-imidazole (SB 203580) and 4-(3-(4-Chlorophenyl)-5-(1-methylpiperidin-4-yl)-1H-pyrazol-4-yl) pyrimidine (SC 409) were obtained from Calbiochem (San Diego, CA). PFBM cells were incubated in low-serum media (1% FBS) for 12 h before inoculation with the specified virus at an MOI of 100, or pretreatment with the specified inhibitor for 2 h followed by infection. For p38 MAPK activation experiments, cells were lysed at the specified time-points in lysis buffer (1% Triton X-100, 50 mM Tris–HCl, 150 mM NaCl, 1 mM EDTA, 1 mM DTT, 50 mM beta-glycerophosphate, 100 mM sodium vanadate, pH 7.4) supplemented with 1x complete protease inhibitor cocktail (Roche). Lysates were clarified by centrifugation at 13,000 rpm in a table-top centrifuge at 4°C for 15 min before freezing at −80°C for later analysis. For immunofluorescence assays, cells were fixed at the specified time-points with 3% paraformaldehyde. For analysis of cytokine production, supernatant was collected 24 h post-innoculation (p.i.) before freezing at −80°C for later analysis. Fixed cells were labeled with the specified antibodies as described previously (6). Cells were viewed on a Nikon Eclipse E600 fluorescence

microscope, and images were captured with a Sensicam EM camera and analyzed with IPLab software.

SDS sample buffer was added to lysates and the reaction was heated at 95°C for 10 min before separation using a 4–20% SDS-PAGE gel at 200 V for 2 h. Gels were electroblotted to PVDF membrane at 200 A for 2 h, blocked with 5% bovine serum albumin and probed with the specified antibody at 4°C for 12 h. Membranes were developed using either anti-rabbit antibody (Southern Biotech, Birmingham AL) or anti-goat antibody (Santa Cruz Biotechnology, Santa Cruz CA) linked to horseradish peroxidase and ECL substrate (Pierce, Rockford IL) and images captured using a Fujifilm LAS-3000 CCD camera. For western blot analysis of TNF-alpha production, supernatants were concentrated 50× using iCon 9 kDa molecular weight cut-off spin columns (Pierce, Rockford IL) and analyzed by western blot as described above. Western blot densitometry analysis of signal intensity was performed using ImageJ software. For quantification of cytokine production, supernatants were processed with the specified ELISA kits (R&D Systems) using standard capture ELISA techniques as specified by the manufacturer.

4.4. Results and Discussion

The p38 MAPK pathway has been shown to be activated by multiple viral pathogens during infection (1, 2, 8, 9, 16, 53). To determine whether the p38 MAPK pathway is activated during the infectious lifecycle of FIPV, primary feline blood-derived mononuclear (PFBM) cells were inoculated with either FIPV-1146 or FIPV-DF2 at an MOI of 100. Untreated cells and infected cells ranging from 15 min to 12 h p.i. were lysed and analyzed by western blot with the anti-phospho-p38 MAPK mAb (3D7). Untreated cells showed a minimal level of p38 MAPK phosphorylation, however addition of either virus isolate caused rapid phosphorylation of p38 MAPK

(~600% increase) within 15 min p.i. (Figures 4.1 A and C). p38 MAPK underwent de-phosphorylation by 60 min and then showed a second phase of phosphorylation later in infection between 6 and 12 h p.i., which was less pronounced (Figure 4.1 A). To determine whether viral replication was required for FIPV-induced p38 MAPK activation, UV-inactivated virus was added to PFBM cells and analyzed by western blot as described above (Figure 4.1 B). UV-treated FIPV also induced p38 MAPK phosphorylation, however the activation was not biphasic, and instead remain sustained throughout the 12 h time-course (Figure 4.1 B). Membranes were re-probed with anti-p38 MAPK (N-20) pAb to show that an equal amount of p38 MAPK was present in each sample (Figures 4.1 A and B). To further confirm that the p38 MAPK pathway is activated by FIPV, PFBM cells were inoculated with FIPV-1146 at an MOI of 100 before fixing the cells for immunofluorescent microscopy. p38 MAPK again showed a rapid phosphorylation by 15 min p.i. while the total amount of p38 MAPK remained unchanged (Figure 4.2). In addition the p38 MAPK in infected cells showed increased nuclear localization as compared to untreated cells, a phenomenon highly associated with the regulation of transcriptional activators (Figure 4.2). These data indicate that the p38 MAPK pathway is activated during infection of PFBM cells by FIPV, and that viral replication is dispensable for this activation to occur.

The p38 MAPK pathway was first discovered by investigating the target of pyridinyl imidazole compounds which blocked LPS-induced cytokine induction in human monocytes (23). To test the effect of pyridinyl imidazole inhibitors on FIPV-induced p38 MAPK phosphorylation, PFBM cells were treated with 10 μM of either SB 203580 or SC 409 (or 0.1% DMSO as a control) for 2 h before inoculating with FIPV-1146 or FIPV-DF2 at an MOI of 100. 15 min p.i. cells were lysed and analyzed by western blot with the anti-phosphop38 MAPK mAb (3D7). Cells which were pretreated with DMSO alone showed rapid FIPV-induced phosphorylation of p38

MAPK, however those which were pretreated with either SB 203580 or SC 409 showed no activation as compared to uninfected cells (Figure 4.3). These data demonstrate that FIPV-induced p38 MAPK activation is blocked by pyridinyl imidazole inhibitors.

Activation of the p38MAPKpathway has been shown to be required for replication of some viruses including the murine coronavirus Mouse Hepatitis Virus (MHV) (2). To investigate whether activation of the p38 MAPK pathway is required for replication of FIPV, PFBM cells were treated with 10 μM of either SB 203580 or SC 409 (or 0.1% DMSO as a control) for 2 h before inoculating with FIPV-1146 or FIPV-DF2. 12 h p.i. cells were fixed and stained for with the anti-FIPV N protein mAb (17B7.1). As shown in figure 4.4, pretreatment with p38 MAPK inhibitors has no significant effect on FIPV replication in PFBM cells. Activation of p38 MAPK by viral pathogens has been shown to induce the production of pro-inflammatory cytokines such as TNF-alpha, IL-1 beta and IL-6 (2, 13, 24, 25; 42, 48, 52). To investigate whether TNF-alpha production in FIPV-infected PFBM cells is regulated by p38 MAPK activation, PFBM cells were treated with 10 μM of either SB 203580, SC 409 or 0.1% DMSO for 2 h before inoculating with FIPV-1146 or FIPV-DF2 at an MOI of 100.

24 h p.i. supernatants were collected, concentrated and analyzed by western blot with the anti-TNF-alpha (N-19) pAb. Cells which were pretreated with DMSO alone showed significant production of TNF-alpha, however those which were pretreated with either SB 203580 or SC 409 showed no detectable production of TNF-alpha as compared to uninfected cells (Figure 4.5 A). To quantify the production of TNF-alpha, infections were performed as described above, except at 24 h p.i. supernatants were collected and analyzed by anti-TNF-alpha capture ELISA. Infected cells which were pretreated with DMSO alone showed significant production of TNF-alpha (N750 pg/ml) however pretreatment with 10 μM SB 203580 and 10 μM SC 409

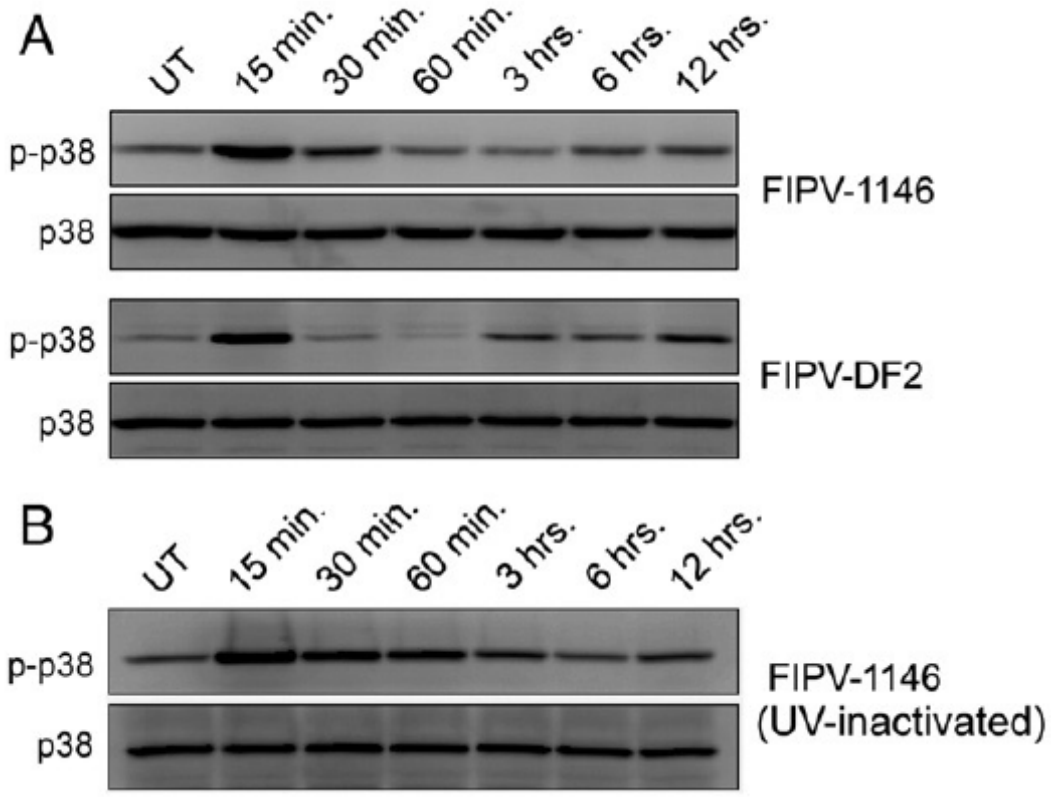

Figure 4.1 FIPV induces phosphorylation of p38 MAPK in PFBM cells. PFBM cells were infected with either untreated FIPV-1146 or FIPV-DF2 viral particles (A), or UV inactivated particles (B), at an MOI of 100. Cells were lysed at the specified times p.i. and analyzed by western blot with the anti-phospho-p38 MAPK mAb (3D7) and re-probed with anti-p38 MAPK (N-20) pAb. Signal intensity from two time-course infections of untreated FIPV-1146 and one time-course infection of untreated FIPV-DF2 were quantified by densitometry analysis with Image J software (C).

Figure 4.1 (continued)

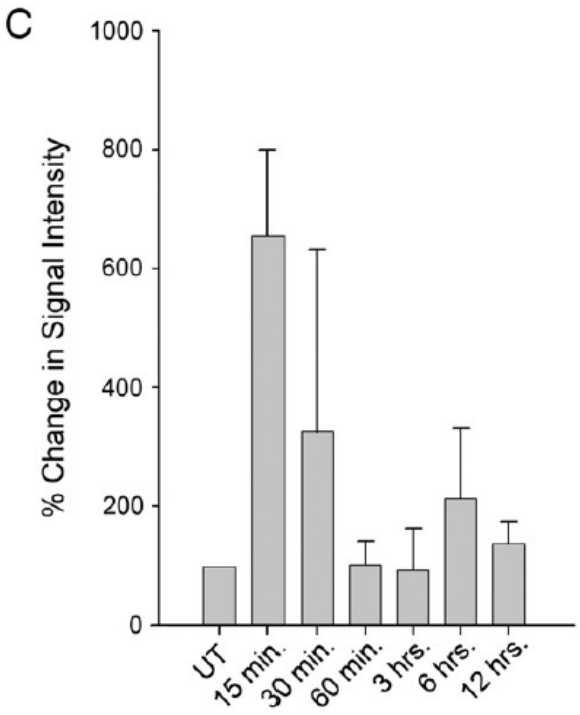

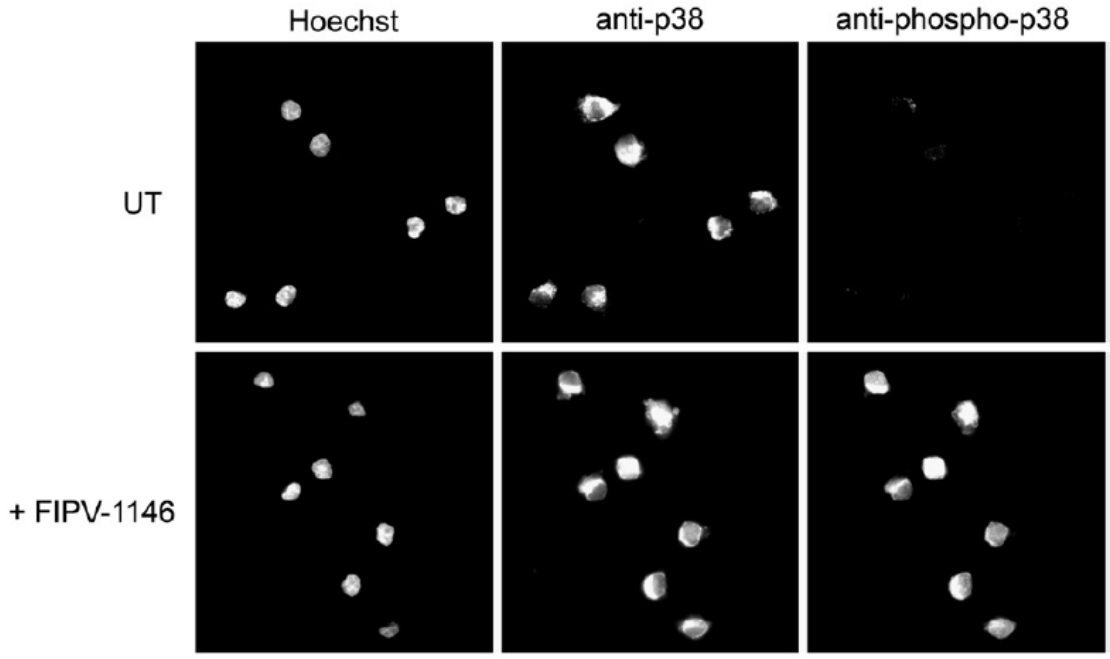

Figure 4.2 Immunofluorescence of FIPV-induced p38 MAPK activation and nuclear re-localization. PFBM cells were infected with FIPV-1146 at an MOI of 100. Cells were fixed at 15 min p.i. and stained with the anti-phospho-p38 MAPK mAb (3D7), the anti-p38 MAPK (N-20) pAb and Hoechst.

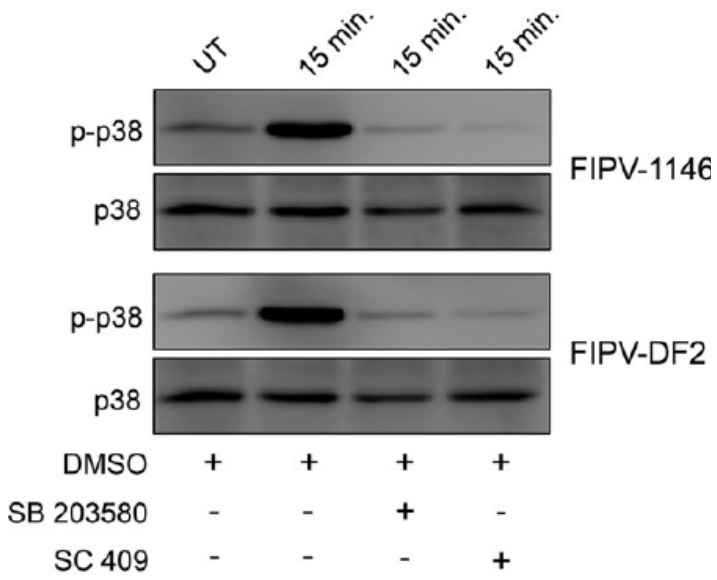

Figure 4.3 Inhibition of FIPV-induced p38 MAPK activation in PFBM cells by the pyridinyl imidazole compounds SB 203580 and SC 409. PFBM cells were pretreated with 10 μM of either SB 203580 or SC 409 (or 0.1% DMSO as a control) for 2 h before inoculating with FIPV-1146 or FIPV-DF2 at an MOI of 100. 15 min p.i. cells were lysed and analyzed by western blot with the anti-phospho-p38 MAPK mAb (3D7) and re-probed with anti-p38 MAPK (N-20) pAb.

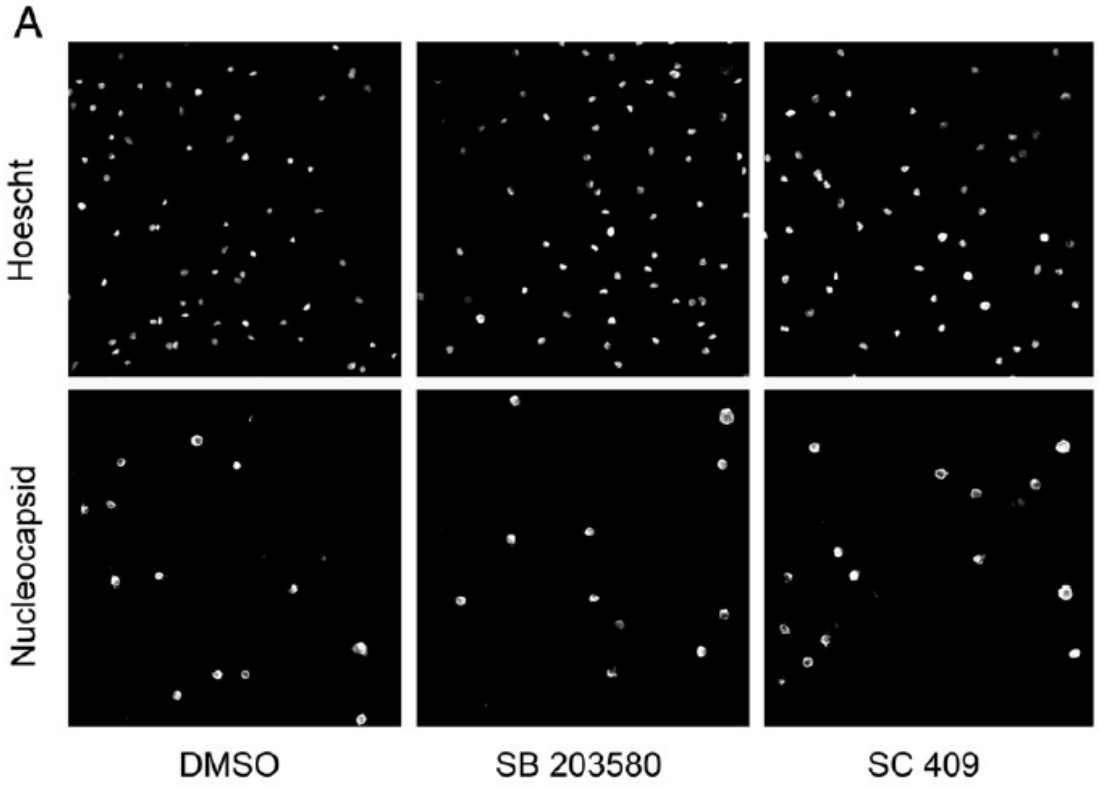

Figure 4.4 Inhibition of the p38 MAPK pathway does not significantly affect FIPV infection of PFBM cells. PFBM cells were pretreated with 10 μM of either SB 203580 or SC 409 (or 0.1% DMSO as a control) for 2 h before inoculating with FIPV-1146 or FIPV-DF2. Cells were fixed 12 h p.i. and stained with the anti-FIPV-N protein mAb (17B7.1) (A). For quantification, N500 cells were scored from three independent replicates of each experimental condition (B). Error bars represent the standard deviation of the mean.

Figure 4.4 (continued)

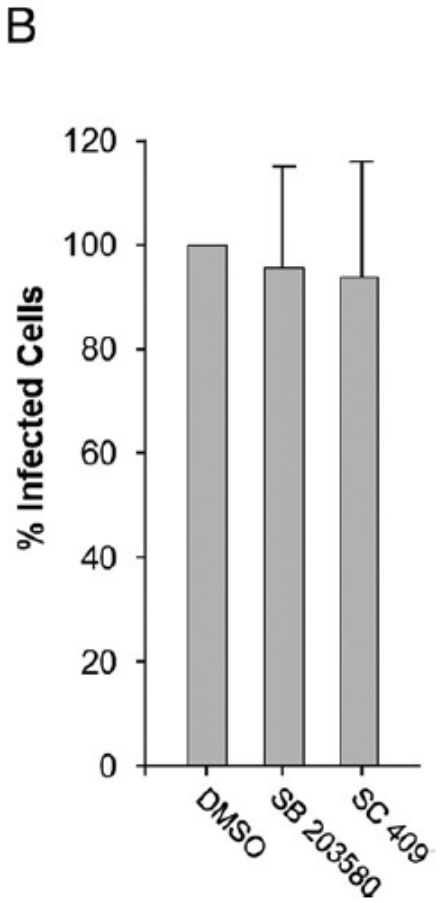

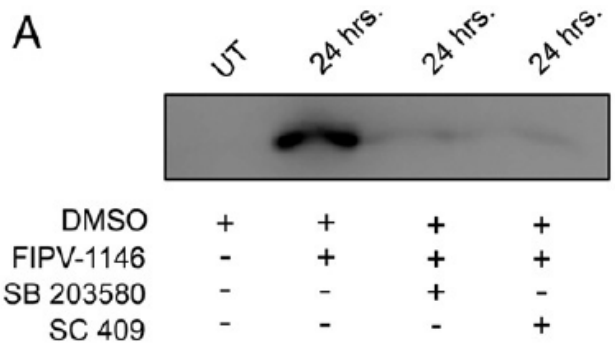

Figure 4.5 FIPV-induced TNF-alpha production by PFBM cells is regulated by p38 MAPK activation. PFBM cells were pretreated with 10 μM of either SB 203580 or SC 409 (or 0.1% DMSO as a control) for 2 h before inoculating with FIPV-1146 or FIPV-DF2 at an MOI of 100. 24 h p.i. supernatants were collected, concentrated and analyzed by western blot with the anti-TNF-alpha (N-19) pAb (A). 24 h p.i. supernatants were collected and TNF-alpha production was quantified by anti-TNF-alpha capture ELISA (B). TNF-alpha produced from untreated cells was below the detection limit of the assay (10 pg/ml).

Figure 4.5 (continued)

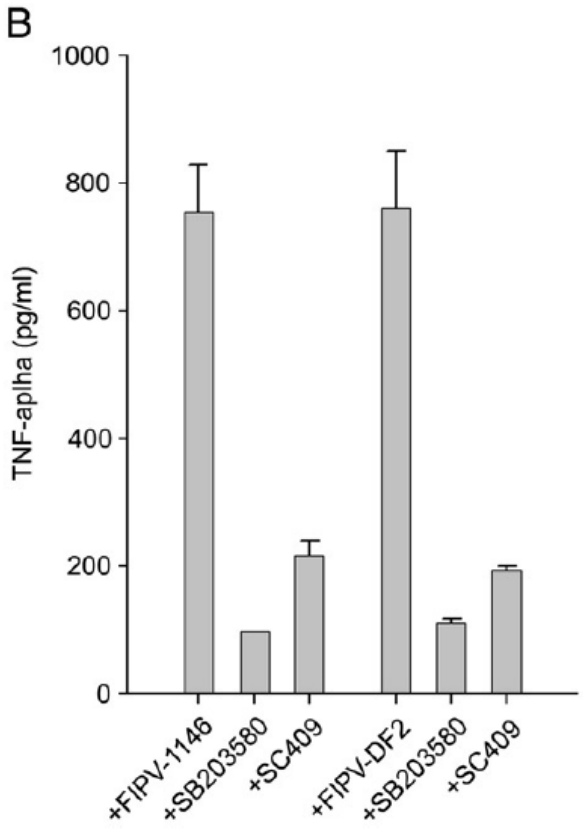

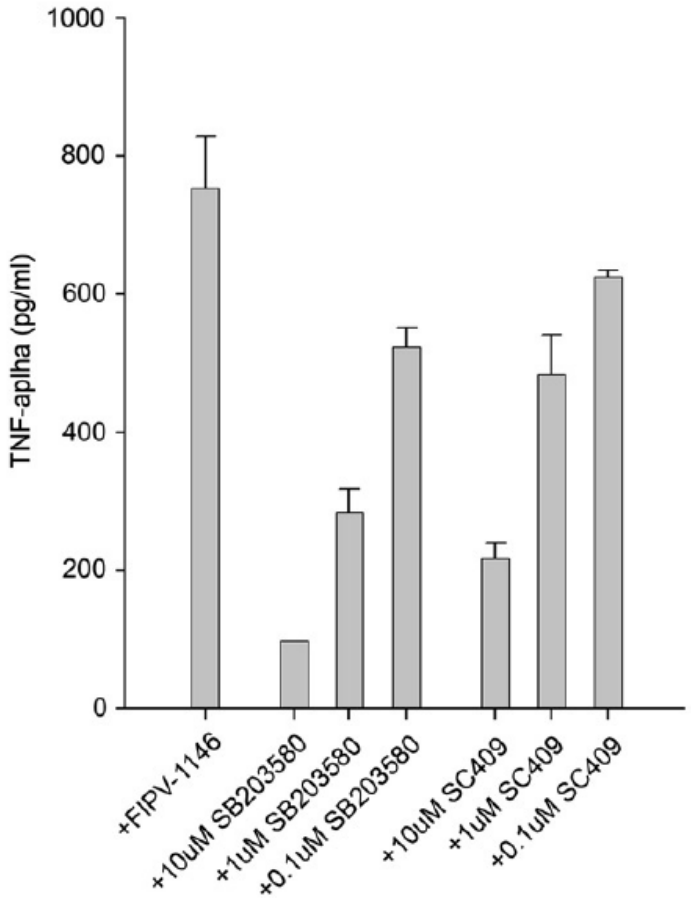

Figure 4.6 FIPV-induced TNF-alpha production is inhibited in a dose-dependent manner by SB 203580 and SC 409. PFBM cells were pretreated with either SB 203580 or SC 409 at a range of concentrations (10 μM, 1 μM or 0.1 μM) or 0.1% DMSO for 2 h before inoculating with FIPV-1146 at an MOI of 100. 24 h p.i. supernatants were collected and TNF-alpha production was quantified by anti-TNF-alpha capture ELISA. TNF-alpha from untreated cells was below the detection limit of the assay (10 pg/ml).

resulted in a 8-fold and 4-fold reduction in TNF-alpha production respectively (Figure 4.5 B). Uninfected cells produced no TNF-alpha, or were below the detection level of the assay. Overall these data indicate that production of the pro-inflammatory cytokine TNF-alpha in FIPV infected PFBM cells is regulated by activation of the p38 MAPK pathway.

To show that the reduction of FIPV-induced TNF-alpha production by SB 203580 and SC 409 was specific to the pyridinyl imidazole inhibitors, PFBM cells were treated with either SB 203580 or SC 409 at a range of concentrations (10 μM, 1 μM or 0.1 μM) or 0.1% DMSO for 2 h before inoculating with FIPV-1146 or FIPV-DF2 at an MOI of 100. As seen in our previous data, PFBM cells which were pretreated with DMSO alone produced significant amounts of TNF-alpha however pretreatment with SB 203580 and SC 409 resulted in a significant reduction in TNF-alpha production in a dose-dependent manner (Figure 4.6).

It is known that individual animals can vary in their reaction to infection by FIPV (21). To determine whether or not FIPV-induced p38 MAPK activation was specific to a single animal, PFBM cells were individually prepared from six additional SPF cats (07PGP2, 07PGV4, 07PGV5, 07FGR2, 07FGV6, 07FJM5). PFBM cells individually purified from each animal were inoculated with FIPV-1146 at an MOI of 100. Untreated cells and infected cells (15 min p.i.) were lysed and analyzed by western blot with the anti-phospho-p38 MAPK mAb (3D7). Consistent with our previous data, untreated cells showed a minimal level of p38 MAPK phosphorylation while addition of FIPV caused a rapid phosphorylation of p38 MAPK in PFBM cells from all six cats (Figure 4.7). Membranes were re-probed with anti-p38 MAPK (N-20) pAb to show that an equal amount of p38 MAPK was present in each sample (Figure 4.7). In addition, the regulation of TNF-alpha production by p38 MAPK was analyzed in PFBM cells from all six SPF cats. PFBM cells from each animal were treated with

10 μM SC 409 or 0.1% DMSO for 2 h before inoculating with FIPV-1146 at an MOI of 100. 24 h p.i. supernatants were collected and analyzed by anti-TNF-alpha capture ELISA. While the baseline level of TNF-alpha production differed slightly amongst all of the cats tested, treatment with the p38 inhibitor SC 409 resulted in the same trend observed in our previous experiments: a significant reduction in TNF-alpha levels (between 3-fold to 8-fold) (Figure 4.8). These data taken together suggest that FIPV-induced activation of the p38 MAPK pathway in PFBM cells represents a common mechanism by which this virus promotes TNF-alpha production in cats.

Cats with FIP have also been reported to show increased levels of the pro-inflammatory cytokines IL-1 beta and IL-6. To investigate whether IL-1 beta and IL-6 production in FIPV-infected PFBM cells is regulated by p38 MAPK activation, PFBM cells were treated with 10 μM of either SB 203580, SC 409 or 0.1% DMSO for 2 h before inoculating with FIPV-1146 at an MOI of 100. 24 h p.i. supernatants were collected and analyzed by anti-IL-1 beta and anti-IL-6 capture ELISA. Infected cells which were pretreated with DMSO alone showed significant production of IL-1 beta (~200 pg/ml) however pretreatment with 10 μM SB 203580 and 10 μM SC 409 resulted in a 7-fold and 4-fold reduction in IL-1 beta production respectively (Figure 4.9). Neither infected nor uninfected PFBM cells produced significant levels of IL-6 (Figure 4.9). Overall, these data indicate that both TNF-alpha and IL-1 beta production in FIPV-infected PFBM cells is regulated by p38 MAPK activation, a situation that does not apply to IL-6.

Modulation of signaling pathways by viruses is becoming recognized as a key pathogenic determinant in viral diseases mediated by aberrant host immunological responses. In the case of FIP, cytokine production is markedly altered between animals with disease as compared to healthy animals, with overproduction of the pro-inflammatory cytokine TNF-alpha in particular being indicative of a poor outcome

(21). Feline TNF-alpha causes apoptosis in feline T-cells (implicating it as the causative agent of T-cell lymphopenia), and upregulates the FIPV receptor APN making target cells more susceptible to infection in vitro (7, 21, 45, 46). It has been shown previously that FIPV-infected monocytes upregulate the expression of TNF-alpha, however the mechanism regulating this process remains undescribed.

In this study we show that infection by FIPV causes a rapid activation of the p38 MAPK pathway in PFBM cells, and that this process directly regulates production of the pro-inflammatory cytokines TNF-alpha and IL-1 beta. As shown in figure 4.1, FIPV-induced p38 MAPK activation in PFBM cells occurs in a biphasic temporal pattern which mimics that observed with other viral pathogens that activate MAPK pathways during infection such as influenza virus. At present we are unable to define the mechanism by which FIPV particles are able to activate the p38 MAPK pathway, however the rapid nature of the initial activation suggests that it occurs early during entry; likely due to interactions between the S protein and its receptor. This model is further supported by the observation that UV-inactivated virus also induce rapid activation of the p38 MAPK pathway. This activation is markedly different than that reported in MHV infected cells, where activation did not occur until 6–12 h p.i., and UV-treated viral particles did not induce phosphorylation of p38 MAPK (2). It is notable that the FIPV receptor APN localizes to lipid rafts (30, 32) which are known to be a signaling portal for the p38 MAPK pathway (4, 15, 33, 44, 49, 54). In fact it has recently been shown that rhinovirus activates the p38 MAPK pathway through the actions of lipid rafts and RhoA (8). Further investigation will be necessary to determine the role of APN and lipid rafts in the initial phase of FIPV-induced p38 MAPK activation and TNF-alpha/IL-1 beta production. Interestingly, UV-inactivated FIPV induced prolonged p38 MAPK activation, rather than the biphasic activation induced by untreated viral particles. This suggests that FIPV may activate p38 MAPK

during entry, but then suppresses p38 MAPK during the early phase of replication. The second phase of FIPV-induced p38 MAPK activation induced by untreated viral particles (6 h p.i.) may be caused by the production of pro-inflammatory cytokines. It has been shown that TNF-alpha can itself activate the p38 MAPK through signaling associated with the cytoplasmic domain of its receptors TNF receptor 1 (TNFR1)-associated death domain protein (TRADD) and TNF receptor-associated factor 2 (TRAF2) (5, 17, 18). Therefore TNF-alpha produced during the initial phase of FIPV-induced p38 MAPK activation, may be the cause of the latter phase of activation. Pretreatment with the pyridinyl imidazole inhibitors SB 203580 and SC 409 blocked production of TNF-alpha and IL-1 beta suggesting that p38 MAPK directly regulates production of the cytokines in FIPV-infected PFBM cells. The upregulation of IL-6 production was not observed in FIPV-infected PFBM cells, suggesting that another cell type may be responsible for its production in cats with FIP. At this time the mechanism by which p38 MAPK regulates pro-inflammatory cytokine production in FIPV-infected PFBM cells is unknown, however regulation of cytokines by MAPKs in analogous systems occurs by affecting either transcriptional regulation, translational regulation, or both (22). For example the recently emerged severe acute respiratory syndrome coronavirus (SARS-CoV) is also known to infiltrate immune cells such as monocytes and macrophages and activate the p38 MAPK pathway (3, 11, 14, 31). SARS-CoV infection causes a p38 MAPK-dependent phosphorylation of downstream transcriptional regulators such as activating transcription factor 1 (ATF-1) and signal transducer and activator of transcription 3 (STAT-3), as well as translational regulators such as MAPK activate protein kinase 2 (MAPKAPK2) and the eukaryotic initiation factor 4E (eIF4E) (27-29). As seen in figure 4.2 it appears that FIPV causes increased p38 MAPK nuclear localization suggesting that the activation of transcription factors likely play a role in pro-inflammatory production in PFBM cells,

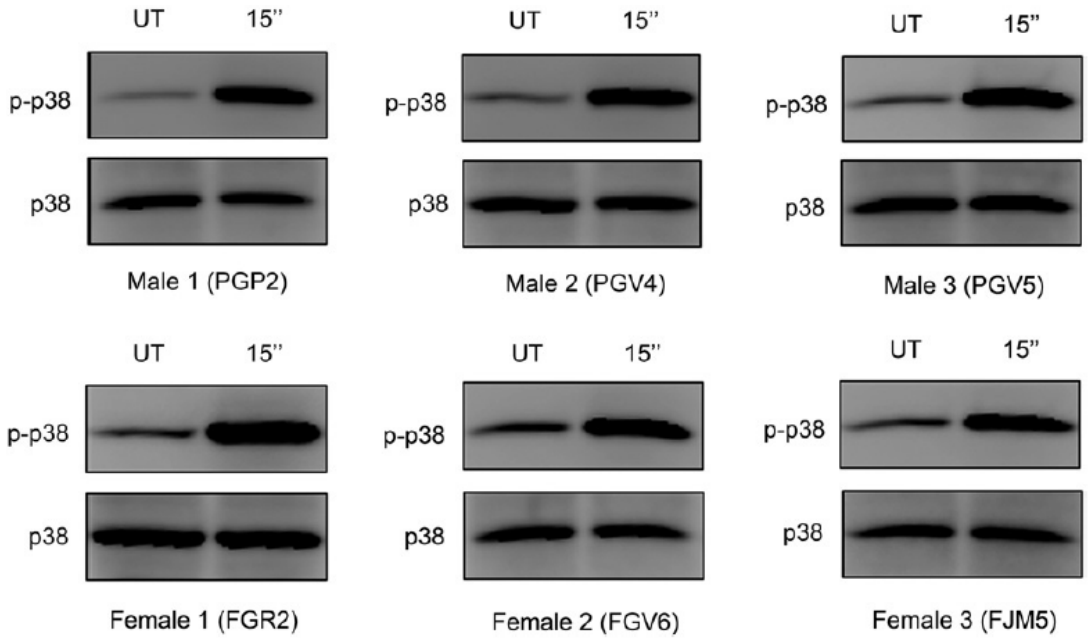

Figure 4.7 FIPV-induced p38 MAPK activation in PFBM cells from six individual SPF cats. PFBM cells were individually prepared from three male (07PGP2, 07PGV4, 07PGV5) and three female (07FGR2, 07FGV6, 07FJM5) SPF cats. Cells from each animal were inoculated with FIPV-1146 at an MOI of 100. 15 min p.i. cells were lysed and analyzed by western blot with the anti-phospho-p38 MAPK mAb (3D7) and re-probed with anti-p38 MAPK (N-20) pAb.

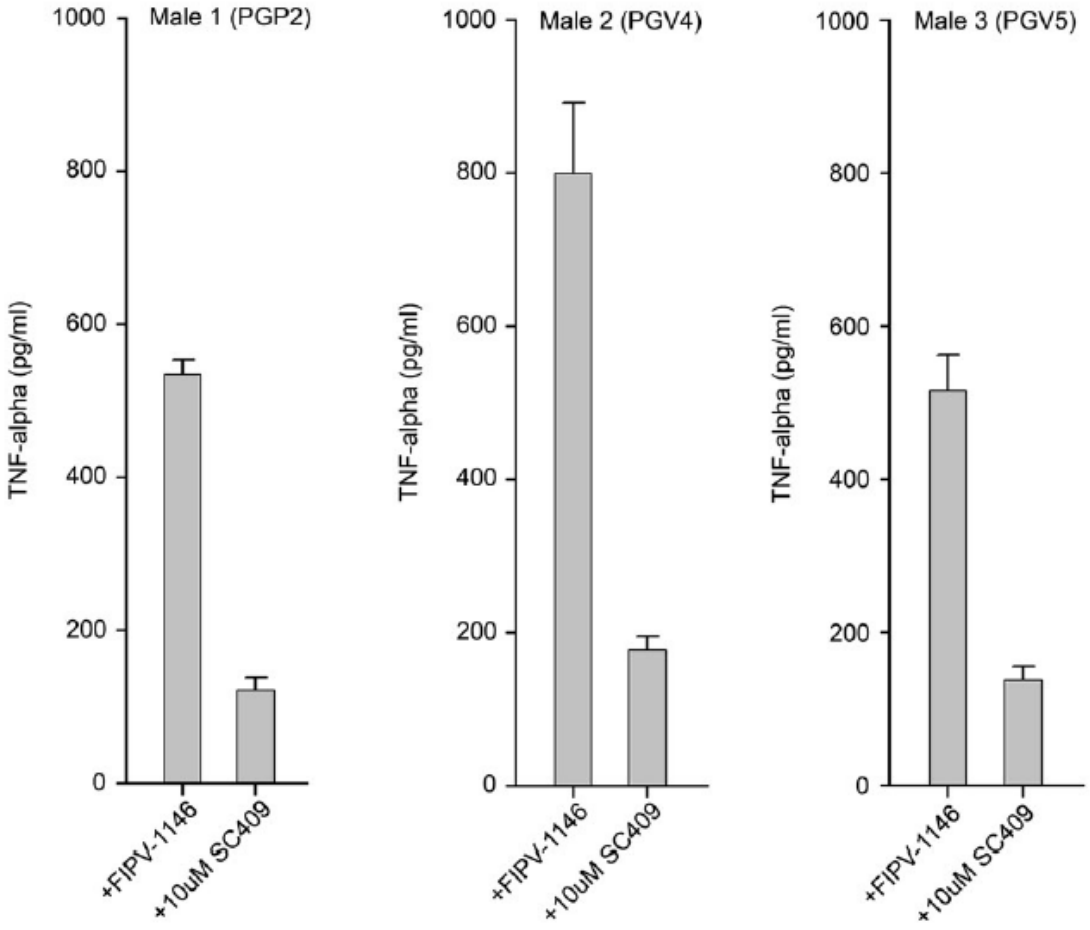

Figure 4.8 FIPV-induced TNF-alpha production by PFBM cells from six SPF cats is inhibited by SC 409. PFBM cells were individually prepared from three male (07PGP2, 07PGV4, 07PGV5) and three female (07FGR2, 07FGV6, 07FJM5) SPF cats. Cells from each animal were inoculated with FIPV-1146 at an MOI of 100. 24 h p.i. supernatants were collected and TNF-alpha production was quantified by anti-TNF-alpha capture ELISA. TNF-alpha from untreated cells was below the detection limit of the assay (10 pg/ml).

Figure 4.8. (continued)

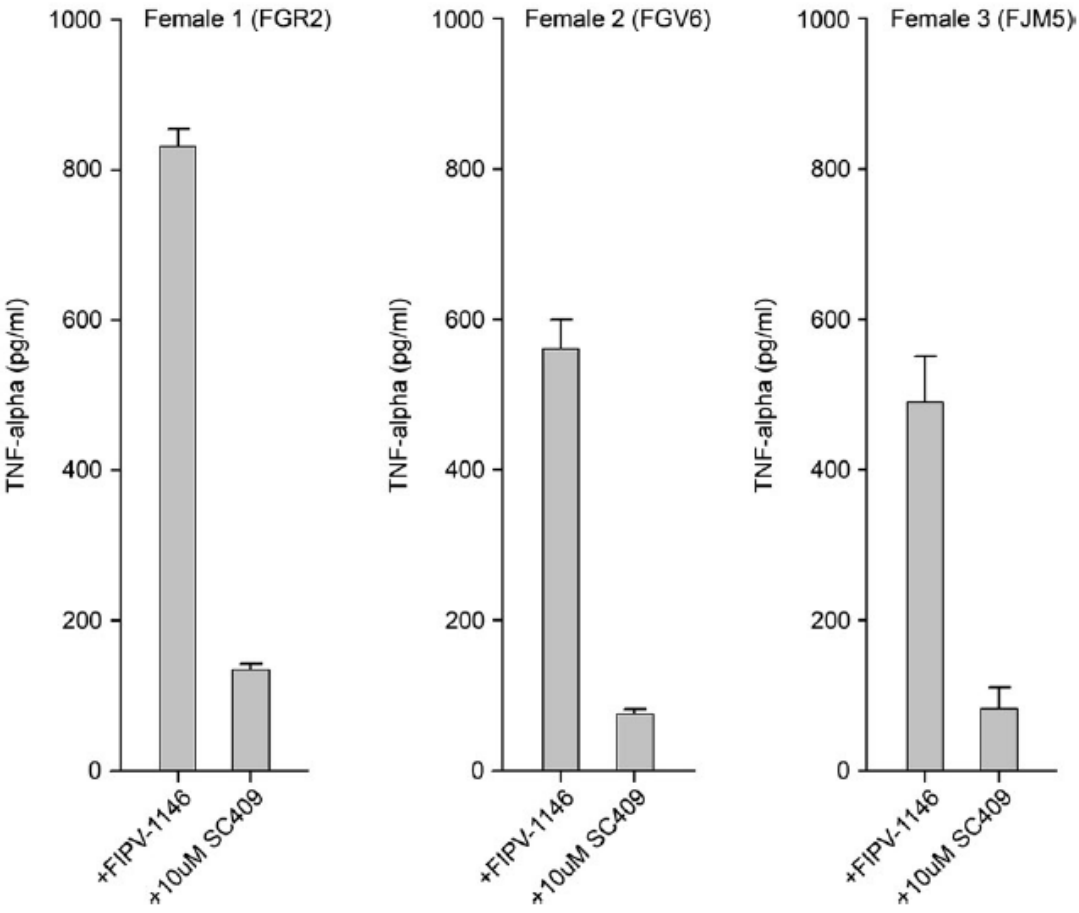

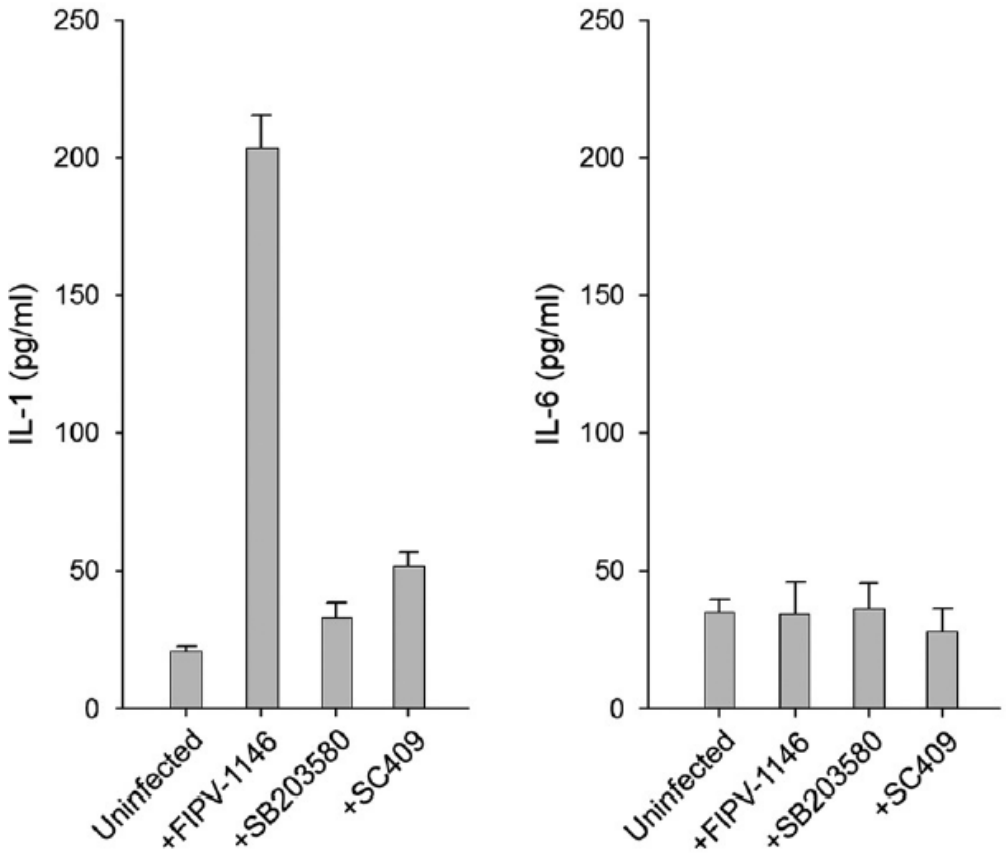

Figure 4.9 Production of IL-l beta and IL-6 by FIPV-infected PFBM cells. PFBM cells were pretreated with 10 μM of either SB 203580 or SC 409 (or 0.1% DMSO as a control) for 2 h before inoculating with FIPV-1146 at an MOI of 100. 24 h p.i. supernatants were collected and IL-1 beta and IL-6 production was quantified by anti IL-1 beta or anti-IL-6 capture ELISA.

however this also does not exclude a role for translational regulation. Future studies examining the role of downstream transcriptional and translational regulators in FIPV-infected PFBM cells should clarify the mechanism regulating this process. Another aspect complicating the treatment of FIP is the diverse reactions to infection displayed by cats with the disease (21). Our results suggest that activation of the p38 MAPK pathway and its regulation of TNF-alpha production is common to PFBM cells of all cats, however further sampling of animals throughout different geographic regions will be required to confirm this conclusion. Pyridinyl imidazole compounds have been shown to be efficacious therapeutic agents for blocking the mediators of chronic inflammatory diseases such as rheumatoid arthritis (22). In fact, several p38 MAPK inhibitors have shown promise in animal models of inflammatory diseases and some have even reached human clinical trials (22). Our results show a clear activation of p38 MAPK by FIPV during infection, and that this activation is responsible for pro-inflammatory cytokine production which is a key contributor to the pathological changes observed in cats with FIP. This raises this possibility that p38 MAPK inhibitors, alone or in conjunction with other therapies, may possess therapeutic benefits in the treatment of cats with FIP.

4.5. Acknowledgments

We thank Marc Antoniak for helpful advice and discussions during the course of this work, and Ed Dubovi for kind provision of reagents. We also thank A Damon Ferguson for technical assistance. ADR was supported grant T32AI007618 (Training in Molecular Virology and Pathogenesis) from the National Institutes of Health. Work in the author's lab was supported by the Winn Feline Foundation and the George Sydney and Phyllis Redmond Miller Trust.

REFERENCES

1. Adamson, A.L., Darr, D., Holley-Guthrie, E., Johnson, R.A., Mauser, A., Swenson, J., Kenney, S., 2000. Epstein–Barr virus immediate-early proteins BZLF1 and BRLF1 activate the ATF2 transcription factor by increasing the levels of phosphorylated p38 and c-Jun N-terminal kinases. J. Virol. 74 (3), 1224–1233.
2. Banerjee, S., Narayanan, K., Mizutani, T., Makino, S., 2002. Murine coronavirus replication-induced p38 mitogen-activated protein kinase activation promotes interleukin-6 production and virus replication in cultured cells. J. Virol. 76 (12), 5937–5948.
3. Belyavsky, M., Belyavskaya, E., Levy, G.A., Leibowitz, J.L., 1998. Coronavirus MHV-3-induced apoptosis in macrophages. Virology 250 (1), 41–49.
4. Calzolari, A., Raggi, C., Deaglio, S., Sposi, N.M., Stafsnes, M., Fecchi, K., Parolini, I., Malavasi, F., Peschle, C., Sargiacomo, M., Testa, U., 2006. TfR2 localizes in lipid raft domains and is released in exosomes to activate signal transduction along the MAPK pathway. J. Cell. Sci. 119 (21), 4486–4498.
5. Carpentier, I., Declercq,W., Malinin, N.L., Wallach, D., Fiers, W., Beyaert, R., 1998. TRAF2 plays a dual role in NF-kappaB-dependent gene activation by mediating the TNFinduced activation of p38 MAPK and IkappaB kinase pathways. FEBS Lett. 425 (2), 195–198.
6. Chu, V., McElroy, L.J., Chu, V., Bauman, B.E., Whittaker, G.R., 2006. The avian coronavirus infectious bronchitis virus undergoes direct low-pH-

dependent fusion activation during entry into host cells. J. Virol. 80 (7), 3180–3188.

7. Dean, G., Olivry, T., Stanton, C., Pedersen, N.C., 2003. In vivo cytokine response to experimental feline infectious peritonitis virus infection. Vet. Microbiol. 97 (1–2), 1–12.
8. Dumitru, C.A., Dreschers, S., Gulbins, E., 2006. Rhinoviral infections activate p38 MAPkinases via membrane rafts and RhoA. Cell. Physiol. Biochem. 17 (3–4), 159–166.
9. Erhardt, A., Hassan, M., Heintges, T., Häussinger, D., 2002. Hepatitis C virus core protein induces cell proliferation and activates ERK, JNK, and p38 MAP kinases together with the MAP kinase phosphatase MKP-1 in a HepG2 Tet-Off cell line. Virology 292 (2), 272–284.
10. Fantuzzi, L., Belardelli, F., Gessani, S., 2003. Monocyte/macrophage-derived CC chemokines and their modulation by HIV-1 and cytokines: a complex network of interactions influencing viral replication and AIDS pathogenesis. 74 5, 719–725.
11. Franks, T., Chong, P.Y., Chui, P., Galvin, J.R., Lourens, R.M., Reid, A.H., Selbs, E., McEvoy, C.P., Hayden, C.D., Fukuoka, J., Taubenberger, J.K., Travis, W.D., 2003. Lung pathology of severe acute respiratory syndrome (SARS): a study of 8 autopsy cases from Singapore. Human Pathol. 34 (8), 743–748.
12. Frevel, M.A., Bakheet, T., Silva, A.M., Hissong, J.G., Khabar, K.S., Williams, B.R., 2003. p38 mitogen-activated protein kinase-dependent and -independent signaling of mRNA stability of AU-rich element-containing transcripts. Mol. Cell. Biol. 23 (2), 425–436.

13. Griego, S.D., Weston, C.B., Adams, J.L., Tal-Singer, R., Dillon, S.B., 2000. Role of p38 mitogen-activated protein kinase in rhinovirus-induced cytokine production by
bronchial epithelial cells. J. Immunol. 165 (9), 5211–5220.

14. Gu, J., Gong, E., Zhang, B., Zheng, J., Gao, Z., Zhong, Y., Zou, W., Zhan, J., Wang, S., Xie, Z., Zhuang, H., Wu, B., Zhong, H., Shao, H., Fang, W., Gao, D., Pei, F., Li, X., He, Z., Xu, D., Shi, X., Anderson, V.M., Leong, A.S., 2005. Multiple organ infection and the pathogenesis of SARS. J. Exp. Med. 202 (3), 415–424.

15. Head, B., Patel, H.H., Roth, D.M., Murray, F., Swaney, J.S., Niesman, I.R., Farquhar, M.G., Insel, P.A., 2006. Microtubules and actin microfilaments regulate lipid raft/caveolae localization of adenylyl cyclase signaling components. J. Biol. Chem. 281 (36), 26391–26399.

16. Holloway, G., Coulson, B.S., 2006. Rotavirus activates JNK and p38 signaling pathways in intestinal cells, leading to AP-1-driven transcriptional responses and enhanced virus replication. J. Virol. 80 (21), 10624–10633.

17. Hsu, H., Xiong, J., Goeddel, D.V., 1995. The TNF receptor 1-associated protein TRADD signals cell death and NF-kappa B activation. Cell 81 (4), 495–504.

18. Hsu, H., Shu, H.B., Pan, M.G., Goeddel, D.V., 1996. TRADD-TRAF2 and TRADD-FADD interactions define two distinct TNF receptor 1 signal transduction pathways. Cell 84 (2), 299–308.

19. Huang, C., Jacobson, K., Schaller, M.D., 2004. MAP kinases and cell migration. J. Cell. Sci. 117 (20), 4619–4628.

20. Kedzierska, K., Crowe, S., 2002. The role of monocytes and macrophages in the pathogenesis of HIV-1 infection. Curr. Med. Chem. 9 (21), 1893–1903. 142.

21. Kiss, I., Poland, A.M., Pedersen, N.C., 2004. Disease outcome and cytokine responses in cats immunized with an avirulent feline infectious peritonitis virus (FIPV)-UCD1 and challenge-exposed with virulent FIPV-UCD8. J. Feline Med. Surg. 6 (2), 89–97.

22. Kumar, S., Boehm, J., Lee, J.C., 2003. p38 MAP kinases: key signalling molecules as therapeutic targets for inflammatory diseases. Nat. Rev. Drug Discov. 2 (9), 717–726.

23. Lee, J., Laydon, J.T., McDonnell, P.C., Gallagher, T.F., Kumar, S., Green, D., McNulty, D., Blumenthal, M.J., Heys, J.R., Landvatter, S.W., Strickler, J.E., McLaughlin, M.M., Siemens, I.R., Fisher, S.M., Livi, G.P., White, J.R., Adams, J.L., Young, P.R., 1994. A protein kinase involved in the regulation of inflammatory cytokine biosynthesis. Nature 372, 739–746.

24. Lee, C., Tomkowicz, B., Freedman, B.D., Collman, R.G., 2005a. HIV-1 gp120-induced TNF-{alpha} production by primary human macrophages is mediated by phosphatidylinositol-3 (PI-3) kinase and mitogen-activated protein (MAP) kinase pathways. J. Leukoc. Biol. 78 (4), 1016–1023.

25. Lee, D.C., Cheung, C.Y., Law, A.H., Mok, C.K., Peiris, M., Lau, A.S., 2005b. p38 mitogenactivated protein kinase-dependent hyperinduction of tumor necrosis factor alpha expression in response to avian influenza virus H5N1. J. Virol. 79 (16), 10147–10154.

26. Leong, A.S., Wong, K.T., Leong, T.Y., Tan, P.H., Wannakrairot, P., 2007. The pathology of dengue hemorrhagic fever. Semin. Diagn. Pathol. 24 (4), 227–236.

27. Mizutani, T., 2007. Signal transduction in SARS-CoV-infected cells. Ann. N. Y. Acad. Sci. 1102, 86–95.

28. Mizutani, T., Fukushi, S., Murakami, M., Hirano, T., Saijo, M., Kurane, I., Morikawa, S., 2004a. Tyrosine dephosphorylation of STAT3 in SARS coronavirus-infected Vero E6 cells. FEBS Lett. 577 (1–2), 187–192.

29. Mizutani, T., Fukushi, S., Saijo, M., Kurane, I., Morikawa, S., 2004b. Phosphorylation of p38 MAPK and its downstream targets in SARS coronavirus-infected cells. Biochem. Biophys. Res. Commun. 319 (4), 1228–1234.

30. Navarrete Santos, A., Roentsch, J., Danielsen, E.M., Langner, J., Riemann, D., 2000. Aminopeptidase N/CD13 is associated with raft membrane microdomains in monocytes. Biochem. Biophys. Res. Commun. 269 (1), 143–148.

31. Nicholls, J., Poon, L.L., Lee, K.C., Ng, W.F., Lai, S.T., Leung, C.Y., Chu, C.M., Hui, P.K., Mak, K.L., Lim,W., Yan, K.W., Chan, K.H., Tsang, N.C., Guan, Y., Yuen, K.Y., Peiris, J.S., 2003. Lung pathology of fatal severe acute respiratory syndrome. Lancet 361 (9371), 1773–1778.

32. Nomura, R., Kiyota, A., Suzaki, E., Kataoka, K., Ohe, Y., Miyamoto, K., Senda, T., Fujimoto, T., 2004. Human coronavirus 229E binds to CD13 in rafts and enters the cell through caveolae. J. Virol. 78 (16), 8701–8708.

33. Olsson, S., Sundler, R., 2006. The role of lipid rafts in LPS-induced signaling in a macrophage cell line. Mol. Immunol. 43 (6), 607–612.

34. Pearson, G., Robinson, F., Beers Gibson, T., Xu, B.E., Karandikar, M., Berman, K., Cobb, M.H., 2001. Mitogen-activated protein (MAP) kinase

pathways: regulation and physiological functions. Endocr. Rev. 22 (2), 153–183.

35. Pedersen, N.C., Black, J.W., Boyle, J.F., Evermann, J.F., McKeirnan, A.J., Ott, R.L., 1984a. Pathogenic differences between various feline coronavirus isolates. Adv. Exp. Med. Biol. 173, 365–380.

36. Pedersen, N.C., Evermann, J.F., McKeirnan, A.J., Ott, R.L., 1984b. Pathogenicity studies of feline coronavirus isolates 79-1146 and 79-1683. Am. J. Vet. Res. 45, 2580–2585.

37. Perlman, S., Gallagher, T., Snijder, E.J., 2008. Nidoviruses. ASM Press, Washington D.C.

38. Raman, M., Chen,W., Cobb, M.H., 2007. Differential regulation and properties of MAPKs. Oncogene 26 (22), 3100–3112.

39. Regan, A., Shraybman, R., Cohen, R.D., Whittaker, G.W., 2008. Differential role for low pH and cathepsin-mediated cleavage of the viral spike protein during entry of serotype II feline coronaviruses. Vet. Microbiol 132, 235–248.

40. Rottier, P.,1999. The molecular dynamics of feline coronaviruses. Vet. Microbiol. 69 (1–2), 117–125.

41. Rottier, P., Nakamura, K., Schellen, P., Volders, H., Haijema, B.J., 2005. Acquisition of macrophage tropism during the pathogenesis of feline infectious peritonitis is determined by mutations in the feline coronavirus spike protein. J. Virol. 79 (22), 14122–14130.

42. Sloan, D.D., Jerome, K.R., 2007. Herpes simplex virus remodels T-cell receptor signaling, resulting in p38-dependent selective synthesis of interleukin-10. J. Virol. 81 (22), 12504–12514.

43. Stoddart, C., Scott, F.W., 1989. Intrinsic resistance of feline peritoneal macrophages to coronavirus infection correlates with in vivo virulence. J. Virol. 63 (1), 436–440.

44. Sugawara, Y., Nishii, H., Takahashi, T., Yamauchi, J., Mizuno, N., Tago, K., Itoh, H., 2007. The lipid raft proteins flotillins/reggies interact with Galphaq and are involved in Gq-mediated p38 mitogen-activated protein kinase activation through tyrosine kinase. Cell. Signal. 19 (6), 1301–1308.

45. Takano, T., Hohdatsu, T., Hashida, Y., Kaneko, Y., Tanabe, M., Koyama, H., 2007a. A "possible" involvement of TNF-alpha in apoptosis induction in peripheral blood lymphocytes of cats with feline infectious peritonitis. Vet. Microbiol. 119 (2–4), 121–131.

46. Takano, T., Hohdatsu, T., Toda, A., Tanabe, M., Koyama, H., 2007b. TNF-alpha, produced by feline infectious peritonitis virus (FIPV)-infected macrophages, upregulates expression of type II FIPV receptor feline aminopeptidase N in feline macrophages. Virology 364 (1), 64–72.

47. Vennema, H., Poland, A., Foley, J., Pedersen, N.C., 1998. Feline infectious peritonitis viruses arise by mutation from endemic feline enteric coronaviruses. Virology 243 (1), 150–157.

48. Wang, W.H., Grégori, G., Hullinger, R.L., Andrisani, O.M., 2004. Sustained activation of p38 mitogen-activated protein kinase and c-Jun N-terminal kinase pathways by hepatitis B virus X protein mediates apoptosis via induction of Fas/FasL and tumor necrosis factor (TNF) receptor 1/TNF-alpha expression. Mol. Cell. Biol. 24 (23), 10352–10365.

49. Wang, R., Town, T., Gokarn, V., Flavell, R.A., Chandawarkar, R.Y., 2006. HSP70 enhances macrophage phagocytosis by interaction with lipid raft-

associated TLR-7 and upregulating p38 MAPK and PI3K pathways. J. Surg. Res. 136 (1), 58–69.

50. Weiss, R., Scott, F.W., 1981. Pathogenesis of feline infectious peritonitis: pathologic changes and immunofluorescence. Am. J. Vet. Res. 42 (12), 2036–2048.

51. Whitmarsh, A.J., 2007. Regulation of gene transcription by mitogen-activated protein kinase signaling pathways. Biochim. Biophys. Acta 1773 (8), 1285–1298.

52. Yurochko, A.D., Huang, E.S., 1999. Human cytomegalovirus binding to human monocytes induces immunoregulatory gene expression. J. Immunol. 162 (8), 4806–4816.

53. Zachos, G., Clements, B., Conner, J., 1999. Herpes simplex virus type 1 infection stimulates p38/c-Jun N-terminal mitogen-activated protein kinase pathways and activates transcription factor AP-1. J. Biol. Chem. 274 (8), 5097–5103.

54. Zeidan, A., Javadov, S., Chakrabarti, S., Karmazyn, M., 2008. Leptin-induced cardiomyocyte hypertrophy involves selective caveolae and RhoA/ROCK-dependent p38 MAPK translocation to nuclei. Cardiovasc. Res. 77 (1), 64–72.

CHAPTER FIVE

CONCLUSION

5.1 Conversion of FECV to FIPV

Feline enteric coronavirus (FECV) infection is ubiquitous in domestic and wild cats throughout the world (2). Conversion of FECV to feline infectious peritonitis virus (FIPV) is the cause of feline infectious peritonitis (FIP), however the factors controlling this process are not understood (25). The inability to distinguish between FECV and FIPV is a major reason why diagnosing FIP is extremely difficult. Currently FIP can be confirmed by positive anti-feline coronavirus immunofluorescent staining of primary monocytes (positive prediction value = 1.00), however false negatives are common with this method (negative prediction value = 0.57) (6). Post-mortem histopathological analysis can confirm cases of FIP with absolute certainty; however this is of little use to veterinarians attempting to treat their patient (6). A simple PCR-based test which could identify the specific mutations responsible for conversion of FECV to FIPV would therefore be invaluable.

Using reverse genetics and spike protein chimeras, mutations controlling the conversion of FECV to FIPV have previously been narrowed down to the S2 region of the spike protein for FCoV-2 (18). The S2 region is responsible for facilitating membrane fusion, suggesting that an alteration in the fusogenic properties of the spike protein could be responsible for the switch. Data in this thesis demonstrates a distinct difference in the requirement for cathepsin cleavage of the spike protein for FECV-1683 and FIPV-1146. FECV-1683 was shown to require cleavage by both cathepsin L (catL) and cathepsin B (catB). FIPV-1146 also requires catB cleavage, but appears to have shed its reliance on catL cleavage. This data was mirrored by the ability of both catL and catB to cleave within the S2 region of FECV-1683 spike, whereas only catB could cleave within the S2 region of the FIPV-1146 spike protein. Also shown here is that FECV-1683 requires low pH for spike protein-mediated fusion to occur, while FIPV-1146 is apparently able to fuse at or near neutral pH. It is possible that the

differential cleavage within the S2 region is responsible for altering the pH-dependent fusogenic properties of the spike protein, thereby fundamentally altering viral tropism.

Within S2 there are only 14 amino acid substitutions between FECV-1683 and FIPV-1146. Our data suggests that one or more mutations within a catL cleavage site might control the switch from FECV to FIPV. CatL has been shown to preferentially cleave at sites with an arginine or lysine at P1, and a bulky hydrophobic residue at P2 (i.e. phenylalanine, tryptophan, tyrosine), and no bulky hydrophobic residues at P3 or P4 (4). An examination of the S2 region of the FECV-1683 spike protein uncovered eight potential catL sites. Of these eight potential sites, only one is mutated in the S2 region of FIPV-1146 (R961G) (Figure 5.1). Interestingly this particular arginine is conserved amongst the spike protein of all reported coronavirus spike proteins (3). The arginine is directly adjacent of the putative coronavirus spike protein fusion peptide, and cleavage at this site has recently been shown to be required for the fusion of coronaviruses such as SARS-CoV and IBV (3, 12, 27). Recent sequencing efforts in our laboratory have also uncovered another FIPV isolate with a mutation at this arginine, only the second such example ever to be reported in a coronavirus (11).

If this conserved arginine is required for coronavirus spike protein-mediated fusion, how can it be mutated in viable FIPV isolates? Data in this thesis also shows that catB is able to cleave in the S2 region of both the FECV-1683 and FIPV-1146 spike proteins, at the same or a closely adjacent site. It is therefore possible that while mutation of the conserved arginine in FIPV-1146 disrupts the catL site, the protein shifts its proteolytic activation solely to catB. CatB also preferentially cleave at sites with an arginine or lysine at the P1 position, however it is unique among the cathepsin family proteases in that in can tolerate an arginine or lysine at the P2 position. An examination of the S2 region of the FIPV-1146 spike protein reveals that a potential catB cleavage site remains intact site just two amino acids upstream of the disrupted

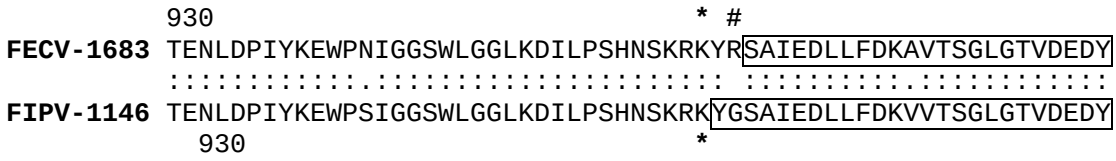

Figure 5.1 Sequence alignment of potential cathepsin cleavage sites upstream of the fusion peptide in the FECV-1683 and FIPV-1146 spike proteins. Potential cathepsin L cleavage sites (#) and cathepsin B cleavage sites (*) are denoted. The putative fusion peptide is boxed. The spike protein of FECV-1683 contains the conserved cleavage arginine at the P1 position of a potential cathepsin L site, directly upstream of the fusion peptide. A mutation in the spike protein of FIPV-1146 (R961G) disrupts the potential cathepsin L cleavage site, while maintaining a potential cathepsin B cleavage site. In this model, two additional amino acids would be added to the N-terminus of the FIPV-1146 fusion peptide.

catL site (Figure 5.1). It is possible that destruction of the catL site in the spike protein of in FIPV-1146 shifts cleavage upstream to the catB site. If this occurred then the fusion peptide would be modified by the addition of two amino acids to the N-terminus (i.e. Y960, G961) (Figure 5.1).

It is known that tyrosine and glycine residues are critical amino acids for the function of other viral fusion peptides (26). In fact, recent studies in our laboratory using liposomal fusion assays have shown that the endogenous FECV fusion peptide requires low pH to mediate fusion; however addition of an YG motif to the N-terminus facilitates efficient fusion at neutral pH (17). Taken together this suggests a model in which FECV requires endocytosis and trafficking to late endosomes in order to contact cathepsin L and low pH, while FIPV is able to fuse at or near the cell surface (Figure 5.2). This could explain how FIPV is able to infect immune cells such as macrophages, which rely upon the harsh environment of a lysosome to disable viral pathogens.

To test this model it will be necessary to pinpoint the cathepsin cleavage sites in the FECV-1683 and FIPV-1146 spike proteins. This may be accomplished purifying spike protein, cleaving with either catL or catB, and subjecting the fragments to N-terminal sequencing. Purification of the spike protein may be accomplished by immunoprecipitation from viral particles using a monoclonal anti-spike antibody, or by expressing and purifying recombinant protein. If the latter method is employed, it will be necessary to remove the transmembrane and cytoplasmic domain in order to facilitate secretion of the protein. This method will also require the addition of a trimerization sequence in order to achieve structural authenticity. In addition, expression in either insect cells (i.e. baculovirus, or S2

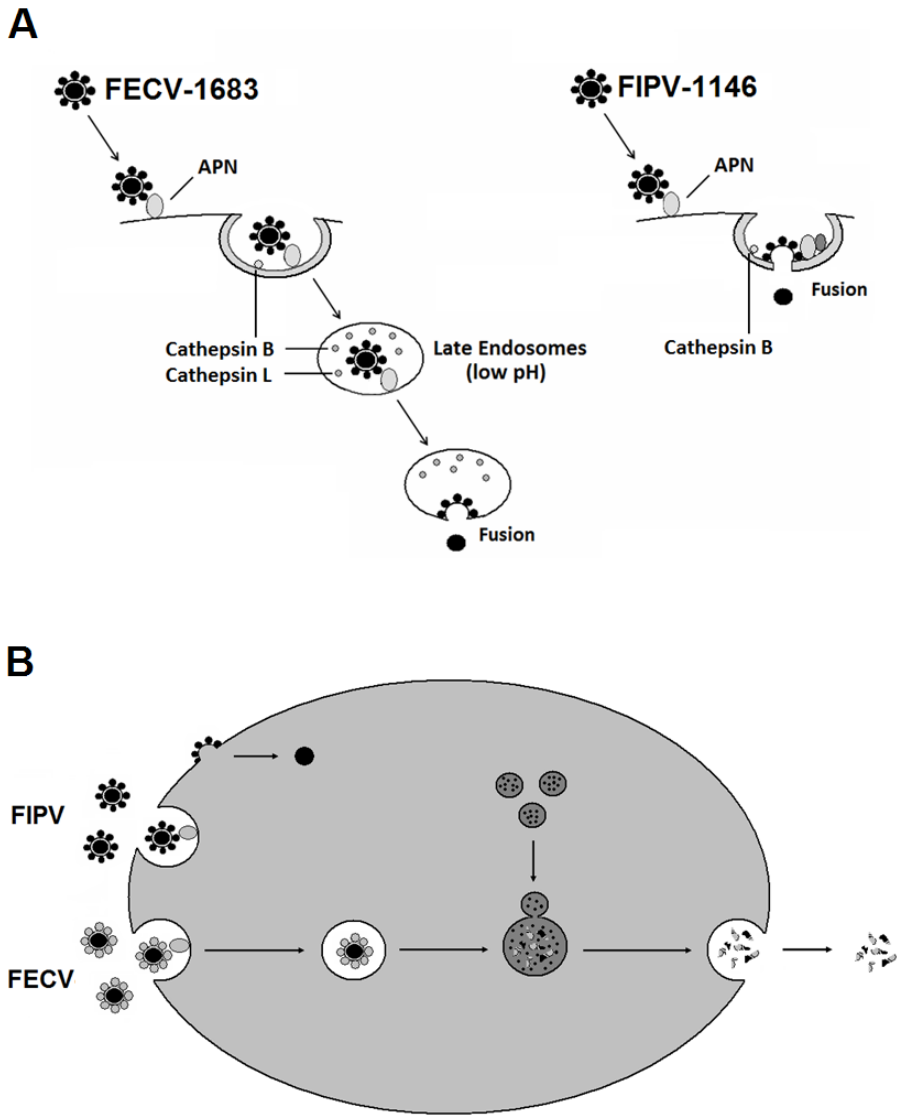

Figure 5.2 A model to explain the different tropisms of FECV and FIPV. FECV binds its receptor Aminopeptidase N (APN) and is endocytosed into the cell. The FECV spike protein requires cathepsin L, cathepsin B and low pH for fusion to occur. FIPV also bind APN, but is able to fuse at the surface due to its modified fusion peptide (A). In a macrophage, this differential entry pathway allows FIPV to avoid destruction by lysosomes (B).

drosophila) or mammalian cells (i.e. 293T cell expression) will be necessary to ensure glycosylation and proper folding of the spike protein.

The recent advent of a feline coronavirus reverse genetics system allows the production of viral particles with mutated spike proteins. In will be interesting to test the phenotype of FECV-1683 viral particles expressing the aforementioned R961G mutation in the spike protein, as well as FIPV-1146 particles with the G961R reversion, in immune cells. In addition particles with the corresponding spike mutation may be produced by the commonly employed retrovirus or VSV pseduovirus systems.

5.2 Dendritic cells and pathogenesis

FIPV is phenotypically distinguished by its ability to infect immune cells, traditionally assumed to be macrophages and monocytes in vivo (20). In this thesis, it is shown that the lectin DC-SIGN is required for efficient cellular entry into immune cells. DC-SIGN is expressed on macrophages, but even more highly expressed on dendritic cells. The role of dendritic cells in FIP has yet to be studied; however they remain a possible "ground zero" for the propagation of FIPV mutants. Dendritic cells are produced in a so-called "immature" form in which they sample their extracellular environment by endocytosis (23). If they contact and recognize a threat (e.g. bacterial lipopolysaccharide, viral antigen, etc.) they become activated, or "mature" dendritic cells. Unlike macrophages, activated dendritic cells migrate from their respective tissue to the lymph nodes in order to elicit an immune response (8). This is significant since the lymph nodes have been implicated as an epicenter of FIPV infection in vivo (16). It is therefore possible that dendritic cells which become infected by FIPV in the gut, then migrate to the lymph node thereby spreading the virus systemically.

The majority of data in this thesis was generated using human DC-SIGN (hDC-SIGN) since feline DC-SIGN (fDC-SIGN) had yet to be characterized. However a search of recently available genomic shotgun sequencing data identified fDC-SIGN (Appendix 1). Studies on the interactions of FIPV and fDC-SIGN are likely to yield interesting results in the future.

In addition to facilitating the systemic spread of FIPV, dendritic cells may also play a key role in outcome of disease. Dendritic cells control the type of T-helper cell differentiation (T_h1 vs. T_h2) in vivo by means of cytokine production (9). As previously discussed, the type of immune response mounted against feline coronavirus infection has a decisive role in the eventual outcome of disease. Therefore FIPV-infected dendritic cells are likely to play a vital role in FIP pathogenesis early during infection. Examination of the cytokines produced by FIPV-infected dendritic cells in vitro may illuminate the contribution of these cells in controlling the T-helper cell differentiation.

5.3 Potential treatment strategies for FIP

FIP is a significant disease of domestic cats, with some populations seeing disease incidence up to a 12%, depending on breed and age (2). There are currently no effective treatments for FIP, and euthanasia is recommended for cats with the disease (1). The development of an effective vaccine has proven elusive. Early vaccine candidates were found to enhance disease, rather than prevent it, by the process of antibody-dependent enhancement of macrophage infection (15). Currently there is only one licensed vaccine on the market called Primucell FIP (Pfizer), however its use is not recommended by the American Association of Feline Practitioners Feline Vaccine Advisory Panel (1). The vaccine is a live-modified temperature sensitive vaccine based on a serotype 2 feline coronavirus, and therefore

does not cross-protect against the more common serotype 1 strains (15). In addition, the vaccine cannot be administered until 16 weeks of age, when most kittens are already seropositive for feline coronavirus (15). Depending on disease severity, treatment may be attempted with immunosuppressants such as glucocorticoids and cyclophosphamide, however this will not prevent an eventual fatal outcome (1).

This thesis identifies and characterizes two specific targets which could be explored for their potential therapeutic value in patients with FIP. The first target is cathepsin B, which is shown here to be required for infection by feline coronaviruses. This work demonstrates that the feline coronavirus spike protein is cleaved during cellular entry by cathepsin B (catB), and that inhibiting this protease blocks viral infection in primary immune cells. If a cat diagnosed with FIP were treated with a general cysteine protease inhibitor (e.g. E-64-d), or a specific catB inhibitor (e.g. CA074-Me), it might inhibit viral infection. If infection was halted, the use of conjunctive immunosuppressive therapy might then be able to treat the underlying disease process, and allow damaged tissue to heal. Multiple studies have documented the efficacy and safety of these cathepsin protease inhibitors in mice (5, 7, 10, 13, 14, 21, 22, 24). In fact, treatment of infected mice with the cysteine protease inhibitor E-64-d has been shown to switch the host immune response from a T_h2 antibody-mediated response, to a T_h1 cell-mediated response (13). This is noteworthy considering that a strong T_h1 response has been correlated with immunity to FIP; while a strong T_h2 response has been correlated with the development of FIP (15).

Another potential therapeutic target to explore is the activation of p38 MAPK in FIPV-infected immune cells. It is shown in this thesis that FIPV activates the p38 MAPK signaling pathway in immune cells, resulting in the production of the pro-inflammatory cytokines TNFα and IL-1β. The specific p38 MAPK inhibitors used in this study have been shown to be efficacious and nontoxic in vivo (19, 28). If a cat

diagnosed with FIP were treated with a p38 inhibitor (e.g. SC-409), this may reduce the amount of pro-inflammatory cytokines produced in the patient. In combination with immunosuppressive therapy, or an anti-viral such as E-64-d, this treatment may have potential therapeutic value in cats with FIP.

Pre-clinical toxicity and pharmacokinetic analyses are planned in cats to demonstrate the efficacy and safety of E-64-d, CA074-Me, and SC-409. Oral, subcutaneous, intramuscular, and intravenous methods of administration will be tested. If no toxicity is observed, and the inhibitors are bioactive in vivo, then double-blinded placebo controlled studies will be conducted with SPF cats experimentally infected with FIPV. Cats would be treated with either cathepsin inhibitor, p38 MAPK inhibitor, both, or placebo, with or without conjunctive immunosuppressive therapy. The development and severity of disease would be monitored to determine the therapeutic value of these treatments. If any of these treatments are successful in alleviating disease in an experimental infection, then patients with confirmed cases of FIP (by immunofluorescent staining of primary monocytes) at the Cornell University Hospital could be enrolled for a clinical trial.

In summation, the difficulty in treating FIP is akin to that of human immunodeficiency virus (HIV) in humans. Both diseases are caused by a virus with 100% mortality rates, and both have proven refractive to the development of an effective vaccine. In the case of HIV, treatment has defaulted to an array of antivirals (including protease inhibitors) which have been applied with varying degrees of success at prolonging and improving the quality of life for patients. This may be the best approach for the treatment of cats with FIP. The novel treatment strategies recommended in this thesis may improve the quality of life in cats with FIP, and at best, could completely alleviate disease.

REFERENCES

1. Cornell University Feline Health Center. 2008, Feline Infectious Peritonitis (FIP).
2. Addie, D., S. Belak, C. Boucraut-Baralon, H. Egberink, T. Frymus, T. Gruffydd-Jones, K. Hartmann, M. J. Hosie, A. Lloret, H. Lutz, F. Marsilio, M. G. Pennisi, A. D. Radford, E. Thiry, U. Truyen, and M. C. Horzinek. 2009. Feline infectious peritonitis ABCD guidelines on prevention and management. J Feline Med Surg 11:594-604.
3. Belouzard, S., Chu, V., Whittaker, G. 2009. Activation of the SARS coronavirus spike protein via sequential proteolytic cleavage at two distinct sites. Proc Natl Acad Sci U S A 106:5871-6.
4. Choe, Y., Leonetti, F., Greenbaum, D., Lecaille, F., Bogyo, M., Brömme, D., Ellman, J., Craik, C. 2006 Substrate profiling of cysteine proteases using a combinatorial peptide library identifies functionally unique specificities. J Biol Chem 281:128424-32.
5. Doh-ura, K., Ishikawa, K., Murakami-Kubo, I., Sasaki, K., Mohri, S., Race, R., Iwaki, T. 2004. Treatment of transmissible spongiform encephalopathy by intraventricular drug infusion in animal models. J Virol 78:4999-5006.
6. Hartmann, K., Binder, C., Hirschberger, J., Cole, D., Reinacher, M., Schroo, S., Frost, J., Egberink, H., Lutz, H., Hermanns, W. 2003. Comparison of different tests to diagnose feline infectious peritonitis. J Vet Intern Med 17:781-90.
7. Hook, V., Kindy, M., Hook, G. 2008. Inhibitors of cathepsin B improve memory and reduce beta-amyloid in transgenic Alzheimer disease mice

expressing the wild-type, but not the Swedish mutant, beta-secretase site of the amyloid precursor protein. J Biol Chem 283:7743-53.

8. Johnson, L., Jackson, D. 2008. Cell traffic and the lymphatic endothelium. Ann N Y Acad Sci:119-33.

9. Kaiko, G., Horvat, J., Beagley, K., Hansbro, P. 2008. Immunological decision-making: how does the immune system decide to mount a helper T-cell response. Immunology 123:326-38.

10. Komatsu, K., Inazuki, K., Hosoya, J., Satoh, S. 1986. Beneficial effect of new thiol protease inhibitors, epoxide derivatives, on dystrophic mice. Exp Neurol 91:23-9.

11. Licitra, B., Whittaker, G. 2009. Unpublished data.

12. Madu, I., Roth, S., Belouzard, S., Whittaker, G. 2009. Characterization of a highly conserved domain within the severe acute respiratory syndrome coronavirus spike protein S2 domain with characteristics of a viral fusion peptide. J Virol 83:7411-21.

13. Maekawa, Y., Himeno, K., Ishikawa, H., Hisaeda, H., Sakai, T., Dainichi, T., Asao, T., Good, R., Katunuma, N. 1998. Switch of CD4+ T cell differentiation from Th2 to Th1 by treatment with cathepsin B inhibitor in experimental leishmaniasis. J Immunol 161:2120-7.

14. Morimoto, M., Tanabe, F., Kasai, H., Ito, M. 2007. Effect of a thiol proteinase inhibitor, E-64-d, on susceptibility to infection with Staphylococcus aureus in Chediak-Higashi syndrome (beige) mice. Int Immunopharmacol 7:973-80.

15. Pedersen, N. C. 2009. A review of feline infectious peritonitis virus infection: 1963-2008. J Feline Med Surg 11:225-58.

16. Perlman, S., Dandekar, A. 2005 Immunopathogenesis of coronavirus infections: implications for SARS. Nat Rev Immunol 12:917-27.

17. Roth, S., Whittaker, G. 2009. Unpublished data.

18. Rottier, P., Nakamura, K., Schellen, P., Volders, H., Haijema, B. 2005 Acquisition of macrophage tropism during the pathogenesis of feline infectious peritonitis is determined by mutations in the feline coronavirus spike protein. J Virol 79:14122-30.

19. Schindler, J., Monahan, J., Smith, W. 2007. p38 pathway kinases as anti-inflammatory drug targets. J Dent Res 86:800-11.

20. Stoddart, C., Scott, F. 1989 Intrinsic resistance of feline peritoneal macrophages to coronavirus infection correlates with in vivo virulence. J Virol 63:436-40.

21. Tsubokawa, T., Solaroglu, I., Yatsushige, H., Cahill, J., Yata, K., Zhang, J. 2006. Cathepsin and calpain inhibitor E64d attenuates matrix metalloproteinase-9 activity after focal cerebral ischemia in rats. Stroke 37:1888-94.

22. Van Acker, G., Saluja, A., Bhagat, L., Singh, V., Song, A., Steer, M. 2002. Cathepsin B inhibition prevents trypsinogen activation and reduces pancreatitis severity. Am J Physiol Gastrointest Liver Physiol 283:794-800.

23. van Niel, G., Wubbolts, R., Stoorvogel, W. 2008. Endosomal sorting of MHC class II determines antigen presentation by dendritic cells. Curr Opin Cell Biol 20:437-44.

24. Vasiljeva, O., Reinheckel, T., Peters, C., Turk, D., Turk, V., Turk, B. 2007. Emerging roles of cysteine cathepsins in disease and their potential as drug targets. Curr Pharm Des 13:387-403.

25. Vennema, H., Poland, A., Foley, J., Pedersen, N. 1998 Feline infectious peritonitis viruses arise by mutation from endemic feline enteric coronaviruses. Virology 243:150-7.

26. White, J., Delos, S., Brecher, M., Schornberg, K. 2008. Structures and mechanisms of viral membrane fusion proteins: multiple variations on a common theme. Crit Rev Biochem Mol Biol 43:189-219.

27. Yamada, Y., Liu, D. 2009 Proteolytic activation of the spike protein at a novel RRRR/S motif is implicated in furin-dependent entry, syncytia formation and infectivity of coronavirus infectious bronchitis virus in cultured cells. J Virol Epub ahead of print.

28. Yu, J., Tripp, C., Russell, J. 2003. Regulation and phenotype of an innate Th1 cell: role of cytokines and the p38 kinase pathway. J Immunol 171:6112-8.

APPENDIX 1

IDENTIFICATION OF FELINE DC-SIGN

Dendritic cell-specific intercellular adhesion molecule-3-grabbing non-integrin (DC-SIGN), also known as CD209, is a C-type lectin expressed on the surface of a variety of immune cells. DC-SIGN non-specifically binds glycosylated proteins in a calcium-dependent manner, and is an integral part of the immune system's ability to sample the host environment. It is conserved in a wide range of mammals including humans and other primates, dogs, pigs, cows, horses and mice. DC-SIGN has not been identified in felines; however both feline immunodeficiency virus (FIV) and feline infectious peritonitis virus (FIPV) have been shown to interact with human DC-SIGN (hDC-SIGN) in vitro.

Shotgun sequencing data of the feline genome has recently been released at 2X coverage, though annotation has yet to be completed. In order to identify feline DC-SIGN (fDC-SIGN), feline genomic sequence was analyzed using the NCBI BLAST search engine with the canine DC-SIGN sequence as a template. From this search the feline DC-SIGN gene was assembled with 98% intron coverage from 4 sections of shotgun sequencing data (gb|ACBE01052350.1| Felis catus c495301847.Contig1b10, gb|AANG01184685.1| Felis catus cont1.184684, gb|ACBE01052349.1| Felis catus c448001196.Contig1, gb|AANG01554893.1| Felis catus cont1.554892). Reverse-transcription PCR (RT-PCR) primers were designed from this sequence (5'fDCSIGN-fwd: ATGTGTGACCCCAAGGAGCCGGAT, and 3'fDCSIGN-rev: TCAGAGGCC CGGGCAGGGGGACGA). Primary feline blood mononuclear cells were isolated as previously described and RNA was extracted using the QIAGEN RNA extraction kit as specified by the manufacturer. RT-PCR yielded a 0.8 kb band which was subsequently cloned into pTOPO2.1. Sequencing using the pTOPO universal primers T7 and SP6 confirmed the identity of the band as feline DC-SIGN (Figure A1.1).

fDC-SIGN is most closely related to canine DC-SIGN (85.7%), porcine DC-SIGN (62.5%), bovine DC-SIGN (62.5%) and equine DC-SIGN (59.4%) (Figure

A1.3A). fDC-SIGN shares only 41.8% homology with hDC-SIGN (Figure A1.3A). Similar to other DC-SIGN sequences which have been reported, fDC-SIGN possesses eight conserved cysteines, and nine acidic amino acids involved in calcium binding (Figure A1.2).

The fDC-SIGN gene was subcloned into the pEF4-myc-his vector, and then subcloned into the mammalian expression vector pCDNA3.1 while retaining the C-terminal myc tag. fDC-SIGN-myc was expressed in murine NIH-3T3 cells using lipofectamine transfection (Figure A1.4). Studies are currently underway to examine the role of fDC-SIGN in the entry of FIPV.

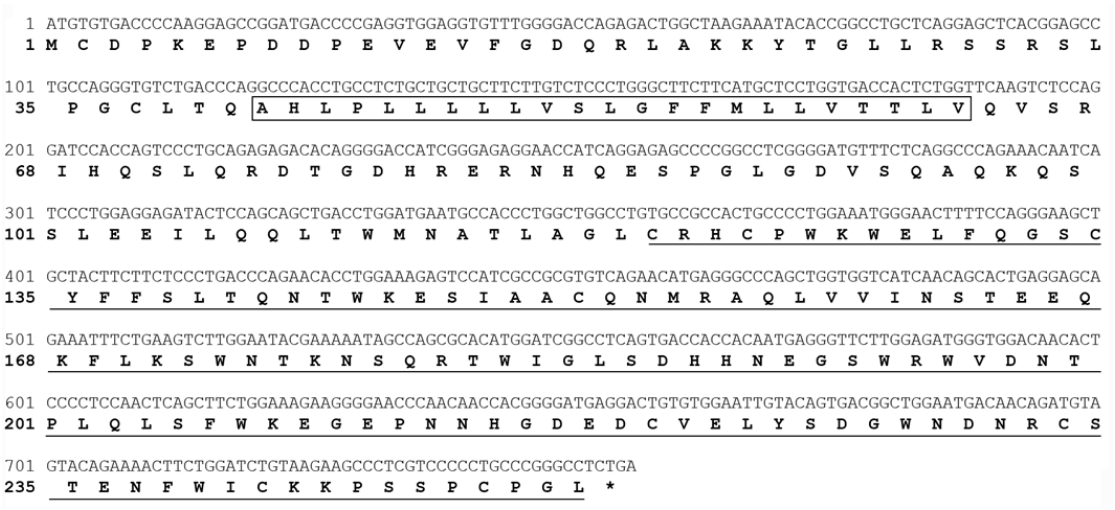

Figure A1.1 The nucleotide and amino acid sequence of feline DC-SIGN. The nucleotide sequence of feline DC-SIGN (fDC-SIGN) is shown as the top line in regular font. The amino acid sequence of fDC-SIGN is shown as the bottom line in bolded font. The transmembrane domain is boxed, and the glycan binding domain is underlined.

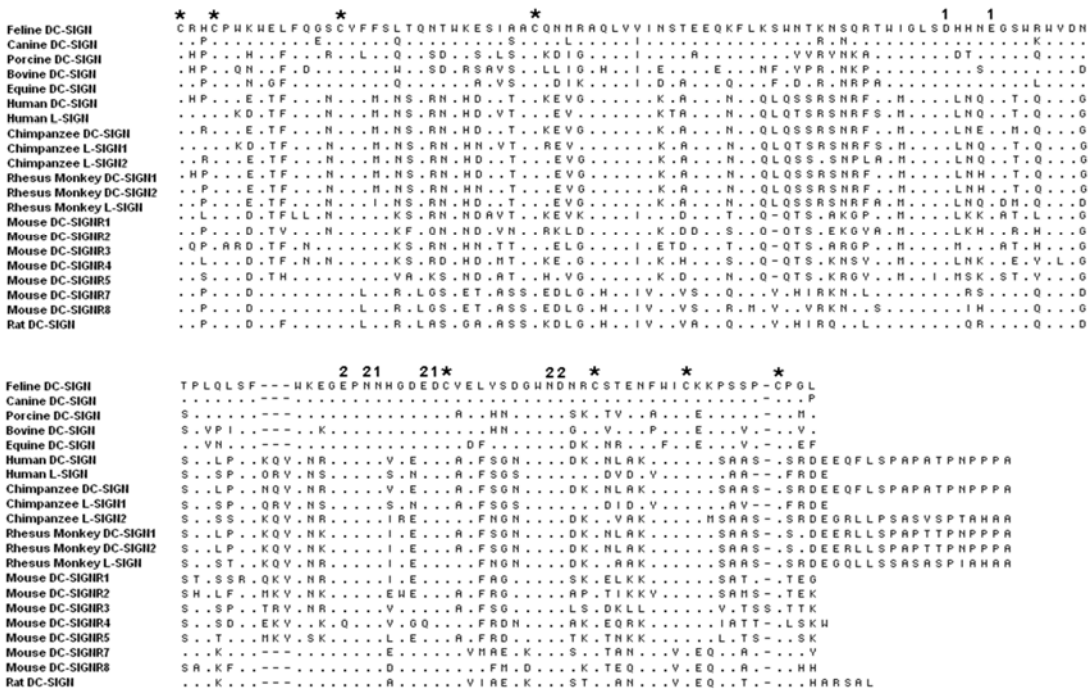

Figure A1.2 Alignment of DC-SIGN sequences. fDC-SIGN is shown aligned with significant DC-SIGN sequences from other mammals. Also shown are the conserved cysteines (*), and the amino acids involved in the first (1) and second (2) calcium-binding sites.

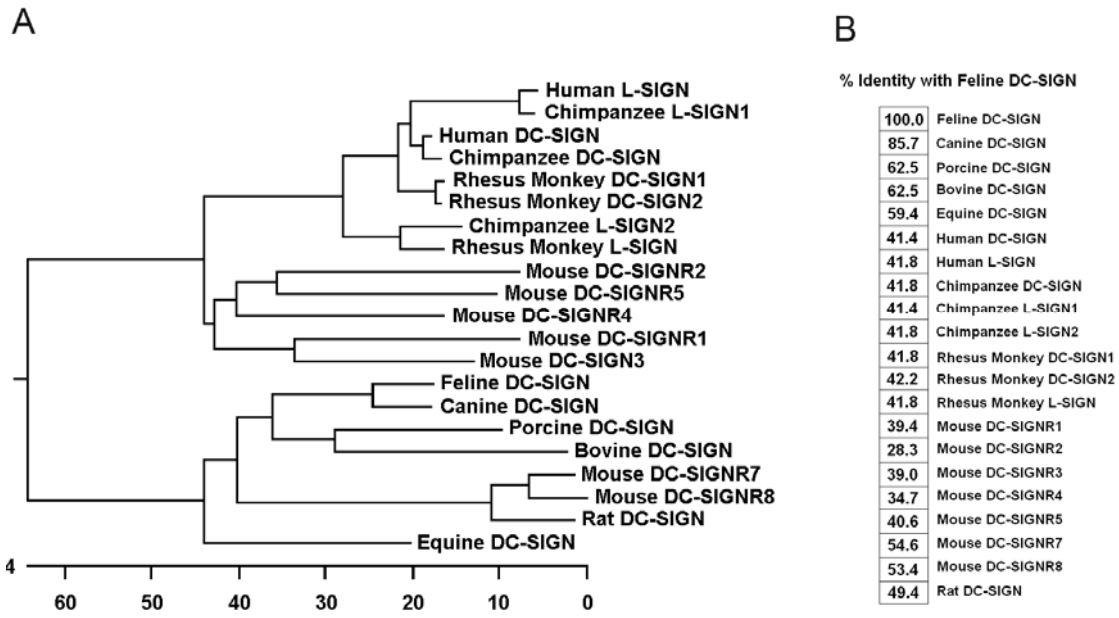

Figure A1.3 Phylogenetic analyses of feline DC-SIGN. A phylogenetic tree of DC-SIGN seqeuences generated by Clustal W allignemnt (A). The percent homology between fDC-SIGN and other mammalian DC-SIGN sequences is shown (B).

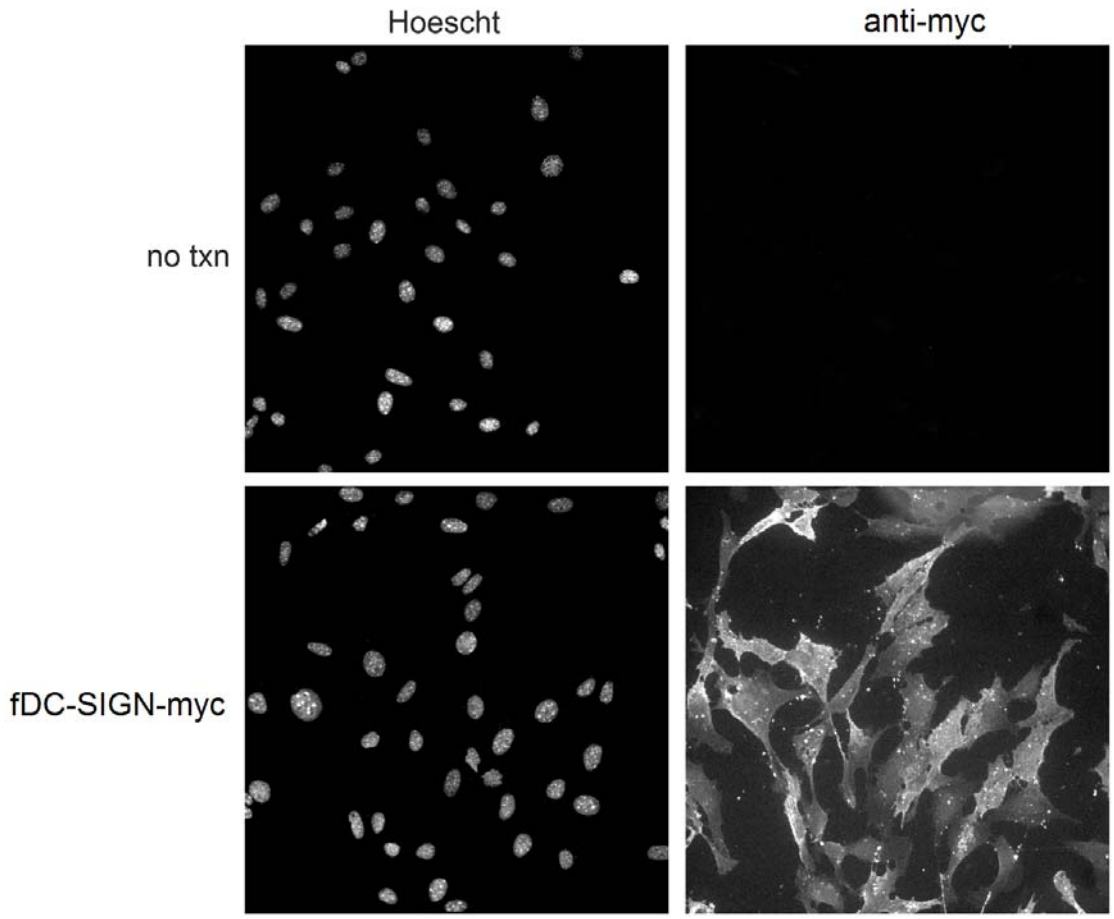

Figure A1.4 Expression of feline DC-SIGN. pCDNA3.1-fDCSIGN-myc was transfected in NIH-3T3 cells using lipofectamine. Cells were fixed with paraformaldehyde and stained with mouse anti-myc (9E10), and anti-mouse alexfuor 488. fDC-SIGN expression was visualized by immunofluorescent microscopy.

APPENDIX TWO

SEROTYPE 1 FIPV UTLIZES CATHEPSIN B AND DC-SIGN

In chapters three and four it is shown the serotype 2 feline coronaviruses (FCoV-2) utilize cathepsin B (catB) and DC-SIGN for cellular entry in cultured and primary cells. However FCoV-2 make up only a small amount of field isolates. Serotype 1 feline coronaviruses (FCoV-1) comprise up to 80% of field isolates, however they are difficult (but not impossible) to isolate and grow in culture.

A series of limited experiments with FCoV-1 were carried out in order to determine if they also rely on cathepsins and DC-SIGN. As shown in figure A2.1, serotype 1 FIPV-BLACK infection is dependent on catB, but independent of cathepsin L (catL) and low pH. The same characteristics were observed for FIPV-UCD2 (data not shown). It was also investigated whether FCoV-1 utilize DC-SIGN. As shown in figure A2.2, both FIPV-BLACK and FIPV-UCD2 infection is significantly enhanced by DC-SIGN expression. This suggests that although serotype 1 and 2 feline coronaviruses possess markedly different spike proteins, they are likely to utilize similar cellular entry pathways. Even more significant, this suggests that both serotypes would be susceptible to cathepsin inhibitors.

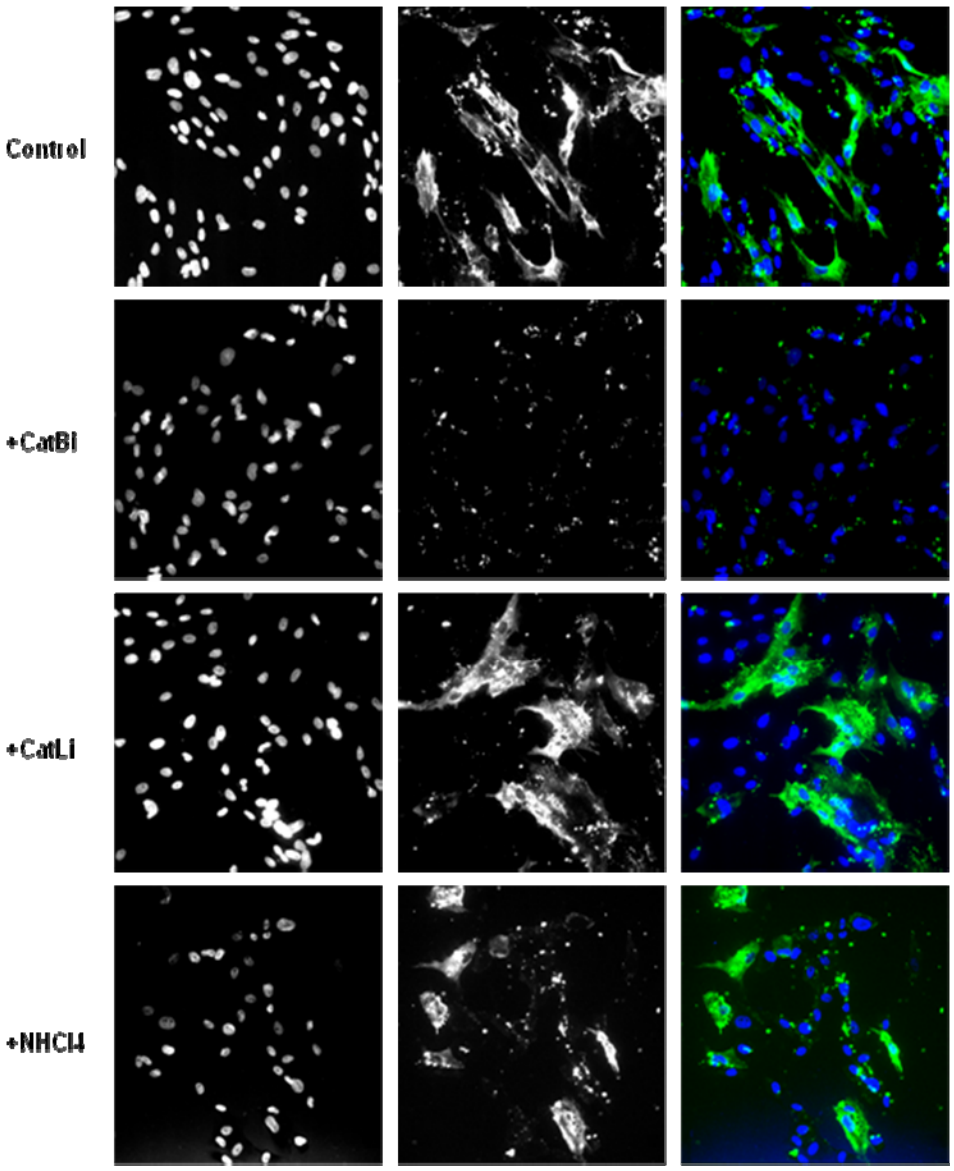

Figure A2.1 Serotype 1 feline coronavirus FIPV-BLACK requires cathepsin B for infection. AKD cells were pretreated with either cathepsin B inhibitor (CA074-Me), cathepsin L inhibitor (Z-FY-(t-Bu)-DMK), the lysomotrophic agent NH_4Cl, or DMSO (control). After 2 hours they were infected with FIPV-BLACK and incubated at 37ºC for 12 hours. Cells were then fixed in paraformaldehyde and stained with feline anti-FIP-1 antisera and anti-feline FITC.

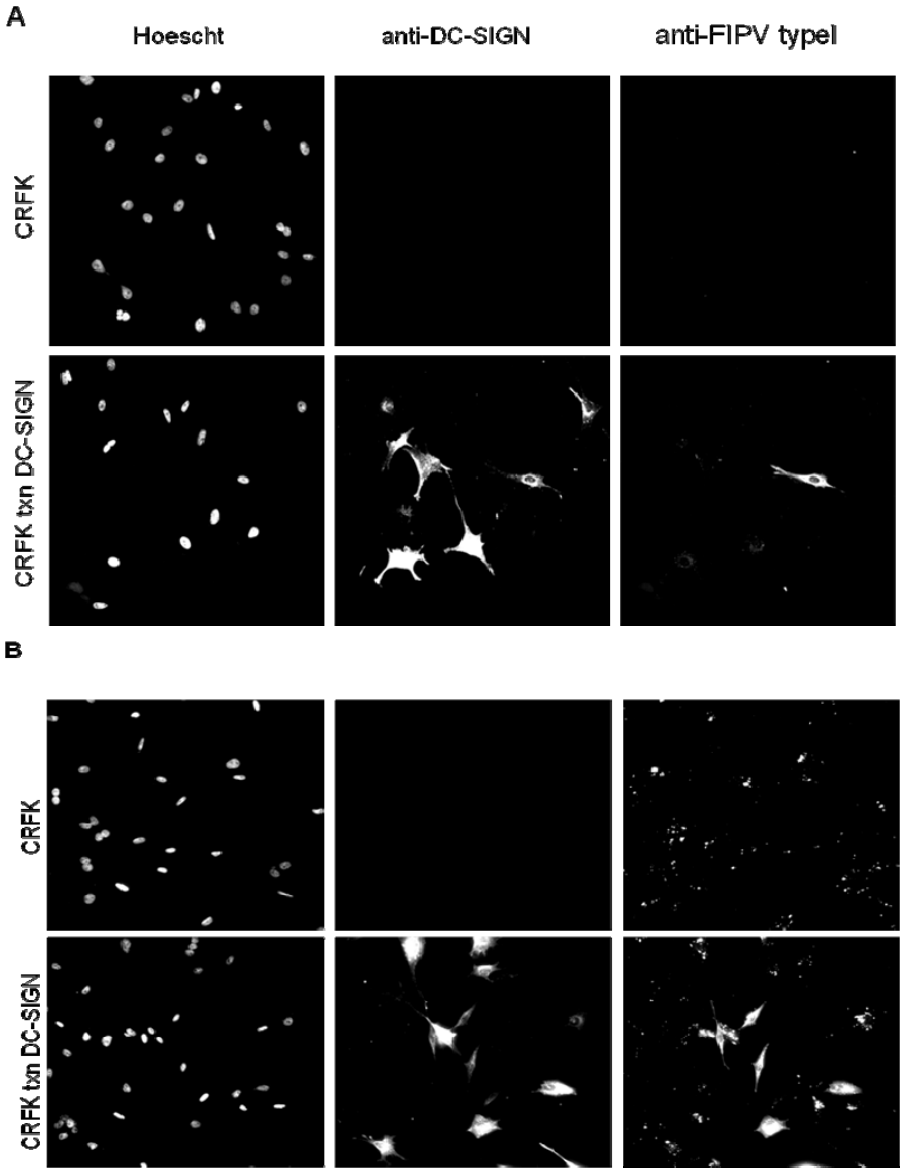

Figure A2.2 Serotype 1 feline coronaviruses FIPV-BLACK and FIPV-UCD2 utilize DC-SIGN for infection. CRFK cells and CRFK cells transfected with human DC-SIGN (hDC-SIGN) were infected with either FIPV-BLACK (A) or FIPV-UCD2 (B). Cells were incubated for 12 hours at 37ºC, fixed in paraformaldehyde, and stained with feline anti-FIP-1 antisera and anti-feline FITC.

APPENDIX THREE

CANINE AND PORCINE CORONAVIRUSES UTILIZE CATHEPSIN B

The spike protein of serotype 2 canine coronavirus (CCoV-2) and transmissible gastroenteritis virus (TGEV) share extensive homology with that of serotype 2 feline coronavirus (FCoV-2). As shown in chapter four, the spike protein of FCoV-2 is dependent on proteolytic activation by cathepsin B (catB). It was therefore investigated whether CCoV-2 and TGEV are also dependent on catB for infection. As shown in figure A3.1, infection by CCoV-2 and TGEV are both blocked by the catB inhibitor CA074-Me.

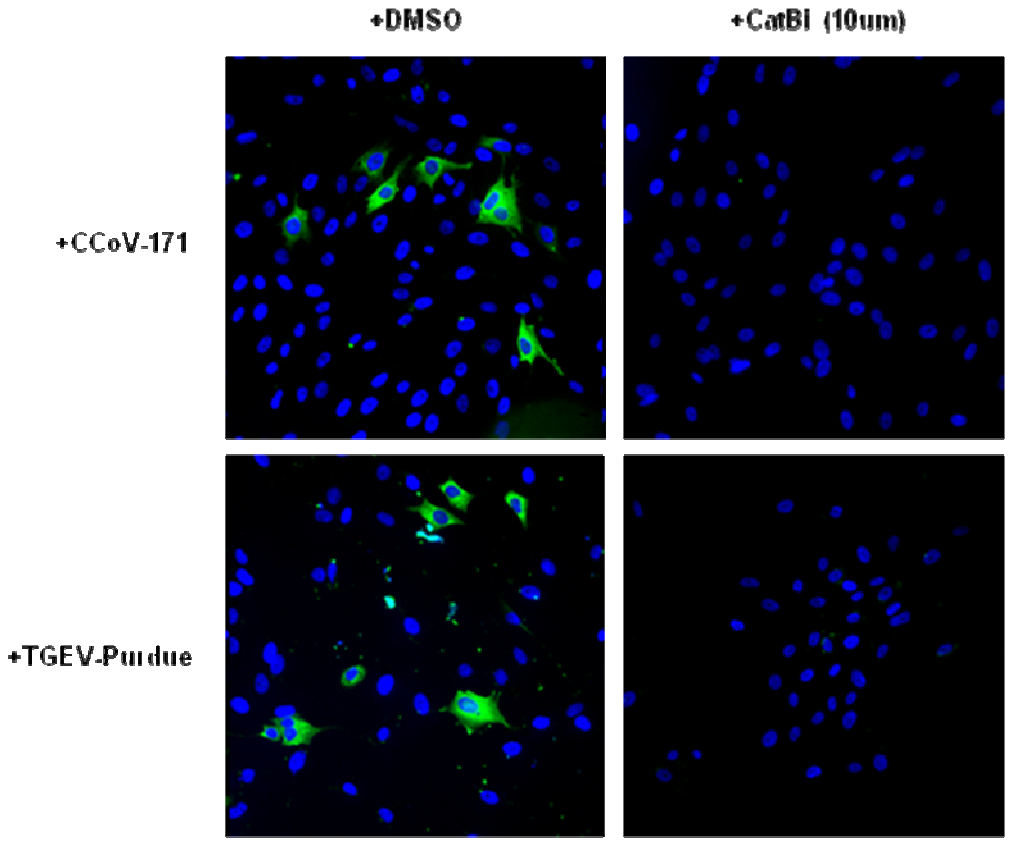

Figure A3.1 Infection by CCoV-2 and TGEV is dependent on cathepsin B. A72 cells were pretreated with either cathepsin B inhibitor (CA074-Me), or DMSO (control). After 2 hours they were infected with either CCoV-171 or TGEV-Purdue and incubated at 37ºC for 8 hours. Cells were then fixed in paraformaldehyde and stained with mouse anti-spike 18A7.4 and anti-mouse alexfluor 488.